BK_{Ca}-IP_3R DECOUPLING IN HYPERTENSION

A Dissertation
Submitted to the Graduate Faculty
of the
North Dakota State University
of Agriculture and Applied Science

By

Sayeman Islam Niloy

In Partial Fulfillment of the Requirements
for the Degree of
DOCTOR OF PHILOSOPHY

Major Department:
Pharmaceutical Sciences

June 2022

Fargo, North Dakota

North Dakota State University
Graduate School

Title

BK_{Ca}-IP_3R Decoupling in Hypertension

By

Sayeman Islam Niloy

The Supervisory Committee certifies that this ***disquisition*** complies with North Dakota State University's regulations and meets the accepted standards for the degree of

DOCTOR OF PHILOSOPHY

SUPERVISORY COMMITTEE:

Dr. Chengwen Sun
Chair

Dr. Stephen T. O'Rourke

Dr. Sijo Mathew

Dr. Alison Ward

Approved:

6/30/2022
Date

Dr. Jagdish Singh
Department Chair

ABSTRACT

Hypertension is a significant risk factor for cardiovascular diseases and a leading cause of worldwide morbidity and mortality. Dysregulation of intracellular Ca^{2+} in vascular smooth muscle (VSM) cells is one major contributor to the development of vascular hypercontractility and remodeling in hypertension. Plasma membrane (PM)-localized large-conductance, Ca^{2+}-activated K^+ (BK_{Ca}) channels prevent hypercontractility through membrane hyperpolarization in response to vasoconstrictor-induced activation of inositol trisphosphate receptors (IP_3Rs), localized on the sarcoplasmic reticulum (SR). However, loss of close contact or coupling between BK_{Ca} and IP_3R may diminish the BK_{Ca}-mediated protection against hypercontractility and hypertrophy and contribute to the development of hypertension. The overall goal of this study was to understand the role of BK_{Ca}-IP_3R coupling in the development of vascular hypercontractility and remodeling. I used a hypertensive animal model, spontaneously hypertensive rat (SHR), to study the impact of the loss of this coupling. My hypothesis was that there is a loss of communication between the IP_3 receptors and the BK_{Ca} channels in SHR VSM cells leading to reduced BK_{Ca} current after IP_3R activation.

My first objective was to determine the role of functional coupling of BK_{Ca} and IP_3R in vascular hypercontractility and hypertrophy development. Based on the findings, one can conclude that in SHR mesenteric VSM cells, there is a loss of functional IP_3R-BK_{Ca} coupling, and it might be involved in vascular hypercontractility and hypertrophy.

My second objective was to examine and compare the molecular coupling of BK_{Ca} and IP_3R between normotensive and hypertensive rats. My data suggest that the molecular connection between BK_{Ca} and IP_3R is disrupted in SHR VSM cells. My results also suggest that this loss of connection is not due to downregulation of junctophilin-2 (JPH2) but may be due to defective tethering of JPH2 to the PM.

Together, this research provides an improved understanding of the crucial roles played by BK_{Ca}-IP_3R coupling in hypertension. An understanding of ion channel coupling under disease conditions may provide relevant caveats where BK_{Ca} channels are considered a therapeutic target. I expect that the knowledge gained from my studies will fundamentally advance the field of ion channel-based therapeutics, especially in cardiovascular disorders.

ACKNOWLEDGEMENTS

I want to express my sincere gratitude to my mentor, adviser, and guide, Dr. Chengwen Sun, whose commitment and enthusiasm made this research work possible. His scientific knowledge, timely advice, and judicial scrutiny allowed me to improve my critical thinking skills, punctuality, and creativity.

I am also thankful to my thesis advisory committee: Dr. Stephen T. O'Rourke, Dr. Sijo Mathew, and Dr. Alison Ward, for their precious time and advice regarding my research work. I would also like to express my gratitude to Dr. Yagna Jarajapu for his mentorship, emotional support, and help with research techniques. Special thanks to Dr. Alison Ward, Dr. Ang Guo, Dr. Wenjuan Fang, Dr. Premanand Balraj, Saimon Mia, Richard Lamptey, Santo Kalathingal Anto, Sanjay Arora, and Kishore Chittimalli for helping me with various experiments. Without their help finishing my research work wouldn't have been possible.

I would also like to thank Dr. Jagdish Singh, chairman of the department of pharmaceutical sciences, for his motivation and great sense of humor.

I want to acknowledge AHA and APS for providing travel awards to attend several national-level conferences. My gratitude to Dr. Jodie Haring, Megan Ruch, and Dr. Mohammad Jiyan for their help and advice on laboratory animal husbandry.

I would like to express my heartfelt appreciation to my family members, especially my dear mother. Their unconditional love propelled me through the tough times and allowed me to complete my research work. Finally, I thank my lord, Allah, the Almighty, for giving me the opportunity to accomplish my lifelong dream of earning a Ph.D.

DEDICATION

To Almighty Allah and My Lovely Family

TABLE OF CONTENTS

LIST OF FIGURES

LIST OF ABBREVIATIONS

ACh	Acetylcholine
ANG II	Angiotensin II
α -SMA	α smooth muscle actin
ATP	Adenosine triphosphate
BK_{Ca}	Large-conductance Ca^{2+}-activated K^+ channel
Co-IP	Co-immunoprecipitation
DAG	Diacylglycerol
DAPI	4',6-diamidino-2-phenylindole
DMEM	Dulbecco's modified Eagle medium
DTT	Dithiothreitol
E-Syt	Extended synaptotagmin
IP_3	Inositol 1,4,5-trisphosphate
IP_3R	Inositol 1,4,5-trisphosphate receptor
JPH	Junctophilin
LTCC	L-type Ca^{2+} channel
MORN	Membrane occupation and recognition nexus
MLC	Myosin light-chain
MLCK	Myosin light-chain kinase
NE	Norepinephrine
PIP2	Phosphatidylinositol 4,5-bisphosphate
PLC	Phospholipase C
PM	Plasma membrane
PRC	Proximity restriction and clustering domain
Orai	Ca^{2+} release-activated Ca^{2+} channel protein

ROC.....	Receptor-operated Ca^{2+} channel
SD.....	Sprague-Dawley
SEM.....	Standard Error of Mean
SHR.....	Spontaneously hypertensive rat
SMP.....	Synaptotagmin-like mitochondrial lipid-binding protein
SOC.....	Store-operated Ca^{2+} channel
SR.....	Sarcoplasmic reticulum
RyR.....	Ryanodine receptor
STIM.....	stromal interaction molecule
TMEM.....	transmembrane protein
2-BP.....	2-bromopalmitate
VAP.....	VAMP-associated protein
VSM	Vascular smooth muscle
WST-1.....	4-[3-(4-iodophenyl)-2-(4-nitrophenyl)-2H-5-tetrazolio]-1, 3-benzene disulfonate

CHAPTER 1: INTRODUCTION

Hypertension or high blood pressure is a multifactorial medical condition where small resistant arteries (<300μm) play a crucial role (Intengan & Schiffrin, 2000). While high blood pressure is often the result of elevated cardiac output and peripheral vascular resistance, patients with established hypertension display normal cardiac output but increased peripheral vascular resistance (Mayet & Hughes, 2003). Numerous studies have shown that structural and functional abnormalities of blood vessels play an important role in developing and maintaining high blood pressure in hypertensive patients. These abnormalities of resistant arteries include increased sensitivity to vasoconstrictors, thickened walls and narrower lumen, and abnormal intracellular concentration of some ions. The reason behind these changes cannot be attributed to a single factor, as age, race, gender, duration of high blood pressure, location of the vascular bed etc., can all play an important role.

Cells that make up the arterial wall express many classes of ion channels that control the flow of ions into and out of cells. By controlling the intracellular ionic composition, ion channels regulate excitability, contraction, relaxation, signaling molecule release, and gene expression of cells (Hibino et al., 2010; Catterall and Swanson, 2015; Zamponi et al., 2015). Abnormal expression and functioning of ion channels are thus implicated in the development of hypertension, atherosclerosis, coronary artery disease, stroke, and increased or erratic peripheral vascular resistance (Yahagi et al., 2017; Brown et al., 2018). Considering the critical role played by ion channels in the pathophysiology of vascular diseases, studies have been conducted for decades to find the most appropriate therapeutic approach targeting the ion channels. Yet most medications available today are small molecules and peptide modulators that lack specificity in targeting channelopathies and often have side effects (Hutchings, Colussi & Clark, 2019). Given the diverse structural and functional features of ion channels, drug discovery in this high potential area has proven to be challenging. Advancing the knowledge of

the role of ion channels in regulating blood pressure will be critical in finding a new class of treatments for hypertension in the future.

Calcium-Dependent Contraction of Vascular Smooth Muscle Cell

The arterial wall consists of 3 layers. The thinnest, innermost layer contains endothelial cells. The outermost layer contains fibroblasts, collagen fiber, and nerve endings. The substantial middle layer contains vascular smooth muscle (VSM) cells. VSM cells are specialized cells, as they can contract and relax in response to hormones, vasoactive peptides, and reactive oxygen species (ROS) (Hill & Meininger, 2016). Increasing the intracellular free Ca^{2+} concentration ($[Ca^{2+}]_i$) is the main mechanism through which VSM cells contract and activate various transcription factors. An increase in $[Ca^{2+}]_i$ happens through Ca^{2+} entry from the extracellular space through PM-localized Ca^{2+} channels and Ca^{2+} released from the intracellular Ca^{2+} stores (Thillaiappan et al., 2017). The sarcoplasmic reticulum (SR) is the largest intracellular Ca^{2+} store in VSM cells, so the SR-localized Ca^{2+} channels, like the inositol trisphosphate receptor (IP_3R) and ryanodine receptors (RyR) channels play a crucial role in $[Ca^{2+}]_i$ regulation (Thillaiappan et al., 2017; Zhao et al., 2010; Saleem et al., 2014).

The first step of Ca^{2+}-induced VSM contraction is the binding of free Ca^{2+} to calmodulin. This Ca^{2+}–calmodulin complex then activates and induces a conformational change in the MLC kinase (MLCK) enzyme. Activated MLCK induces phosphorylation of myosin light chains (MLC) in the presence of ATP and stimulates the formation of cross-bridge leading to myosin–actin interaction and vascular contraction (Allen & Walsh, 1994).

Malfunction of processes responsible for regulating Ca^{2+} homeostasis can lead to increased Ca^{2+} influx, increased Ca^{2+} release from the SR, decreased SR Ca^{2+} uptake, and increased activation of the PLC-DAG-IP_3 pathway leading to increased Ca^{2+} signaling. If remained unchecked, persistently high $[Ca^{2+}]_i$ causes exaggerated contractile responses to vasoactive agonists and increased activation of proto-oncogenes, like c-myc, c-fos, and c-Ha-ras that increase protein synthesis leading to vascular hypertrophy (Marban & Koretsune, 1990).

Proto-oncogenes are converted to oncogenes when activated. Oncogenes stimulate the growth of myocytes through multiple pathways. They activate mitogen-activated protein kinases (MAPK). c-Jun N-terminal Kinase (JNK), p38, Rho-kinase, etc., all of which are capable of producing a hypertrophic response in myocytes (Finkle, 1999; Wehbe et al., 2019; Simpson, 1988).

Since peripheral vascular resistance is one of the main regulators of blood pressure, arterial hypercontractility and hypertrophy lead to significantly high peripheral vascular resistance and hypertension.

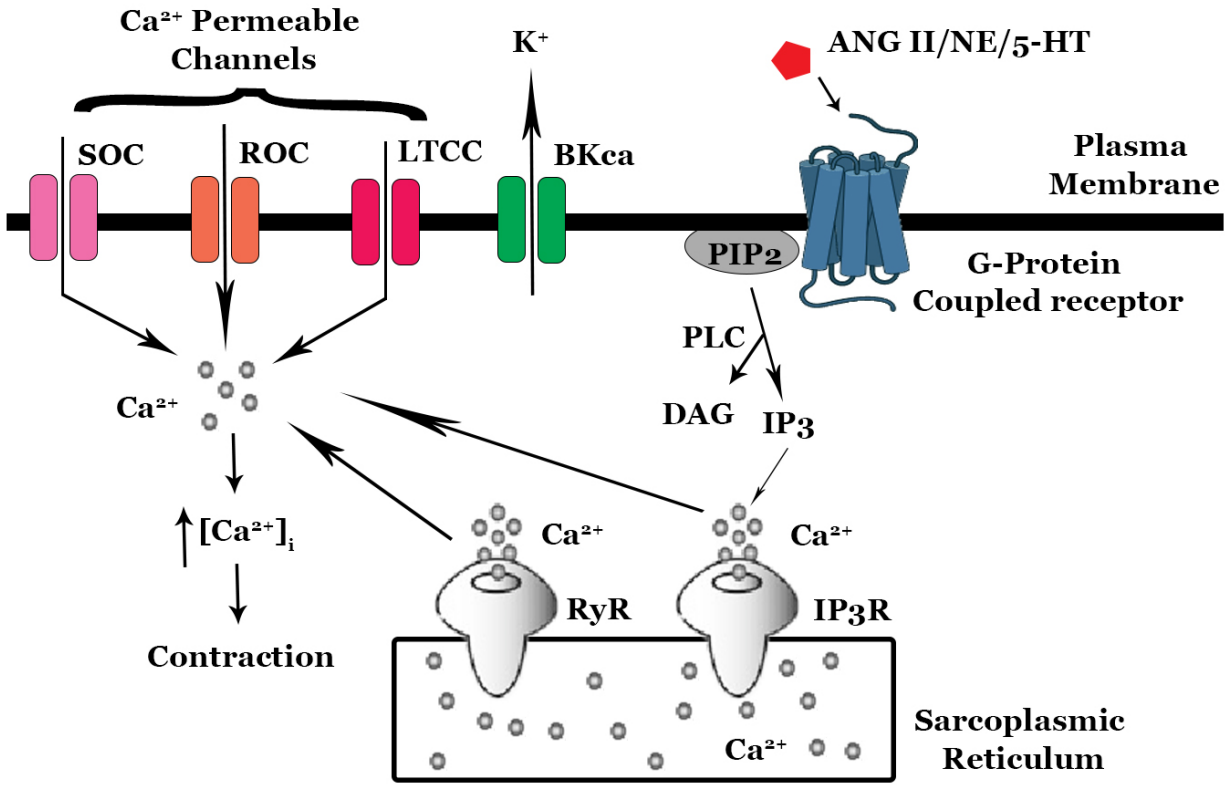

Figure 1. Ca^{2+} regulates vascular smooth muscle cell contraction. Vasoconstrictors induce VSM cell contraction by increasing the Ca^{2+}-influx through store-operated Ca^{2+} channel (SOC), receptor-operated Ca^{2+} channel (ROC), and voltage-gated L-type Ca^{2+} channel (LTCC) or Ca^{2+}-release from the SR through inositol trisphosphate receptor (IP_3R) channel and ryanodine receptor (RyR) channel. Intracellular free Ca^{2+} binds to a messenger protein, calmodulin. Ca^{2+}–calmodulin complex activates and induces a conformational change in myosin light-chain kinase (MLCK). Activated MLCK induces phosphorylation of myosin light chains (MLC), leading to myosin–actin interaction and VSM cell contraction.

BK_{Ca} Channel

Large conductance Ca^{2+} activated K^+ channels, also known as BK_{Ca} or KCNMA1 or MaxiK or Kca1.1 channels, are widely expressed in many types of smooth muscle cells. Compared to other K^+ channels, they have a significantly larger unitary conductance ranging from 200 to 300pS, making them a critical player in regulating peripheral vascular resistance and thus blood pressure (Lee & Cui, 2010). BK_{Ca} channels have a unique ability to be activated independently by membrane depolarization and an increase in Ca^{2+} concentration. When activated, these channels modulate the membrane potential and intracellular Ca^{2+} concentration through a rapid efflux of K^+ ions.

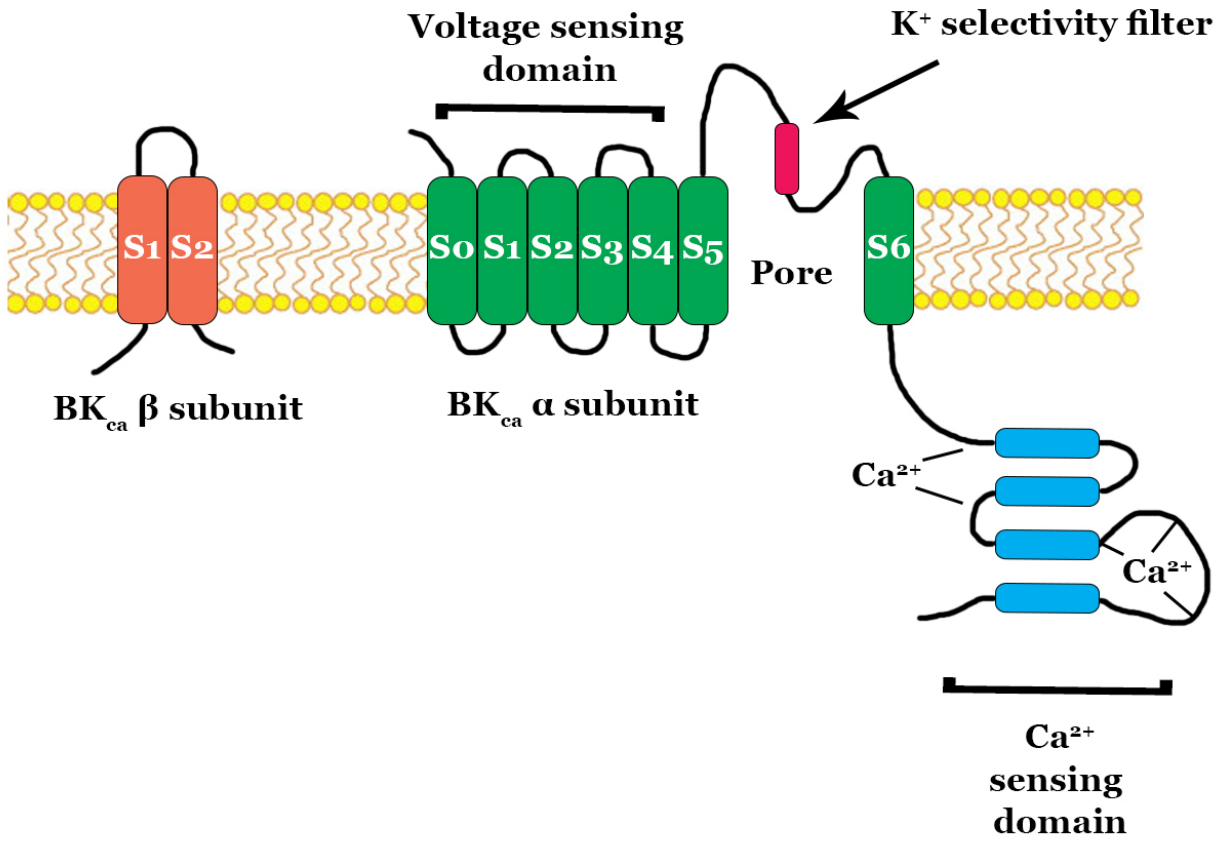

Figure 2. Molecular structure of large-conductance Ca^{2+}-activated K^+ (BK_{Ca}) channel. Each BK_{Ca} channel contains 4 α-subunits and 4 β-subunits in a 1:1 ratio in VSM cells (Petkov, 2014).

BK_{Ca} channels are expressed by a single Slo1 gene and are made up of α, β, and the recently discovered γ subunits (Figure 2). The 4 α subunits in the BK_{Ca} channels are responsible

for forming the ion-selective pore, similar to other voltage-gated K^+ (K_v) channels; however, unlike the K_v channels, the α subunits are also surrounded by the regulatory β and γ subunits. The α subunits have seven transmembrane segments, from S0 to S6. The N(amino)-terminal of the subunit resides at the extracellular side, while the much larger C(carboxy)-terminal, consisting of close to 800 amino acids, is found in the cytoplasm. The C-terminal has the regulatory domains called RCK-domains, responsible for K^+ conductance (Yuan et al., 2010). These domains contain negatively charged aspartic acid residues and act as binding sites for Ca^{2+} (Schreiber & Salkoff, 1997; Moczydlowski, 2004). The C-terminal also contains binding sites for kinase and phosphatase enzymes. The transmembrane segments of the α subunit are tasked with distinct functions, playing a critical role in the regulation of BK_{Ca} channels. The S0 segment, which is unique to BK_{Ca} channels, is needed for the interaction between the α subunits and the regulatory β subunits (Wallner et al., 1996). This interaction is believed to modulate the voltage sensitivity of BK_{Ca} channels (Morrow et al., 2006; Koval et al., 2007). The S1-S4 transmembrane segments form the voltage-sensing domain (VSD) of BK_{Ca} channels (Yellen, 2002). This domain contains positively charged amino acid residues that can sense a rise in voltage and move upwards to the extracellular side (Adelman et al., 1992; Atkinson et al., 1991; Butler et al., 1993). Similar to K_v channels, the S5-S6 transmembrane segments of each α subunit form the pore-gate domain (PGD), which is tasked with controlling K^+ permeation (Yellen, 2002). Changes in voltage and binding of ligands to the ligand-binding sites on the carboxy tail, alter the structure of the pore-gate domain and allow the flow of K^+ through the pore (Piskorowski & Aldrich, 2006). Amino acid residues localized in this domain are capable of attracting potassium ions, which contributes to the large K^+ conductance of BK_{Ca} channels (Flynn & Zagotta, 2001).

The auxiliary β subunits contain two transmembrane segments, called TM1 and TM2 (Hermann, Sitdikova & Weiger, 2015). Unlike the α subunit, the N- and C-terminals of β subunit reside in the cytoplasm. Depending on the tissue, the β subunits in BK_{Ca} channels can be

different in their expression and function. In Vascular smooth muscle cells, the β1 is the predominantly expressed subtype, while β2, β3, and β4 subtypes are more commonly found in neurons (Weiger, et al., 2000). β subunits depending on the tissue, can increase or decrease BK_{Ca} channel activity in response to elevated intracellular Ca^{2+}, modulate channel kinetics, control channel inactivation in response to BK_{Ca} channel blockers such as iberiotoxin and modify voltage sensitivity of BK_{Ca} channels (Wallner, Meera & Toro, 1996; Wallner, Meera & Toro, 1999; Tseng-Crank et al., 1996; Brenner et al., 2000).

BK_{Ca} channels also have γ subunits interacting with the α subunits. These subunits are rich with leucine, have molecular weights of around 35 kDa, and apparently control the voltage- and Ca^{2+}-sensitivity of BK_{Ca} channels (Yan & Aldrich, 2012; Nimigean & Magleby, 1999). These subunits contain only a single transmembrane domain and an extracellular N-terminal, and a cytoplasmic c-terminal tail (Li & Yan, 2016). Like the β subunits, γ subunits are also capable of regulating the gating kinetics, ligand sensitivity, and activation/inactivation characteristics of BK_{Ca} channels (Almassy & Begenisich, 2012; Xia et al., 2000; McManus et al., 1995; Cox & Aldrich, 2000; Wang & Brenner, 2006).

While BK_{Ca} channels have been found to express in intracellular organelles such as mitochondria and nucleus, they are more commonly localized in the plasma membrane of many excitable cells (Contreras et al., 2013). In mesenteric vascular smooth muscle cells, BK_{Ca} channels are co-localized with voltage-gated Ca^{2+} channels, mainly the L-type Ca^{2+} channels (LTCCs) (Berkefeld et al., 2006). LTCCs are voltage-sensitive and typically begin to activate at membrane potentials positive to -10 mV to cause depolarization through Ca^{2+} influx (Xu & Lipscombe, 2001). The Ca^{2+} release channels, such as ryanodine receptors and IP_3 receptors localized on the sarcoplasmic reticulum, have Ca^{2+} binding sites. Ca^{2+} entering through the LTCCs can activate these channels and trigger the release of Ca^{2+} from the SR through the process known as calcium-induce calcium release (CICR). Ca^{2+} influx from extracellular space and Ca^{2+} released from intracellular Ca^{2+} stores raise the cytosolic Ca^{2+} concentration. If this rise

in Ca^{2+} is not controlled, Ca^{2+} level can continue to increase above the optimal level and permanently activate Ca^{2+}-dependent intracellular processes that can cause hypercontractility and narrowing of the artery through VSM cell hypertrophy. Cells have BK_{Ca} channels localized in the plasma membrane to provide a negative-feedback regulatory mechanism to prevent an excessive rise in intracellular Ca^{2+} concentration. Since these channels are both Ca^{2+} and voltage-sensitive, they are activated as a result of increased intracellular Ca^{2+} and voltage, causing a massive K^+ efflux. Efflux of K^+ causes cell hyperpolarization, which results in the closure of LTCCs, preventing further Ca^{2+} influx and vascular hypercontractility.

Outside their function in blood vessels, BK_{Ca} channels also control action potential and neuronal excitability, modulate neurotransmitter release at central nervous system nerve terminals, provide cardioprotection, regulate bladder contractility and excitability, prevent hearing loss, play an important role in circadian rhythm, regulate fibroblast activation and migration, control endocrine secretion, and influences endogenous rhythm structure (Chen and Petkov, 2009; Hristov et al., 2011; Salkoff et al., 2006; Womack and Khodakhah, 2004; Shruti et al., 2008; Soltysinska et al., 2014; Lovell & McCobb, 2001; Scruggs et al., 2020). As a result, pharmacological modulation of BK_{Ca} channels using naturally occurring and synthetic compounds presents a wide array of therapeutic opportunities.

IP_3 Receptor (IP_3R)

Inositol 1,4,5-trisphosphate receptors (IP_3Rs) are intracellular Ca^{2+} release channels, mainly localized on the membrane of the sarcoplasmic reticulum (SR) (Berridge, 1993). Aside from the SR, IP_3Rs are also expressed in the Golgi apparatus and the nucleus (Rodriguez-Prados et al. 2015; Echevarría et al. 2003). When activated by IP_3, clusters of these channels open and let Ca^{2+} out of the SR and create localized Ca^{2+} signals in the cytosol, called Ca^{2+} puffs (Zhao et al., 2008). IP_3Rs also regulate store-operated Ca^{2+} entry (SOCE) in cells, as IP_3-induced Ca^{2+} release from the SR promotes interaction between the stromal interaction molecule 1 (STIM1) on the SR and the calcium release-activated calcium modulator 1 (Orai1) Ca^{2+} channel in the PM

(Prakriya & Lewis 2015). STIM1-Orai1 interaction is necessary for refilling Ca^{2+} stores inside the cells through the Ca^{2+} tunneling process (Petersen, Courjaret, & Machaca, 2017).

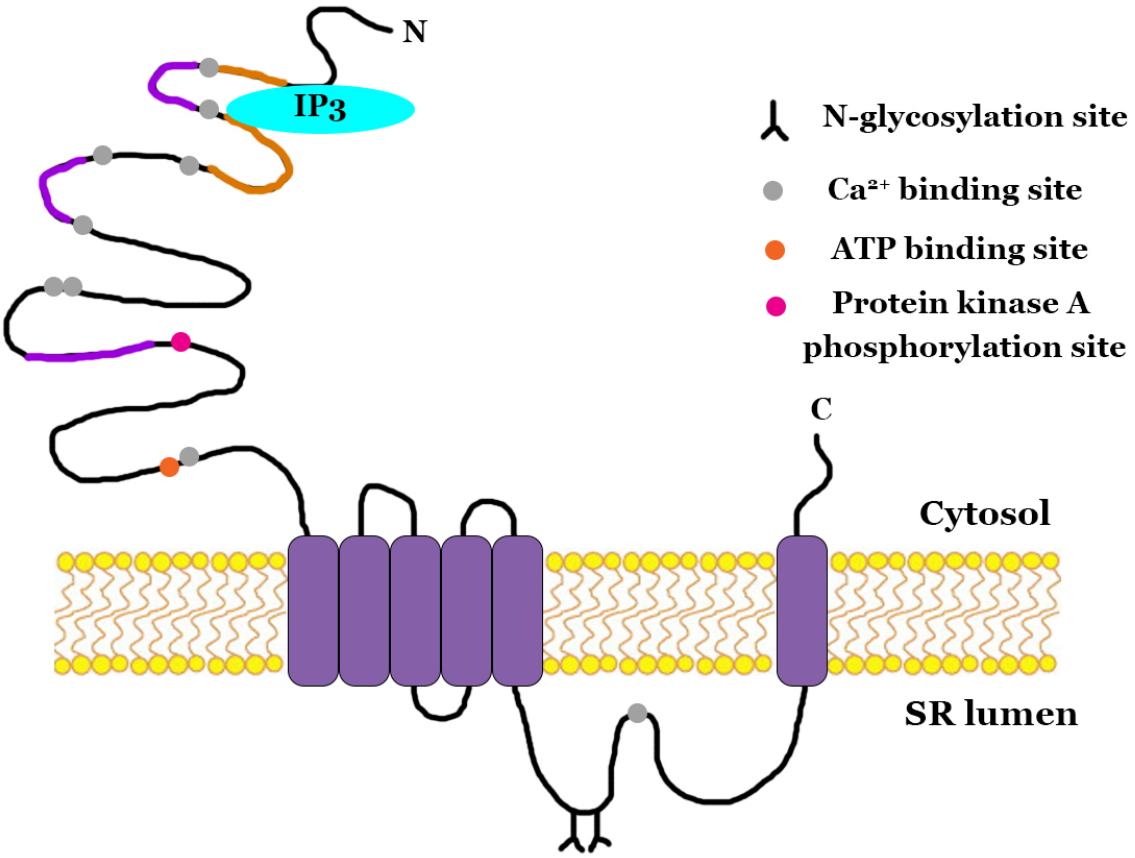

Figure 3. Molecular structure of inositol trisphosphate receptor (IP_3R) channel. Each IP_3R channel contains N-terminal region in the cytoplasm containing 6 transmembrane domains and C-terminal domain. The N-terminal regions contains the ATP, IP_3 and Ca^{2+} binding sites, which module IP_3R functionality. The N-glycosylation sites are in the luminal region.

So far, 3 IP_3R subtypes have been discovered in mammals, known as IP_3R1, IP_3R2 and IP_3R3, encoded by ITPR1, ITPR2, and ITPR3 genes, respectively (Lin et al., 2016). While these 3 subtypes are closely related and similar in size (around 2700 residues), their expression is significantly different between tissues (Taylor et al., 1999). In vascular smooth muscle cells, all 3 subtypes are expressed, although IP_3R1 is the predominantly expressed IP_3R subtype (Zhao et al., 2008). Aside from their difference in expression patterns, the subtypes also have different affinities for IP_3. Experiments have shown that the IP_3R2 subtype has the highest affinity for IP_3, while IP_3R3 has the lowest (Iwai et al., 2007). IP_3Rs, like their relative, the Ryanodine receptor

(RyR) channels, are large-conductance Ca^{2+} channels capable of creating a large localized Ca^{2+} signal. The activity of these channels is also regulated by the intracellular Ca^{2+} concentration, as a small increase in cytosolic Ca^{2+} can increase IP_3R activity while large cytosolic Ca^{2+} can inhibit it (Foskett et al., 2007).

IP_3Rs are commonly expressed on the membrane of the sarcoplasmic reticulum, with about 90% of the channel residing in the cytosol (Fan et al., 2015). Each channel is a tetramer of IP_3R subunits, resembling a "mushroom" like structure, with the "stalk" of the mushroom planted in the membrane of the SR while the "cap" of the mushroom in the cytosol (Paknejad and Hite, 2018). The stalk contains 24 transmembrane domains (TMD), with each subunit consisting of 6 TMDs (Fan et al., 2018). The transmembrane domains are made up of residues towards the C-terminal of the IP_3R subunit and are called TMD1-6. TMD6 of each subunit forms a twist to create a path for Ca^{2+} conduction (Prole & Taylor, 2019). TMD6 and TMD5 of each subunit are connected through a loop with a carbonyl backbone that works as a selectivity filter for cations (Prole & Taylor, 2019). This cation filtering loop resides in the lumen of the SR and has a Ca^{2+} binding site. TMD6 of each subunit also contains a hydrophobic region which prevents the passage of Ca^{2+} through the channel pore when the channel is in the closed state (Fan et al., 2015). When IP_3Rs are activated, the TMD6s change their conformation to stop the hydrophobic region from blocking the passage of ions (des Georges et al., 2016).

Towards the N-terminal of IP_3R, there is an IP_3 binding core (IBC), where the IP_3 molecule binds and activates IP_3R. In each IBC, there are two domains called α and β domains (Paknejad and Hite, 2018). Between these domains, there is an abundance of positively charged amino acid residues which are critical for binding to IP_3 (Paknejad and Hite, 2018). IP_3 molecules contain 3 negatively charged phosphate groups. These groups interact with the positively charged residues in the IP_3 binding core and help the IP_3 molecule dock into the IBC. Arg and Lys have been identified as essential IBC residues for the docking process (Yoshikawa et al., 1996).

In the N-terminal, there is another domain called the suppressor domain (Yoshikawa et al., 1996). As the name suggests, this domain is tasked with reducing the affinity of IBC to IP_3. While the mechanism through which the suppressor domain inhibits IP_3 binding to the IBC domain is not well understood, it is believed that the suppressor domain is capable of binding to the IP_3 binding site in IBC and altering the orientation of the IBC, thus blocking IP_3 from docking (Bosanac et al., 2004). This suppressor domain is also capable of binding to various regulator proteins, like calmodulin (CaM), Ca^{2+}-binding protein 1 (CaBP1), etc. and regulating the IP_3R activity (Kasri et al., 2004; Yang et al., 2002).

After IP_3 or other regulatory proteins bind to the binding regions in the N-terminal of the channel, the signal is transferred to the C-terminal of the channel through a domain called transducing domain. This domain has binding sites for many small function modulatory molecules, such as Ca^{2+}, CaM, protein kinase C (PKC), protein kinase G (PKG), protein kinase A (PKA), Caspase 3, ATP, Calcium/calmodulin-dependent protein kinase II (CaMKII), etc. (Sienaert et al., 1996; Ferris, Huganir & Snyder, 1990; Yamada et al., 1995; Hirota, Furuichi & Mikoshiba, 1999; Supattapone et al., 1988; Ferris et al., 1991; Koga et al., 1994).

When a ligand, for example, Angiotensin II, 5-HT or Norepinephrine, binds to its G protein-coupled receptor (GPCR), the α-subunit of Gq protein activates an enzyme phospholipase C (PLC). Activated PLC then cleaves a cellular membrane phospholipid called phosphatidylinositol 4,5-bisphosphate (PIP2) into 2 compounds, Inositol trisphosphate (IP_3) and diacylglycerol (DAG). The binding of IP_3 to IP_3R triggers the opening of the Ca^{2+} channel and thus the release of Ca^{2+} into the cytoplasm.

IP_3Rs play a critical role in the regulation of blood pressure, as SR Ca^{2+} release is important for myogenic tone regulation (Boittin et al., 1999; Jaggar and Nelson, 2000). Ca^{2+} waves produced by IP_3Rs not only raise the cytosolic Ca^{2+} concentration but also activate PM-localized voltage and Ca^{2+}-sensitive Ca^{2+} and K^+ channels (Hill et al., 2001). These receptor channels are also believed to be upregulated in hypertensive patients, making a case for their

role in the development of hypertension (Linde et al., 2012; Abou-Saleh et al., 2013). Outside the cardiovascular system, IP_3Rs also play a critical role in the secretion of endocrine glands, generation of glucose, development of the embryo, neuronal growth and migration, oxidative phosphorylation, lysosomal activity, autism, tumor formation, and Alzheimer's disease (Futatsugi et al., 2005; Wang et al., 2012; Kume et al., 1997; Uchida et al., 2010; Takei et al., 1998; Cardenas et al., 2016; Xu and Ren, 2015; Berridge, 2016).

SR-PM Junctions

SR-PM junctions are specialized cellular microdomains where various junctional tethering proteins bring the plasma membrane (PM) and the sarcoplasmic reticulum (SR) close to each other and form SR-PM coupling sites (Manford et al., 2012). These junctional sites are formed to fulfill the need for communication between PM and different cell organelles. A typical SR-PM junction has a 10-30nm gap between the SR and the PM, which is enough for communication between PM- and SR-localized proteins, lipid transfer, and Ca^{2+} signaling (Chen, Quintanilla & Liou, 2019; Wu et al., 2006). While commonly detected in muscle cells and neurons, these junctions are also found in limited numbers in non-excitable cells like Jurkat T-cells and HeLa cells (Wu et al., 2006; Orci et al., 2009).

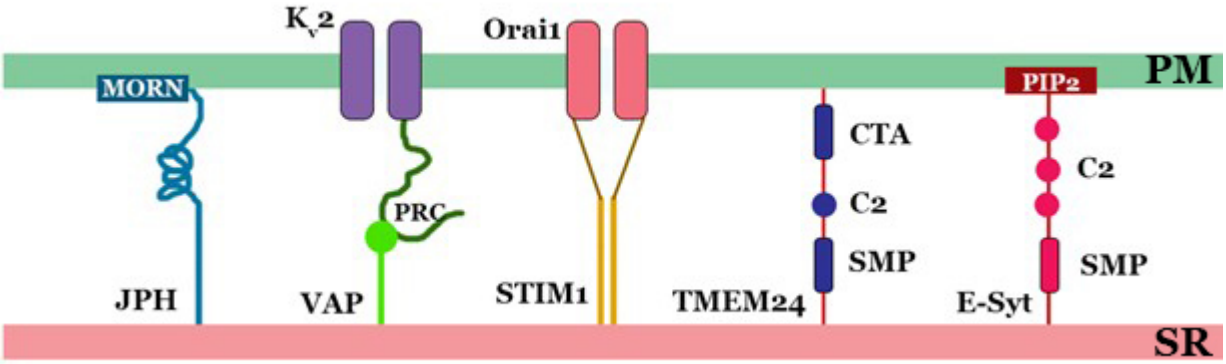

Figure 4. Tethering proteins at SR-PM junctions of VSM cells. SR-PM peripheral coupling sites are responsible for maintaining appropriate spacing between the plasma membrane (PM) and the sarcoplasmic reticulum (SR). This is critical for effective Ca^{2+} signaling and BK_{Ca}-mediated vascular relaxation. JPH, Junctophilin; MORN, membrane occupation and recognition nexus motif; SMP, synaptotagmin-like mitochondrial lipid-binding protein; C2, C-terminal domain; K_{v2}, voltage-gated K^+ channel, Orai1, Ca^{2+} release-activated Ca^{2+} channel protein 1; STIM1, stromal interaction molecule 1; TMEM24, transmembrane protein 24; PRC, proximity restriction and clustering domain; VAP, VAMP-associated protein, E-Syt, extended synaptotagmin; PIP2, phosphatidylinositol 4,5-bisphosphate.

Junctional proteins: The SR-PM junctions are possible due to the interactions between various tethering proteins and the PM/SR. In mammalian cells, many types of SR-PM tethering proteins have been discovered. Principal among them is the Junctophilin (JPH), which is usually found in excitable cells, like the muscle cells and neurons (Takeshima et al., 2000; Nishi et al., 2003). These proteins contain multiple conserved protein domains, each with its own function. The membrane occupation and recognition nexus (MORN) domain binds the JPH protein to the PM, the alpha helix domain bridges the gap between the PM and SR, and the C-terminal transmembrane domain connects the JPH protein to the membrane of the SR (Garbino et al., 2009; Takeshima et al., 2000;). While mainly characterized as a structural protein holding the peripheral SR-PM coupling sites, JPH proteins also play a critical role in Ca^{2+} handling and excitation-contraction coupling in excitable cells (Pritchard et al., 2019).

PM-localized voltage-gated K^+ channel clusters can also function as SR-PM tethering proteins. These clusters are usually made up of K_v2.1 (KCNB1), and K_v2.2 (KCNB2) channels and are usually found in dendrites, axons, and soma of neurons (Chen, Quintanilla & Liou, 2019).

These channels contain a domain called the proximal restriction and clustering (PRC) domain consisting of 26 amino acids (Lim et al., 2000; Fox et al., 2015). This domain is responsible for the clustering of the potassium channels and binding of these clusters to the membrane of the SR (Lim et al., 2000). Recent research has reported that this PRC domain interacts with an SR localized protein called VAMP-associated proteins (VAPs) (Johnson et al., 2018). Interaction between the PRC domain and VAP is believed to be behind the SR-PM tethering ability of K_v2 channel clusters (Johnson et al., 2018).

Alongside JPH proteins, another ubiquitously expressed SR transmembrane protein is the Stromal Interaction Molecule 1 (STIM1) protein. This protein, alongside the calcium release-activated calcium channel protein 1 (Orai1), plays a critical role in store-operated Ca^{2+} entry (SOCE) (Chen et al., 2016). STIM1 not only acts as an SR-PM tethering protein but also acts as an SR Ca^{2+} sensor. When the SR is depleted of Ca^{2+}, the STM1 protein translocates closer to the PM-localized Orai1 and binds to the STIM1 binding site of Orai1 (Chen et al., 2016). The binding of Orai1 to STIM1 opens the Orai1 channels and permits Ca^{2+} entry into the cell and subsequent refilling of SR (Chen et al., 2016). During the SOCE process, the STIM1-Orai1 combination acts as tethering molecules to keep sites of PM and SR closer together (Wu et al., 2016).

Other SR membrane proteins like E-Syt1, E-Syt2, and E-Syt3 contain synaptotagmin-like mitochondrial-lipid binding protein (SMP) and C2 domains (Giordano et al., 2013). These proteins are predominantly expressed in the SR-PM junctional regions and translocate closer to the PM when the cytosolic Ca^{2+} level gets too high (Giordano et al., 2013). There they bind to a membrane phospholipid called Phosphatidylinositol 4,5-bisphosphate or PIP2 and act as SR-PM tethers (Chang et al., 2013).

ORP5 and ORP8 are also SR membrane proteins that bind to PM-localized PI 4-phosphate (PI4P) and contribute to the formation of SR-PM junctions (Chung et al., 2015). These proteins contain pleckstrin homology (PH) and an OBSP-related domain (ORD) which are necessary for the interaction with PI4P (Chen, Quintanilla & Liou, 2019).

Role of SR-PM junctions in Ca^{2+} signaling in VSM cells: SR-PM junctions play a vital role in muscle contraction, the release of neurotransmitters, migration, and apoptosis of different cells by regulating the level of Ca^{2+} in the cytosol (Berridge, Lipp & Bootman, 2000; Lewis, 2011; Dupont et al., 2011). For tight regulation of intracellular Ca^{2+} concentration ($[Ca^{2+}]_i$), proper communication between the PM and SR is critical. To avoid widespread activation of Ca^{2+}-sensitive processes, the level of $[Ca^{2+}]_i$ is kept low, around 50 to 100 nM (Chang, Chen & Liou, 2017). This level of intracellular Ca^{2+} is maintained through cooperation between the Sarco/endoplasmic reticulum Ca^{2+}-ATPase (SERCA) and plasma membrane Ca^{2+}-ATPase (PMCA) pumps, Ca^{2+} channels at the SR and the PM, and K^+ channels at the PM (Chang, Chen & Liou, 2017). These ion channels are in constant communication with each other to regulate intracellular Ca^{2+}. One of the factors that can influence this communication is the distance between these channels localized in the PM and SR. SR-PM junctions bring the PM-localized ion channels and SR-localized ion channels closer together and make proper communication possible (Chang, Chen & Liou, 2017).

SR-PM junctions in muscle cells bring the distance between the PM and SR close to 9-12nm, which is vital for the excitation-contraction coupling (Henkart, Landis & Reese, 1976). When the muscle cell membrane is depolarized, the PM localized voltage-sensitive dihydropyridine receptor (DHPR) channels open and cause Ca^{2+} influx. This increases the local Ca^{2+} concentration in the cytosol and stimulates the opening of SR-localized ryanodine receptor (RyR) channels through a process called "Ca^{2+}-induced Ca^{2+} release" (Endo, 2009). SR releases Ca^{2+} into the cytosol through RyR channels and depolarizes the cell even more. Further depolarization activates the PM-localized voltage-gated Ca^{2+} channels (VGCC), causing further Ca^{2+} entry and muscle contraction (Collier et al., 2000). This whole process requires constant communication between the DHPR, RyR, and VGCC channels. SR-PM junctions make this communication possible by bringing them close together. Aside from excitation-contraction coupling, the SR-PM junction is also necessary for the refilling of intracellular Ca^{2+} stores like

the SR. STIM1 and Orai1 proteins localized in the SR-PM junctions in muscle cells and bind to each other when the level of Ca^{2+} in the SR is low (Chen et al., 2016). This simultaneously makes the store-operated Ca^{2+} entry efficient and prevents unnecessary activation of Ca^{2+}-sensitive processes in the cytosol during the refilling process by keeping the Ca^{2+} entry localized.

So, it is evident that SR-PM junctions are necessary for inter-organelle signaling and Ca^{2+} signaling regulation.

JPH2 in SR-PM Tethering

So far, 4 isoforms of the junctophilin (JPH) protein have been discovered, known as JPH1-4. The expression of these isoforms is tissue-specific, as JPH1 is highly expressed in skeletal muscle, JPH2 in heart and blood vessels, and JPH3 & JPH4 in nervous tissue (Takeshima et al., 2000; Nishi et al., 2003). All the members of the junctophilin family have been found to tether the SR membrane to the PM. Structure-wise, all 4 isoforms have multiple repeats of highly conserved 'membrane occupation and recognition nexus' (MORN) motifs at the N-terminal (Garbino et al., 2009). The MORN motifs are 14 amino acids long and share about 75%-90% homology across all species (Garbino et al., 2009). They are also responsible for targeting the JPH protein to the lipid bilayer of the PM (Minamisawa et al., 2004). Mutations occurring within these motifs have been reported to interfere with the binding of the JPH protein to the PM (Garbino et al., 2009). Each JPH protein has 8 of these motifs divided into 2 groups, with the first group consisting of motifs 1-6 and the second group consisting of motifs 7 to 8 (Takeshima et al., 2000). These two groups are connected by a highly conserved joining region, whose function still remains unknown.

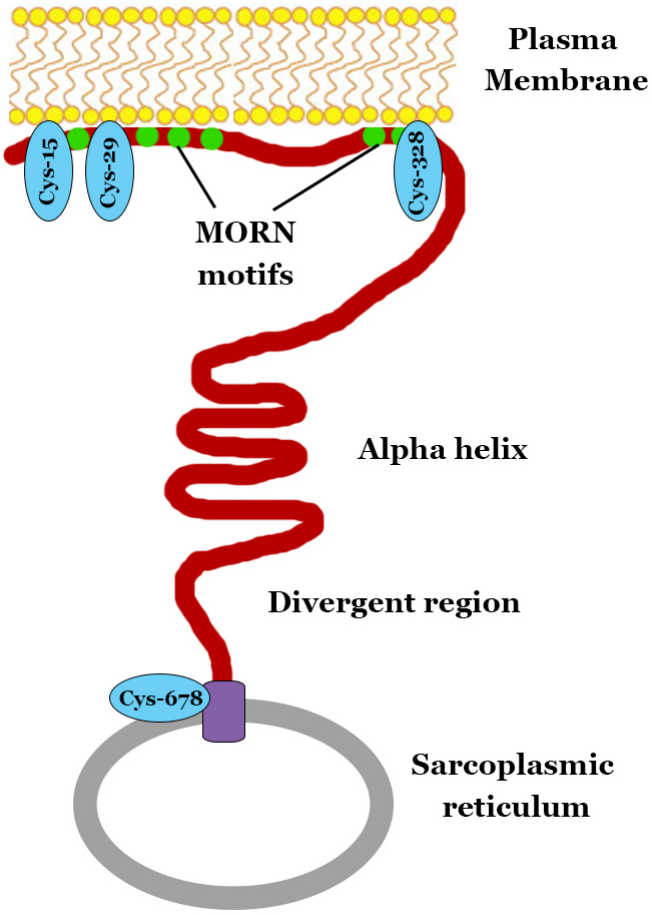

Figure 5. Molecular structure of junctophilin-2 (JPH2). Each JPH2 molecule has 8 MORN motifs at the N terminus and 3 Cys residues. C-terminal regions has a transmembrane domain and 1 Cys residue. Helical and coiled domains are between the N and C terminal. MORN, membrane occupation and recognition nexus.

The N- and C-terminals of the JPH protein is connected by a ~100 amino acid long region called the α-helical domain (Takeshima et al., 2000). This domain is about 10.5nm long and responsible for maintaining the gap between the PM and the SR in SR-PM junctions (Takeshima et al., 2000). This region of the JPH protein contains an extensive secondary structure containing an α-helix. The α-helical domain is followed by another highly conserved region called the divergent region. Despite being highly conserved, this region has small sections, which display a high degree of divergence between different isoforms of JPH protein (Garbino et al., 2009). Lack of conservation in these areas is believed to be the reason behind isoform-specific functions of JPH proteins (Landstrom, Beavers & Wehrens, 2014). While not

proven, it is hypothesized that these variable regions may play a crucial role in selecting the binding partner of the JPH protein. The divergent region is followed by the transmembrane (TM) segment of the JPH protein. This segment contains the C-terminal, which anchors the JPH protein to the SR membrane. The TM segment contains 22 amino acids (Garbino & Wehrens, 2010).

According to Pritchard et al. (2019), JPH2 is the predominantly expressed junctophilin isoform in vascular smooth muscle cells, and knockdown of the JPH2 gene results in loss of SR-PM contact areas in these cells. The binding of JPH2 protein to the PM/SR membrane is stabilized by a reversible lipidation strategy called S-palmitoylation (Jiang et al., 2019). In brief, s-palmitoylation is a common posttranslational modification employed by proteins to associate with membranes (Zaręba-Kozioł et al., 2018). In this process, palmitoyl chains are covalently attached to the cysteine residues of the transmembrane protein (Zaręba-Kozioł et al., 2018). This attachment increases the affinity of the protein for lipids on the plasma membrane and makes it possible to dock into the lipid compartments of the PM. S-palmitoylation process is dependent on the activity of two enzymes, palmitoyltransferase, and acyl protein thioesterase. Palmitoyltransferase is responsible for attaching palmitate to the cysteine residues, while acyl protein thioesterase removes palmitate from the cysteine residues (Zaręba-Kozioł et al., 2018).

The JPH2 protein has 4 cysteine residues, 3 (Cys-15, Cys-29, and Cys-328) of them in the MORN region of the N-terminal and 1 (Cys-678) of them at the C-terminal TM domain (Jiang et al., 2019). Through metabolic labeling with palmitate–alkyne, Cu(I)-catalyzed azide-alkyne cycloaddition (CuAAC) reaction and co-immunoprecipitation, Jiang et al. (2019) showed that all 4 cysteine residues of JPH2 go through the S-palmitoylation process, enabling it to attach to PM and SR.

Role of SR-PM Junctions in Communication Between BK_{Ca} and SR Ca^{2+} Channels

BK_{Ca} channels rely on localized Ca^{2+} signals to regulate VSM cell membrane potential and VSM contractility. BK_{Ca} channels require micromolar concentrations of intracellular Ca^{2+} to be activated at the normal resting membrane potential (Piskorowski & Aldrich, 2002). The basal concentration of Ca^{2+} in the cytoplasm of unstimulated VSM cells is 50-100 nM (Foskett, J. K., White, C., Cheung, K. H., & Mak, 2007), too low to activate BK_{Ca} channels at normal resting membrane potential. Ca^{2+}-release channels localized on the membrane of the SR can produce localized Ca^{2+} transients with a very high Ca^{2+} concentration (10 to 100 μM) (Jaggar et al., 2000). These transients create Ca^{2+} microdomains with steep Ca^{2+} concentration gradients that rapidly form and dissipate near the opening of the channel. While the Ca^{2+} concentration adjacent to the open channel may be ~100μM, the concentration may dip below 1μM as close as 1–2 μm from the channel opening (Naraghi, M., & Neher, 1997; Ríos, E., & Stern, 1997). SR-PM junctions bring SR-localized Ca^{2+}-release channels within 10-150 nm of BK_{Ca} channels (Poteser et al., 2016) and thus are vital for BK_{Ca} activation mediated by SR Ca^{2+} release.

Knowledge Gaps and Significance of This Research

While the interest in studying the importance of SR-PM coupling sites has grown tremendously in the last decade, little is known about their role in the development of hypercontractility and hypertrophy. This research investigated novel mechanisms for the development of hypertension using a hypertensive animal model to study the impact of the loss of these coupling sites on BK_{Ca}-IP_3R coupling and vascular diseases. The pathophysiology of hypertension in spontaneously hypertensive rat (SHR) rat strains is applicable to human hypertension, with cardiac pathology developing gradually over time and then decompensating (Breckenridge, 2013). While this frequently studied animal model is known to suffer from vascular hypercontractility and hypertrophy (Touyz, Tolloczko & Schiffrin, 1994; Marche, Herembert & Zhu, 1995), there hasn't been any research conducted on the possible role of the loss of SR-PM coupling sites and BK_{Ca}-IP_3R coupling on the development of hypertension and

hypertrophy in this model to our knowledge. This present study allowed us to test these hypotheses on this highly relevant animal model for the first time.

This research also focused on identifying the cellular mechanisms underlying enhanced vascular contractility in hypertension. Many intracellular signaling pathways contribute to pathological vascular contraction and remodeling, such as inflammation, oxidative stress, lipid accumulation, degradation of the extracellular matrix, etc. (Libby, 2002; Henning, Bourgeois & Harbison, 2018). Due to the heterogeneity of vascular dysfunction, it is challenging to pinpoint single biological processes responsible for vascular disease. This project was aimed at offering a better understanding of the complexity of arterial contractility and remodeling and helping unravel the role of ion channel coupling in the development of cardiovascular disease (CVD).

The impact of this study also expands beyond the scope of vascular dysfunction. BK_{Ca}-IP_3R interaction is not limited to muscle cells and cellular contraction. It has been reported that their interaction promotes human breast cancer cell proliferation (Mound, Rodat-Despoix, Bougarn, Ouadid-Ahidouch & Matifat, 2013). While Weaver, Olsen, McFerrin & Sontheimer (2007) reported that BK_{Ca} channels promote glioma cell invasion only when they are in proximity to the IP_3 receptors in the brain. As a result, this study on BK_{Ca}-IP_3R coupling will not only further the understanding on vascular hypercontractility and remodeling but also accelerate the progress in this area of research for other diseases.

The central hypothesis of this research was that the functional- and molecular coupling between BK_{Ca} and IP_3R is disrupted in the Spontaneously hypertensive rat (SHR), contributing to the development of vascular hypercontractility and remodeling. The following specific aims were set to test the central hypothesis and accomplish the overall objective of this research:

Aim 1: To determine the role of functional coupling of BK_{Ca} and IP_3R in the development of vascular hypercontractility and hypertrophy. Whole-cell patch-clamp experiment identified that the BK_{Ca} current density is significantly lower in SHR compared to SD in response to a vasoconstrictor. The hypothesis was that this lack of BK_{Ca} activity is related to the loss of

communication between the IP_3 receptors and the BK_{Ca} channels. The goal of this aim was to determine if the Ca^{2+}- and voltage-sensitivity of BK_{Ca} channels is altered in mesenteric VSM cells of SHR. The focus was also on examining BK_{Ca} current density in response to IP_3-induced intracellular Ca^{2+} release and the effect of BK_{Ca} block on vascular hypercontractility, cellular hypertrophy, and proliferation in both SHR and SD rats.

Aim 2: To examine the molecular mechanisms involved in the BK_{Ca}-IP_3R uncoupling in VSM cells of SHR as compared with SD rats. The goal of this aim was to examine the molecular mechanisms involved in the loss of close contact between BK_{Ca} and IP_3R in SHR VSM cells. The expression of BK_{Ca}, IP_3R, and Junctophilin-2 (JPH2) in mesenteric VSM cells was examined. Co-localization of BK_{Ca} and IP_3R was also evaluated. Moreover, JPH2 palmitoylation-inhibition study in SD mesenteric VSM cells was used to study the loss of JPH2 palmitoylation on BK_{Ca} channel current. The hypothesis was that the co-localization of BK_{Ca} and IP_3R is decreased, and JPH2 palmitoylation is functionally impaired in SHR VSM cells compared to SD.

Together, these studies will have a broad impact on the field by dissecting the crucial roles played by BK_{Ca}-IP_3R coupling in hypertension. In the long term, these studies may reveal novel therapeutic targets for the treatment of hypertension.

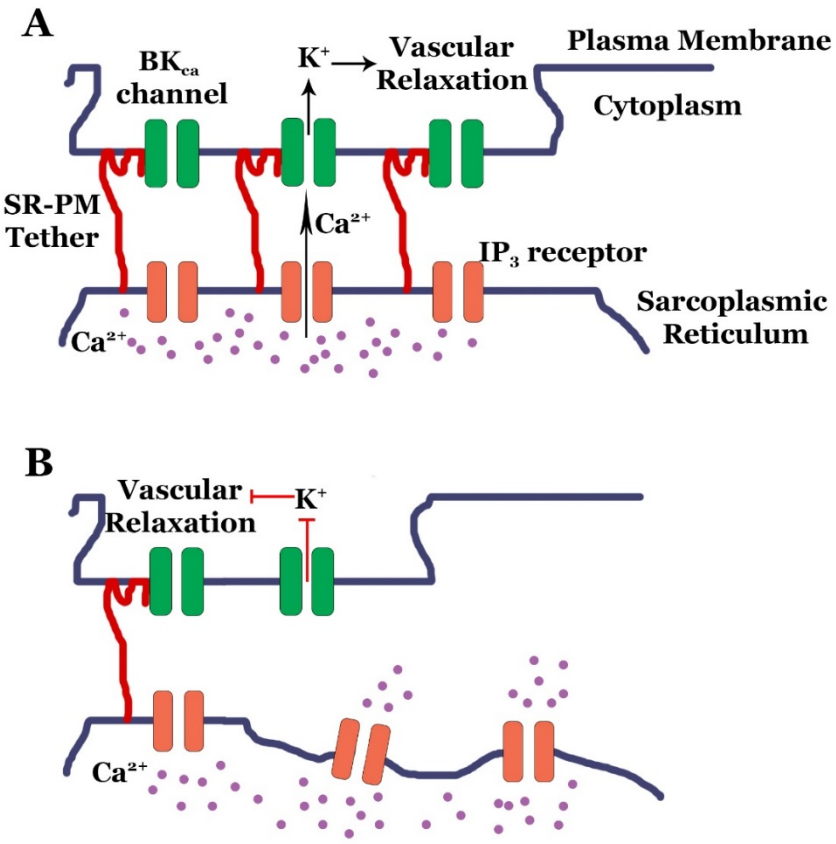

Figure 6. Proposed schematic diagram: proposed defects in the BK_{Ca}-IP_3R coupling in SHR mesenteric VSM cells. A: Normal coupling of BK_{Ca} channels and IP_3 receptors promoting efficient hyperpolarization and vascular relaxation (black arrows). B: Loss of BK_{Ca}-IP_3R coupling in SHR preventing vascular relaxation mediated by SR Ca^{2+} release.

CHAPTER 2: ROLE OF FUNCTIONAL COUPLING OF BK_{Ca}-IP_3R IN THE DEVELOPMENT OF VASCULAR HYPERCONTRACTILITY AND HYPERTROPHY

Introduction

Small resistance arteries of less than 300μm in diameter are one of the main regulators of blood pressure. These arteries control the blood pressure by rapid changes in their lumen diameter through contraction and dilation. A substantial portion of the wall of resistance arteries is made up of excitable vascular smooth muscle (VSM) cells. In response to mechanical, chemical, or electrical stimuli, the intracellular Ca^{2+} concentration ($[Ca^{2+}]_i$) in VSM cells increases and causes cell contraction and growth. (Allen & Walsh, 1994; Touyz et al., 2018).

Increased smooth muscle tone results in increased peripheral vascular resistance with a consequent increase in blood pressure (Schiffrin, 1992). $[Ca^{2+}]_i$ depends on Ca^{2+} entry from the extracellular space or Ca^{2+} release from intracellular Ca^{2+} stores. In VSM cells, voltage-dependent L-type Ca^{2+} channels (LTCC) are the predominant mediator of extracellular Ca^{2+} influx, while the sarcoplasmic reticulum (SR) is the largest intracellular Ca^{2+}-storage organelle (Brozovich et al., 2016). Inositol 1,4,5-trisphosphate receptors (IP_3R) are intracellular Ca^{2+} channels localized in the membrane of the sarcoplasmic reticulum (SR). In response to many stimuli that activate phospholipase C, IP_3Rs release Ca^{2+} from the SR to give local Ca^{2+} signals (Ca^{2+} puffs), and then Ca^{2+} waves that spread across the cell and raise cytosolic Ca^{2+} concentration, thereby causing cell contraction (Zhao et al., 2010; Saleem et al., 2014; Thillaiappan et al., 2017).

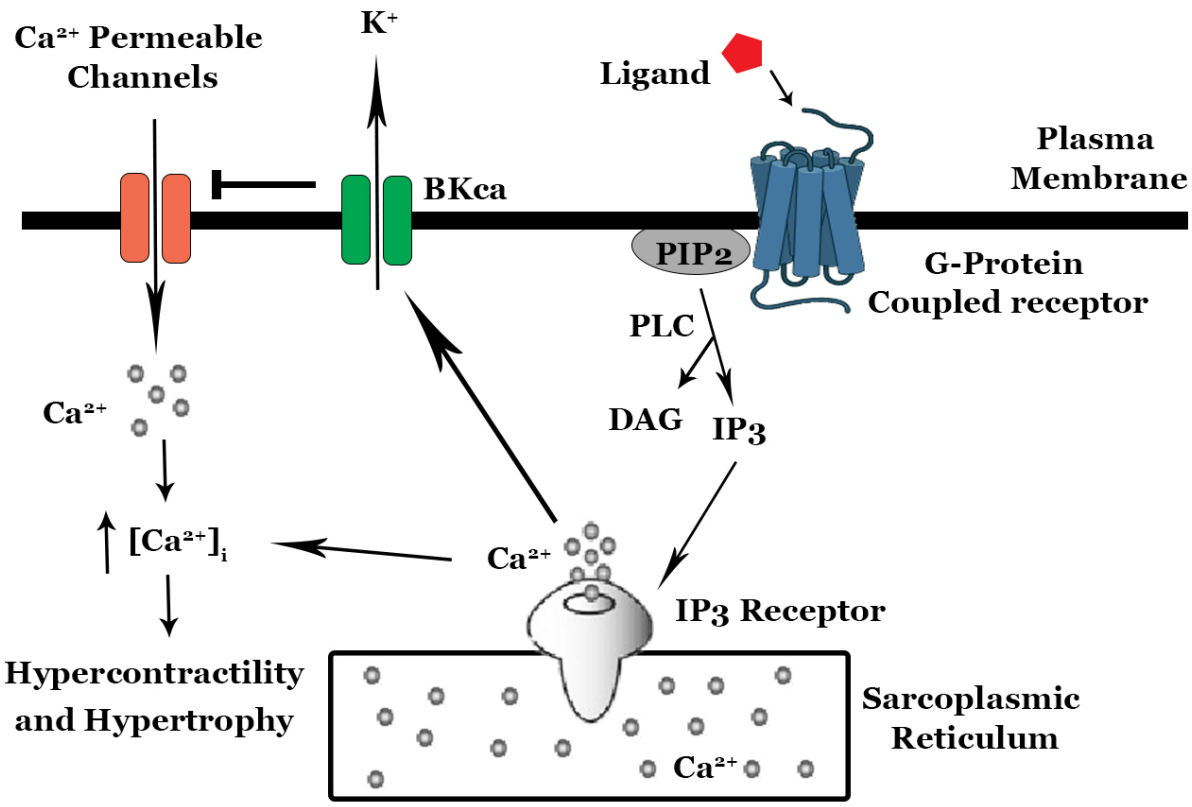

Figure 7. BK_{Ca}-mediated negative feedback mechanism protecting against over-elevation of intracellular Ca^{2+} concentration ($[Ca^{2+}]_i$) and vascular hypercontractility. BK_{Ca} channels regulate Ca^{2+} channels by controlling membrane potential. Ca^{2+} released from the intracellular stores via the IP_3 receptor activates BK_{Ca} channels. An increase in $[Ca^{2+}]_i$ and elimination of K^+ regulate several physiological processes, including vascular tone and VSM cell proliferation. Abbreviations: IP_3R = Inositol 1,4,5-triphosphate receptor, BK_{Ca} = Large-conductance Ca^{2+}-activated K^+ channel, PLC = Phospholipase C, DAG = diacylglycerol, PIP2 = Phosphatidylinositol 4,5-bisphosphate.

In VSM cells, IP_3Rs are coupled to large-conductance Ca^{2+}-activated K^+ (BK_{Ca}) channels such that IP_3R -mediated SR Ca^{2+} release activates the BK_{Ca} channels (Zhao et al., 2010). BK_{Ca} channels belong to the family of voltage-gated potassium channels, but their activity can be independently modulated by either Ca^{2+} or voltage (Szteyn & Singh, 2020; Vetri, Saha Roy Choudhury, Sundivakkam & Pelligrino, 2014). The native BK_{Ca} channel is formed by four pore-forming α (BKα) and ancillary β ($BK\beta_{1-4}$) subunits and has large single-channel conductance of 100–300pS (Marty, 1981). BK_{Ca} channels act as negative feedback regulators of membrane potential and Ca^{2+} homeostasis as their activation hyperpolarizes the membrane potential

through a large efflux of K^+ ions, which in turn closes voltage-dependent L-type Ca^{2+} channels, reduces Ca^{2+} influx, and induces vascular relaxation (Vetri et al., 2014; Zhao et al., 2010).

Electron microscopy studies have revealed that regions of the SR and the PM in VSM cells come very close to each other (10-25nm) and form peripheral coupling sites, which play an essential role in signaling and molecular trafficking between the two membrane compartments (Popescu, Gherghiceanu, Mandache & Cretoiu, 2006; Jiang et al., 2019). These peripheral coupling sites bring the IP_3Rs into proximity of BK_{Ca} channels, which is necessary for the functional coupling between IP_3R and BK_{Ca} (Jiang et al., 2019). Loss of this functional coupling would diminish transient BK_{Ca} channel activity, which in turn would increase $[Ca^{2+}]_i$. Increased $[Ca^{2+}]_i$ causes vascular hypercontractility and activates hypertrophic response genes (Wilkins & Molkentin, 2004; Touyz et al., 2018).

Thus, the present study was designed to increase the understanding of the function of the IP_3R–BK_{Ca} channel Ca^{2+} signaling pathway in opposing vasoconstriction in mesenteric arteries. Here, the hypothesis was that the loss of functional coupling between BK_{Ca} and IP_3R is involved in the development of vascular hypercontractility and hypertrophy in SHR arteries.

Materials and Methods

Chemicals: Crystallized papain, collagenase, and elastase were purchased from Worthington Biochemicals (Freehold, NJ). Mouse anti-smoothelin antibody was purchased from Santa Cruz Biotechnology (Santa Cruz, CA). Mouse Anti-α smooth muscle actin (anti-α SMA) antibody, goat anti-mouse secondary antibody, and norepinephrine (NE) were purchased from Thermofisher Scientific (Waltham, MA). Soybean trypsin inhibitor, DTT, HEPES, and other reagents were obtained from Sigma-Aldrich (St. Louis, MO). Paxilline, angiotensin II (ANG II), and acetylcholine (ACh) were purchased from Cayman Chemical (Ann Arbor, MI). WST-1 reagent was purchased from Abcam (Waltham, MA). Fura-2 AM was purchased from Santa Cruz (California, USA), and cover glass chambers were acquired from CellVis (California, USA).

Blood pressure measurement: Mean arterial pressure was measured without anesthesia, using CODA non-invasive tail-cuff blood pressure measuring system (Kent Scientific corporation, CT, USA). SHR and SD rats of both sexes (8-10 rats of each sex) were warmed at 32-34°C on a heating pad for 10 min before placing them in a plastic restrainer of appropriate size. The tail of the rat was then inserted into a pneumatic pulse-sensitive cuff. Each measurement of blood pressure was obtained by averaging 10 consecutive readings.

Tissue preparation and cell isolation: Third- and fourth-order mesenteric arteries were dissected from 4-6-month-old SHR and normotensive Sprague-Dawley (SD) rats of either sex purchased from Charles River Farms (Wilmington, MA). Mesenteric arteries of at least 3 rats of either sex were used per experiment. At least 3 mesenteric vascular beds were used per experiment for VSM cell isolation. Rats were housed at 22 ± 2°C on a 12 h-12 h light-dark cycle and provided with food and water ad libitum. Rats were euthanized for experiments with an overdose of pentobarbital (150mg/kg). All animal protocols were approved by the North Dakota State University Institutional Animal Care and Use Committee. Enzymatic isolation of single VSM cells was carried out as previously described (Sun et al., 1998). The vessel segments were incubated for 10 minutes in 2 ml of low Ca^{2+} Tyrode's solution: (mM) 145 NaCl, 4 KCl, 0.05 $CaCl_2$, 1 $MgCl_2$, 10 HEPES, and 10 dextrose containing 1 mg/ml albumin, followed by 20 minutes at 37°C in 1.5 mg/ml papain and 1 mg/mL DTT. Finally, the segments were incubated for 80 minutes at 37°C in 2 mg/mL collagenase, 0.5 mg/mL elastase, and 1 mg/ml soybean trypsin inhibitor. Tissues were then triturated gently using a fire-polished wide-bore pipette to release single VSM cells. Cells were either stored in low Ca^{2+} Tyrode's solution at 4°C for electrophysiological experiments within 6h or cultured in $25cm^2$ culture flask, which contained Dulbecco's modified Eagle medium (DMEM) supplemented with 10% fetal bovine serum, penicillin (100U/ml), and streptomycin (100µg/ml). After 6-8 days, cells were subcultured by trypsinization. Cells were passaged as they became confluent and were diluted 1:5. The medium was exchanged every 3 days. Cultures (<5th passage) were maintained under optimal conditions

of 37°C (5% CO_2, 95% air). Cells at the 3rd-5th passages were used for experiments. Immunofluorescence staining of SMC markers, including α-smooth muscle actin (α-SMA; Brisset et al., 2007) and smoothelin (Lino et al., 2018; Sartore et al., 2001), was used to identify the VSM cells.

Real-time $[Ca^{2+}]_i$ imaging: Mesenteric VSM cells were plated in eight-well cover glass chambers (CellVis, California, USA) and incubated for 60 mins with fura-2 AM (4 μM; (Santa Cruz, California, USA) at room temperature, washed and perfused with Hank's balanced salt solution. Real-time Ca^{2+} imaging was performed using an Olympus fluorescence microscope (Fluoview FV300) equipped with a 20x numerical aperture oil immersion lens (with excitation at 340 and 380 nm and emissions at 510 nm). Changes in fluorescence intensities in selected regions of interest were recorded in response to 1μM ANG II, or 5μM NE and results were obtained in the ratio of 340/380-nm wavelengths. To minimize the Ca^{2+} influx and examine the effect of agonists on intracellular Ca^{2+} release, Ca^{2+} imaging experiment was also performed in Ca^{2+}-free environment. Cells were perfused in zero calcium-containing HBSS following initial incubation with Fura-2 AM before the application of 1μM ANG II or 5μM NE. Peak and area under the curve (AUC) above baseline were calculated to assess the net response to the agonists.

Western blotting: $BK_{Ca}\alpha$ and IP_3R protein levels in rat mesenteric arteries were assessed by western blot analysis. Mesenteric arteries from 3 SHR and SD rats of either sex (2 male and 1 female rat of each strain) were isolated and homogenized by mechanical shearing with a Dounce homogenizer in ice-cold RIPA buffer. The Bradford method-based Bio-Rad protein assay kit (Bio-Rad, Hercules, California) was used for the quantification of solubilized protein. Bovine serum albumin (BSA) was used to establish the standard curve. Relative measurement of protein concentration was achieved through comparison with the standard curve. 35μg of protein was loaded in each well for the western blot analysis. Kaleidoscope (Bio-Rad, Hercules, California) was used for band referencing. Proteins were separated on 7.5% polyacrylamide gels by SDS-PAGE and electroblotted onto a nitrocellulose membrane.

Membranes were blocked in TBS-T (0.08% Tween) containing 5% milk for 1h, followed by overnight incubation with rabbit polyclonal anti-KCNMA1 (1:1000) or rabbit polyclonal anti-IP_3R1 (1:1000) primary antibodies at 4°C. After washing with TBS-T, membranes were incubated for 1h with anti-rabbit horseradish peroxidase-conjugated secondary antibodies (1:3000). To ensure equal loading, the membranes were reprobed for β-actin after stripping using mouse monoclonal Anti-β-Actin antibody (1:1000). β-actin is a common housekeeping protein used in the western blot analysis of rodent mesenteric arteries (Stott et al., 2018; Silva et al., 2015; Troiano et al., 2021; Matsumoto et al., 2010). For stripping, a mild stripping buffer containing 199.8 mM glycine and 3.46 mM SDS was used (pH: 2.2). Briefly, the membrane was incubated twice with the stripping buffer for 8 minutes each. Afterwards the membrane was washed 3 times for 5 minutes each with TBST. After washing, the membrane was used again for β-actin staining. Membranes were developed using enhanced chemiluminescence (ThermoFisher Scientific, Waltham, MA), and digital images were obtained using an AGFA CP1000 automatic film processor. Relative protein expression values were obtained by dividing the raw values of $BK_{Ca}\alpha$ and IP_3R1 by the raw values of β-actin.

Vascular function studies: Mesenteric resistance arteries (<200μm diameter) were dissected from SHR & SD rats and mounted in a pressure myograph as described previously (Jadeja, Rachakonda, Bagi & Khurana, 2015). 5 mesenteric arteries from each strain were collected from 3 rats of either sex (2 male and 1 female rat of each strain) for use in this experiment. The mounted segment was bathed in standard Krebs solution (in mM): 112 NaCl, 4.7 KCl, 2.2 $CaCl_2$, 1.2 $MgCl_2$, 25 $NaHCO_3$, 1.2 KH_2PO_4, and 14 dextrose. (Saeki, Suzuki, Yamamura, Takeshima & Imaizumi, 2019). To limit the interference from endothelial cells, decision was made to remove the endothelium of the arteries for this experiment. Endothelial denudation was applied by slowly perfusing 5–8 mL of air through the lumen of the vessels, as described previously (Chai, Wang, Zeldin & Lee, 2013). The vessel chamber was then connected to the DMT 110P pressure myograph (DMT-USA, Inc., Ann Arbor, MI) for measurement of

outer vessel diameter with an automated edge detection system (ImagingSource, Germany). The myograph chamber was connected to a 250-mL reservoir of PSS that was bubbled with a 5% CO_2/95% O_2 gas mixture and circulated with the use of a Masterflex pump at a rate of approximately 10 mL/min. The temperature was maintained at 37°C in the bath chamber.

The vessels were pressurized to 60 mm Hg and allowed to equilibrate for 45 to 60 min. Arteries in which an extraluminal application of 60mM KCl and 10μM NE-induced vasoconstriction to >50% of their resting lumen diameter were considered viable (Endemann, Touyz, Li, Deng & Schiffrin, 1999). Confirmation of endothelial removal was evaluated via loss of vasodilatory response to ACh (10μM) in vessels preconstricted with NE (10μM).

With intraluminal pressure maintained at 60 mmHg, arteries were exposed to different concentrations of NE to obtain cumulative concentration-response curves before and after blocking the BK_{Ca} channels with a selective BK_{Ca}-blocker, paxilline (1μM). Vessel outer diameter was quantified using DMT MyoVIEW 2 (DMT-USA, Inc., Ann Arbor, MI) software, and data are expressed as a percent of initial diameter.

Hypertrophy assay: Mesenteric VSM cells were collected from 3 rats of SHR and SD strain of either sex (2 male and 1 female rat of each strain) and cultured. Cells at 3rd passage were seeded in 35mm dishes with glass coverslips and serum-starved for 24 h before treatment after reaching 70% confluency. Cells were stimulated with either the vehicle (PBS), ANG II (1μM) or BK_{Ca} blocker (paxilline, 1μM), and ANG II (1μM). Cells were incubated with paxilline for 30 minutes before the addition of ANG II. After 48 hours of incubation, images of the cells were taken using a brightfield microscope with a 10x objective for the measurement of total cell area. After the brightfield microscope imaging, cells were washed with PBS, fixed with 4% paraformaldehyde, permeabilized with 0.1% Triton X-100 and blocked with 2% BSA for 1 hour at room temperature. Cells were then stained with mouse anti-α-SMA antibody (1:250) in 0.1% BSA at 4^0C overnight and then labeled with goat anti-mouse secondary antibody conjugated to Alexa Fluor 594 (1:500). The nuclei were stained with 1.5 μg/ml 4',6-diamidino-2-phenylindole

(DAPI). Images were then taken with a Carl Zeiss LSM 900 confocal microscope using a 10x objective. Cell area from the brightfield and fluorescent images were measured using the ImageJ software.

Cell proliferation assay: Cellular proliferation of VSM cells was determined using the WST-1 (4-[3-(4-iodophenyl)-2-(4-nitrophenyl)-2H-5-tetrazolio]-1, 3-benzene disulfonate) reagent. Mesenteric VSM cells were collected from 3 rats of SHR and SD strain of either sex (2 male and 1 female rat of each strain) and cultured. Cells at 3rd passage were plated in a 96-well microplate, grown to 70% confluence, and serum-starved for 24 hours. Following preincubation with either vehicle (PBS), or BK_{Ca} channel blocker (paxilline, 1μM), the cells were treated with ANG II (1μM) for 48h. At the end of the exposure period, the medium was replaced with 100 μl of the (1:10 dilution) WST-1 in a fresh medium in each well and incubated for 3h. Absorbance was measured using a multifunctional microplate reader (SpectraMax M5, Molecular Devices) at 440 nm, with a reference wavelength set at 630 nm.

Electrophysiological recordings: BK_{Ca} channel activity in mesenteric VSM cells was recorded in either the whole-cell configuration or from inside-out patches as described previously (Modgil, Guo, O'Rourke & Sun, 2013; Sun et al., 1998). Atleast 3 VSM cells of each strain were used for the patch clamp experiments. The electrophysiological study involving Adenophostin A was conducted on 3 separate occasions using cells freshly isolated from rats of either sex (2 male and 1 female rat of each strain). Results were obtained by averaging the current density produced by 5-10 VSM cells. 1.5-mm borosilicate glass capillaries were used to fabricate patch electrodes and were filled with prefiltered solutions of different compositions. The currents in cell-attached, whole-cell, and inside-out patch-clamp configurations were recorded at room temperature (20°C to 24°C). Axopatch 200B patch-clamp amplifier (Axon Instruments, Burlingame, CA) was used to control voltage-clamp and voltage-pulse generation, and pCLAMP 10.0 software (Molecular Devices, Sunnyvale, CA) was used to collect the current data. Voltage-activated currents were filtered at 1kHz and digitized at 5 kHz, and leakage current

was subtracted digitally. Series resistance and total cell capacitance were obtained by adjusting series resistance and whole-cell capacitance using the Axopatch 200B amplifier control system. Only acutely dispersed, spindle-shaped, relaxed cells were examined for BK_{Ca} currents in the electrophysiological experiments.

For inside-out excised patches, several drops of cell suspension were placed in a 35mm petri dish containing the following (mM): 145 KCl, 1.1 $MgCl_2$, 0.37 $CaCl_2$, 10 HEPES, 1 EGTA, and 10 dextrose; pH 7.4 (KOH). The recording pipettes (resistance 5-6 MΩ) were filled with a solution containing (in mM): 145 KCl, 1.8 $CaCl_2$, $MgCl_2$ 1.1, and 5 HEPES; pH 7.2 (KOH). Free-Ca^{2+} levels on the cytoplasmic face of the membrane were set by adding the calculated ratio of $CaCl_2$ and EGTA (using Chelator 1.0 software, Schoenmakers, Nijmen, The Netherlands). Patches were excised initially in low free-Ca^{2+} of 0.06μM. BK_{Ca} open-state probability (NPO) and unitary amplitudes of single-channel currents were obtained at different membrane potentials between -70mV to +70mV (20-mV steps) in the presence of 0.3, 1, 1.5 or 3μM [Ca^{2+}]. The NPO calculation was performed as described previously (Sun et al., 1998).

For cell-attached patch-clamp recording, several drops of cell suspension were placed in a 35mm petri dish containing the following (mM): 140 NaCl, 5 KCl, 1.2 $CaCl_2$, 10 HEPES, 1 EGTA, and 10 dextrose; pH 7.4 (NaOH). The recording pipettes (resistance 7-8 MΩ) were filled with a solution containing (in mM): 145 KCl, 1.8 $CaCl_2$, $MgCl_2$ 1.1, and 5 HEPES; pH 7.2 (KOH). The recording was performed with a pipette potential of +50 mV.

Whole-cell BK_{Ca} current was recorded using the whole-cell configuration of the voltage-clamp technique. VSM cells were superfused at a rate of 2.0 ml/min with a solution containing (in mM) 145 NaCl, 5.4 KCl, 1.8 $CaCl_2$, 1 $MgCl_2$, 5 HEPES, 10 dextrose; pH 7.4 (NaOH). The recording pipettes had resistances of 3-4 MΩ; and were filled with a solution containing (in mM) 145 KCl, 5 NaCl, 0.37 $CaCl_2$, 2 $MgCl_2$, 10 HEPES, 1 EGTA, 7.5 dextrose; pH 7.2 (KOH). Only cells with tight seals (>3 GΩ) were selected to break in. For the whole-cell patch-clamp experiment

involving 5-HT, cells were held at −60 mV, and 100-millisecond depolarizing step pulses of 10 mV increments from −20 to +80 mV voltages were applied. For the whole-cell patch-clamp experiment involving Adenophostin A, cells were held at −60 mV, and 100-millisecond depolarizing step pulses of 20 mV increments from −40 to +80 mV voltages were applied. current was divided by the capacitance and expressed as current density.

Calculations and statistical analysis: Statistical analysis was performed using GraphPad Prism version 8.0.0 for Windows (San Diego, CA). Statistical differences between the experimental groups were analyzed using Student's t test or one-way ANOVA followed by Dunnett's or Tukey's post hoc test for multiple comparisons, where appropriate. Statistical significance was established at a minimum of $P \leq 0.05$. All values were expressed as means ± SE. Analysis of Ca^{2+} signals from Ca^{2+} imaging was completed using ImageJ—FIJI software. For whole-cell current amplitude at a given test potential, the peak current was measured using a peak detection routine in pClamp 10 software to generate the current-voltage relationship. Densitometric analysis of the western blot signals was performed using ImageJ software.

Results

SHRs have significantly higher mean arterial pressure compared to normotensive SD rats: Mean arterial pressure (MAP) of 4–6-month-old SHR recorded using the non-invasive tail-cuff method was significantly higher than the age-matched normotensive SD rat (Figure 8). Both male and female of SHR had significantly higher MAP compared to their counterpart of the SD strain. The average MAP of male SHR was 54.75% higher than that of male SD rat (Average MAP was 167.13±9.49 mmHg for male SHR and 108.1±7.88 mmHg for male SD), while the average MAP of female SHR was 45.51% higher than that of female SD rat (Average MAP was 148.56±2.92 mmHg for female SHR and 102.1±5.72 mmHg for female SD). No significant difference in MAP between male and female SD rats was found; however, male SHR had significantly higher MAP compared to female SHR. The average MAP of male SHR was ~11.1% higher than average female SHR MAP (Average MAP was 167.13±9.49 mmHg for male

SHR and 148.56±2.92 mmHg for female SHR). The reason behind male SHR's significantly higher blood pressure has been attributed to sex hormones, as testosterone is known to regulate the sympathetic nervous system, renin-angiotensin system (RAS), and nitric oxide bioavailability (Elmarakby & Sullivan, 2021).

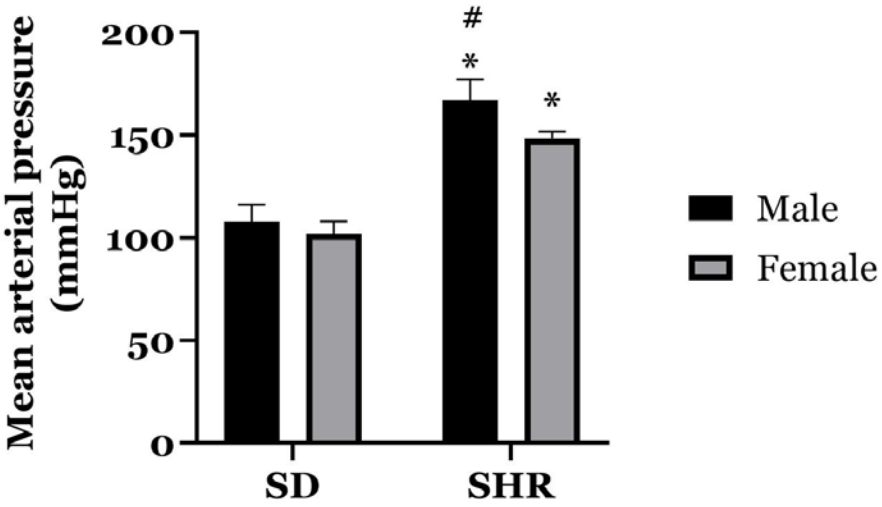

Figure 8. Mean arterial pressure of SD and SHR of both sexes. Systolic and diastolic blood pressure in 4–6-month-old rats were measured by the tail-cuff method. Data are expressed as mean ± SEM (n= 8-10 rats). * $p < 0.05$ as compared with SD of the same sex. # $p < 0.05$ as compared with female SHR.

Cultured VSM cells are of mature contractile smooth muscle cell phenotype:

Two commonly used marker proteins were chosen to detect mature contractile smooth muscle cell phenotype, α-smooth muscle actin (α-SMA) and smoothelin. The immunostaining experiment revealed that the cultured SD and SHR mesenteric VSM cells expressed both α-SMA and smoothelin (Figure 9). This result proves that not only the cultured cells are VSM cells, but they also have the contractile VSM cell phenotype needed for this study.

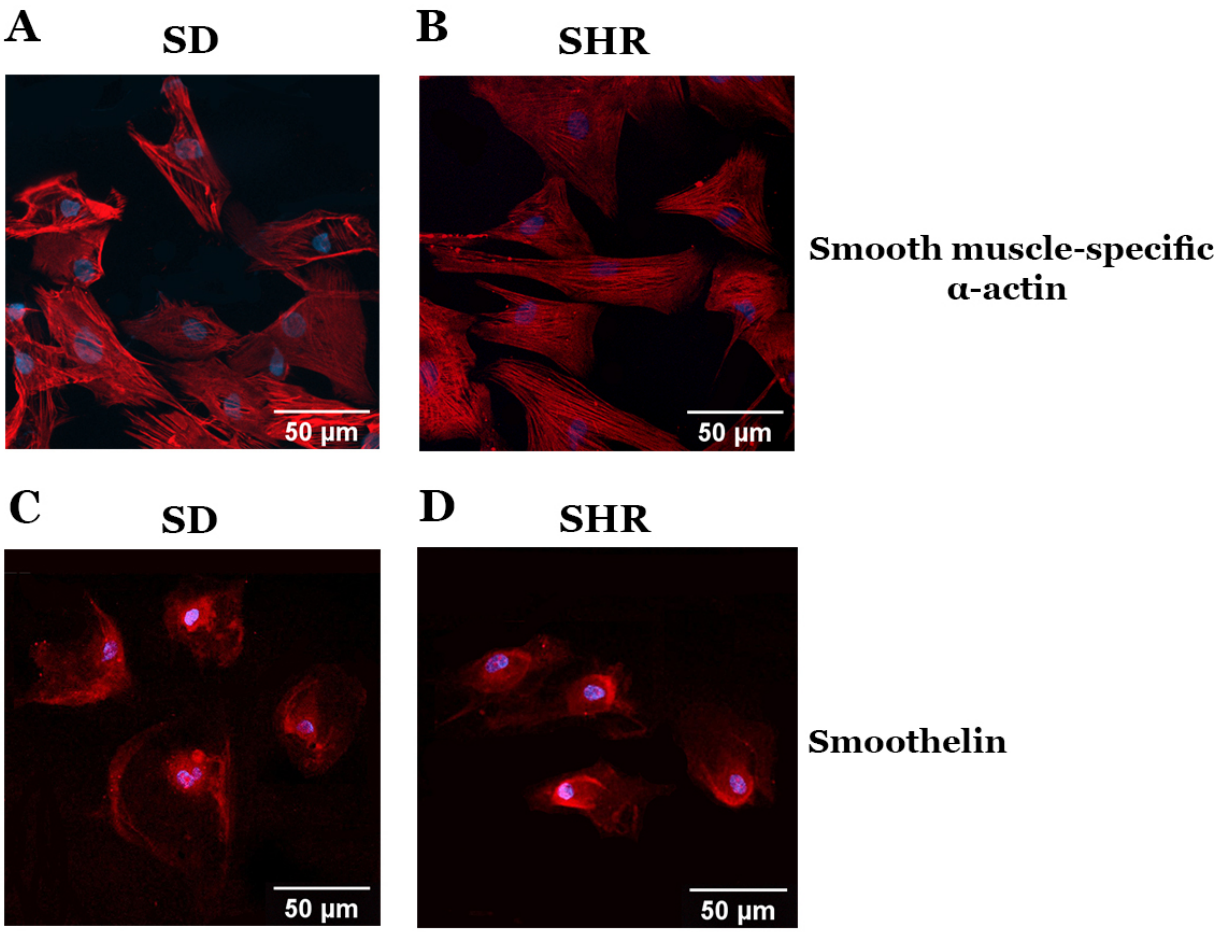

Figure 9. Cultured VSM cell identification: immunofluorescence demonstration of the expression of smooth muscle-specific markers in the culture of VSM cells. Smooth muscle-specific α-actin staining in SD (A) and SHR (B). Smoothelin staining in SD (C) and SHR (D).

Ca^{2+}- and voltage-sensitivity of BK_{Ca} channels are not significantly different between SHR and SD rats: The inside-out patch configuration of patch-clamp was used to examine the possibility that the Ca^{2+}- and voltage-sensitivity of BK_{Ca} channels may be reduced in VSM cells of SHR compared to SD. At <3µM [Ca^{2+}], channels were mainly observed at large test potentials of 50 and 70mV. Raising the [Ca^{2+}] to 3µM lowered the threshold of activation to less positive (+10 and +30mV) and negative test potentials (Figure 11). Figure 10A shows that the unitary amplitudes of single-channel currents obtained at different membrane potentials between -70mV to +70mV (20-mV steps) in the presence of 3µM [Ca^{2+}], were similar for inside-out patches from SD and SHR VSM cells.

The resulting current-voltage relationship in Figure 10A, generated by plotting unitary current amplitude as a function of membrane potential, indicated single-channel conductance of 210 pS (SD) and 211 pS (SHR). Figure 10C shows that BK_{Ca} open probability (NP_O) between SD and SHR VSM cells at different positive membrane voltages in the presence of 1μM $[Ca^{2+}]$ is not significantly different. Figure 11A and 11B illustrate the relationship between BK_{Ca} activity and $[Ca^{2+}]$ at four different $[Ca^{2+}]$ levels in VSM cells from SD and SHR, respectively. NP_O was calculated from 5-minute recordings obtained at +70mV membrane potential in $[Ca^{2+}]$ of 0.3, 1, 1.5 or 3μM (Figure 11C). NP_O values were similar under identical conditions of voltage and $[Ca^{2+}]$ for BK_{Ca} channels in SHR and SD patches, providing no evidence for altered Ca^{2+}- or voltage-sensitivity sensitivity of BK_{Ca} channels in SHR.

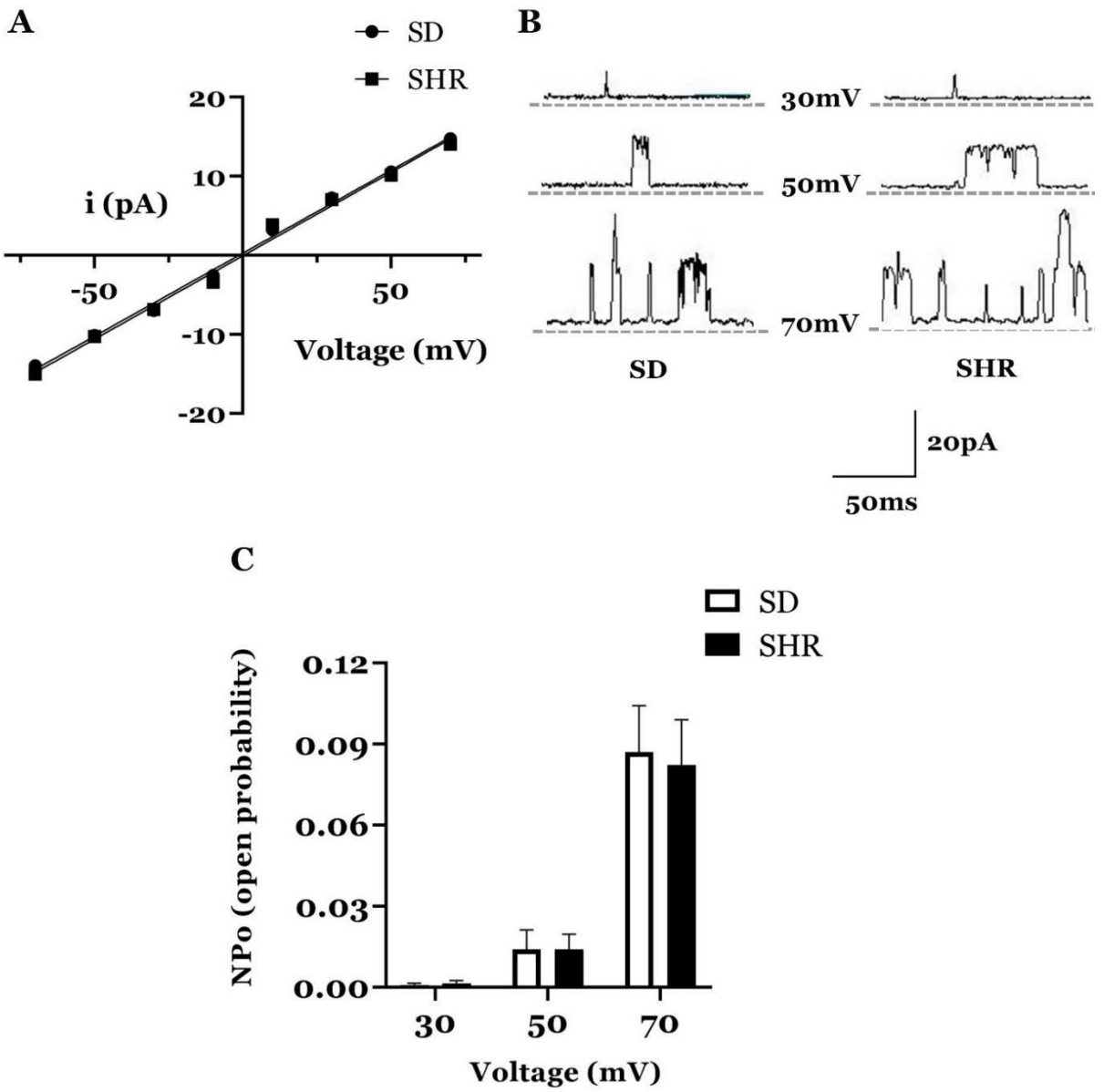

Figure 10. Effects of voltage on the activity of BK_{Ca} channels recorded from inside-out patches of SHR and SD rat mesenteric arterial VSM cells. A: A summary of the i-v relationship for SHR and SD BK_{Ca} channels in 3μM Ca^{2+}, representing data (mean±SEM) from 6 patches in symmetrical (145mM) K^+ solutions. B: Records of unitary currents in the presence of 1μM Ca^{2+} at 30, 50 and 70mV in symmetrical [K^+]. C: Bar graph summarizing the effect of voltage on BK_{Ca} open probability (NP_o) in 1μM Ca^{2+} (n= 6 patches). Values are mean±SEM.

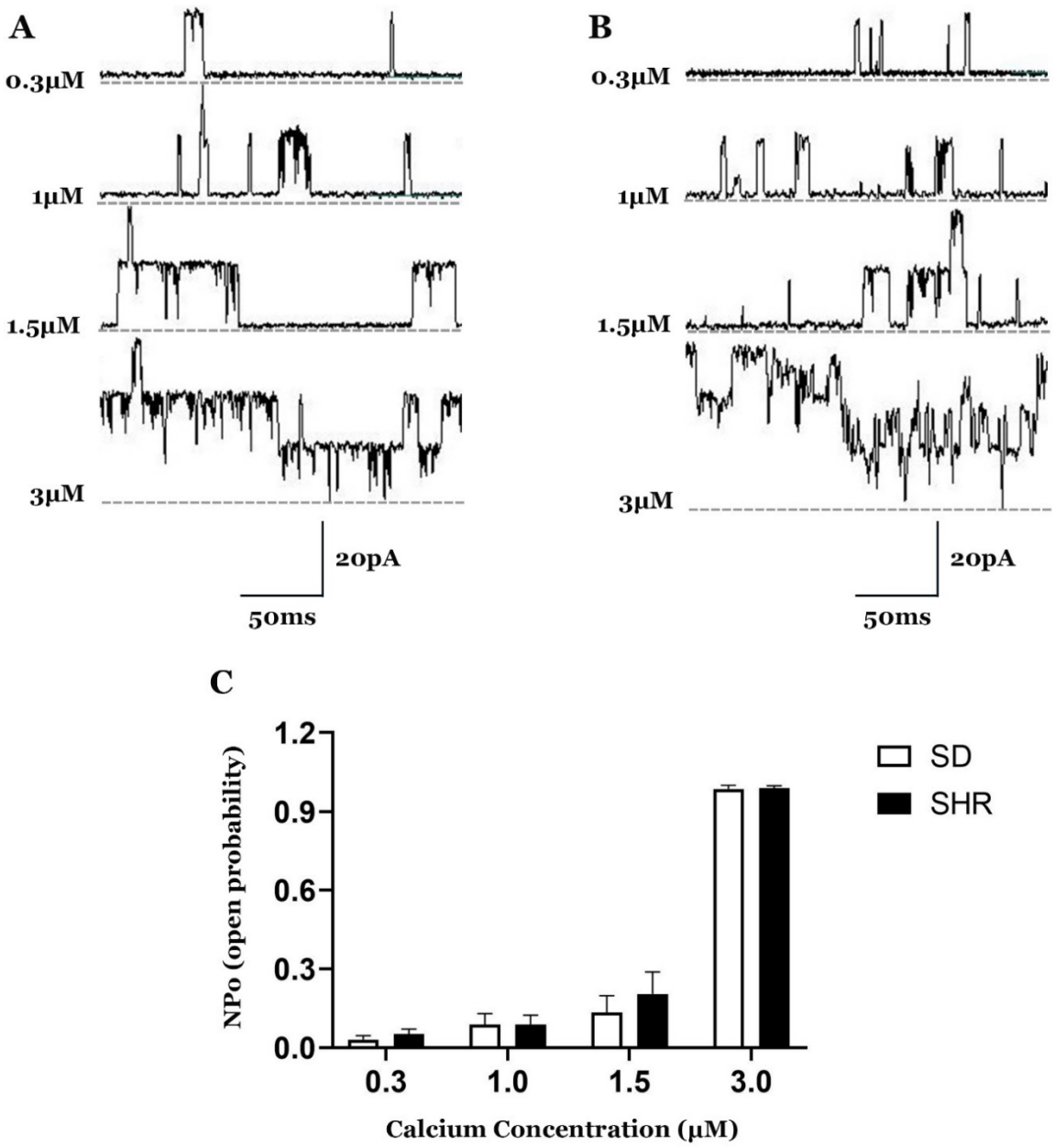

Figure 11. Effects of Ca^{2+} on the activity of BK_{Ca} channels recorded from inside-out patches of SHR and SD rat mesenteric arterial VSM cells. A-B: Records of unitary currents at +70mV in the presence of 0.3, 1, 1.5 and 3µM Ca^{2+} in symmetrical $[K^+]$ for SD (A) and SHR (B). C: Bar graph summarizing the effect of calcium on BK_{Ca} open probability (NPo) at +70mV (n= 6 patches). Values are mean±SEM.

Intracellular Ca^{2+} transients are significantly larger in SHR compared to SD:

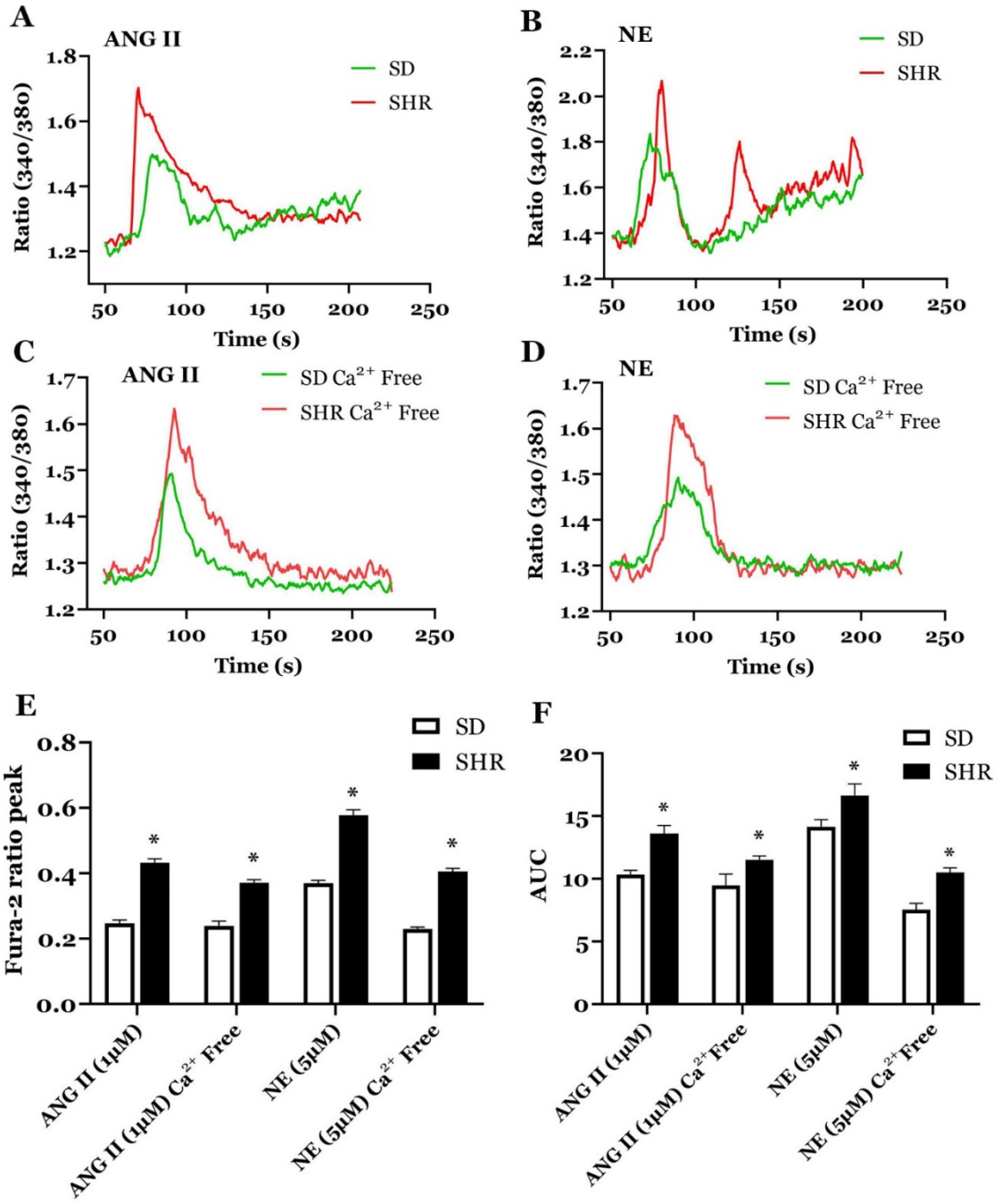

Figure 12. Difference in intracellular Ca^{2+} transients between SD and SHR rats. A-B: Representative examples of intracellular Ca2 + transients recorded from fura 2/AM-loaded VSM cells in response to 1μM ANG II (A) or 5μM NE (B). C-D: Representative examples of intracellular Ca^{2+} transients recorded from fura 2/AM-loaded VSM cells in response to 1μM ANG II (C) or 5μM NE in Ca^{2+}-free HBSS (D). E-F: Bar graphs summarizing the peak and area under the curve (AUC) above baseline of intracellular Ca^{2+} transients. Values are mean±SEM (n=10 transients in total from cells isolated from 2 male and 1 female rat of each strain). *P<0.05 indicates a significant difference from the corresponding SD value.

To examine the amplitude and area of the Ca^{2+} transients in SD and SHR VSM cells, confocal microscopy was used in VSM cells loaded with Fura-2 AM (4μM). Cells were exposed to either 1μM ANG II or 5μM NE, which are known to stimulate the production of IP_3 in VSM cells. $[Ca^{2+}]_i$ response after their application was evaluated using 340/380 nm excitation ratio for fura-2. Both ANG II and NE application triggered Ca^{2+} transients in VSM cells in HBSS containing 1.3mM Ca^{2+}. Ca^{2+} transients in SHR VSM cells had significantly higher peaks and area under the curve compared to VSM cells from SD rats (Figure 12E & 12F). Representative traces of $[Ca^{2+}]_i$ response to ANG II and NE in both SD and SHR VSM cells are shown in Figure 12A and 12B, respectively. To examine Ca^{2+} transients generated by Ca^{2+} released from intracellular Ca^{2+} stores only, cells were bathed in Ca^{2+}-free HBSS and then exposed to ANGII or NE. Even in Ca^{2+}-free environment, Ca^{2+} transients produced in SHR VSM cells were significantly larger than SD for both ANGII and NE (Figure 12E & 12F). Representative traces of $[Ca^{2+}]_i$ response in Ca^{2+}-free HBSS to ANG II and NE in both SD and SHR VSM cells are shown in Figure 12C & 12D respectively. The result from this experiment provides evidence towards smaller Ca^{2+} transients not being a factor behind reduced BK_{Ca} activation in response to IP_3-induced SR Ca^{2+} release in SHR.

$BK_{Ca}\alpha$ and IP_3R1 expression in SHR VSM cells is not significantly different compared to SD: Western blot analysis was performed to examine the expression of $BK_{Ca}\alpha$ and IP_3R1 in SD and SHR mesenteric VSM cells. Relative protein expression values were obtained by dividing the raw values of $BK_{Ca}\alpha$ and IP_3R by the raw values of loading control, β-actin. In this experiment, $BK_{Ca}\alpha$ and IP_3R1 expression levels were not significantly different between SD and SHR mesenteric arteries. Representative blots showing expression of $BK_{Ca}\alpha$ (~110 kDa) and IP_3R1(~240 kDa) in SD and SHR VSM cells are shown in Figure 13A and 13B, respectively. Bar graphs summarizing the relative quantification of $BK_{Ca}\alpha$ and IP_3R1 in SD and SHR VSM cells are shown in Figure 13C and 14D respectively. Data from this experiment

indicate that reduced $BK_{Ca}\alpha$ and IP_3R1 expression in SHR is not a factor behind reduced BK_{Ca} activation in response to IP_3-induced SR Ca^{2+} release.

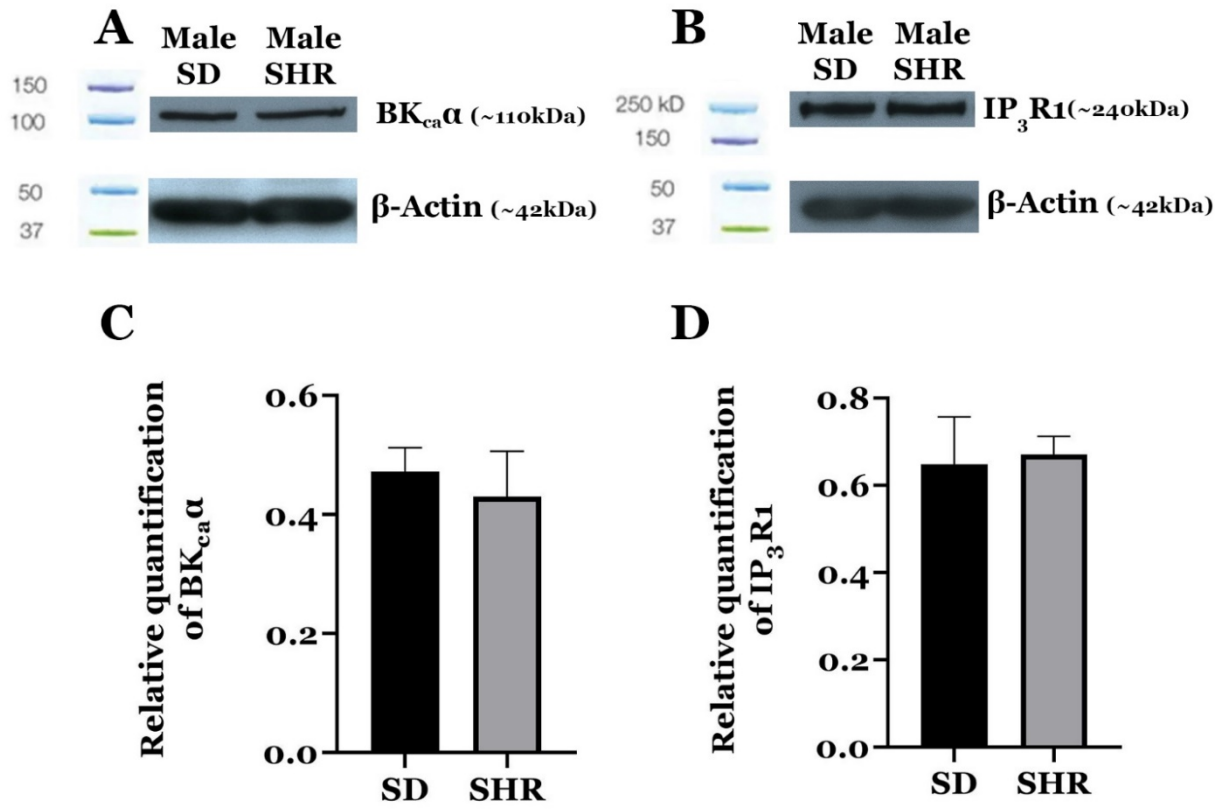

Figure 13. Expression of $BK_{Ca}\alpha$ and IP_3R1 in SD and SHR mesenteric VSM cells. A-B: Representative blots showing expression of $BK_{Ca}\alpha$ (~110 kDa) and IP_3R1(~240 kDa) in small mesenteric arteries dissected from SHR and SD rats. C-D: Bar graph summarizing the relative quantification of $BK_{Ca}\alpha$ and IP_3R1 in small mesenteric arteries dissected from SHR and SD rats (n= 3 rats). Values are mean±SEM.

The expression of $BK_{Ca}\alpha$ and IP_3R1 between male and female SHR mesenteric VSM cells was also compared. The results indicated that $BK_{Ca}\alpha$ and IP_3R1 expression levels were not significantly different between SD and SHR mesenteric arteries. Representative blots showing expression of $BK_{Ca}\alpha$ (~110 kDa) and IP_3R1(~240 kDa) in male and female SHR VSM cells are shown in Figure 14A and 14B, respectively. Bar graphs summarizing the relative quantification of $BK_{Ca}\alpha$ and IP_3R1 in male and female SHR VSM cells are shown in Figure 14C and 14D, respectively.

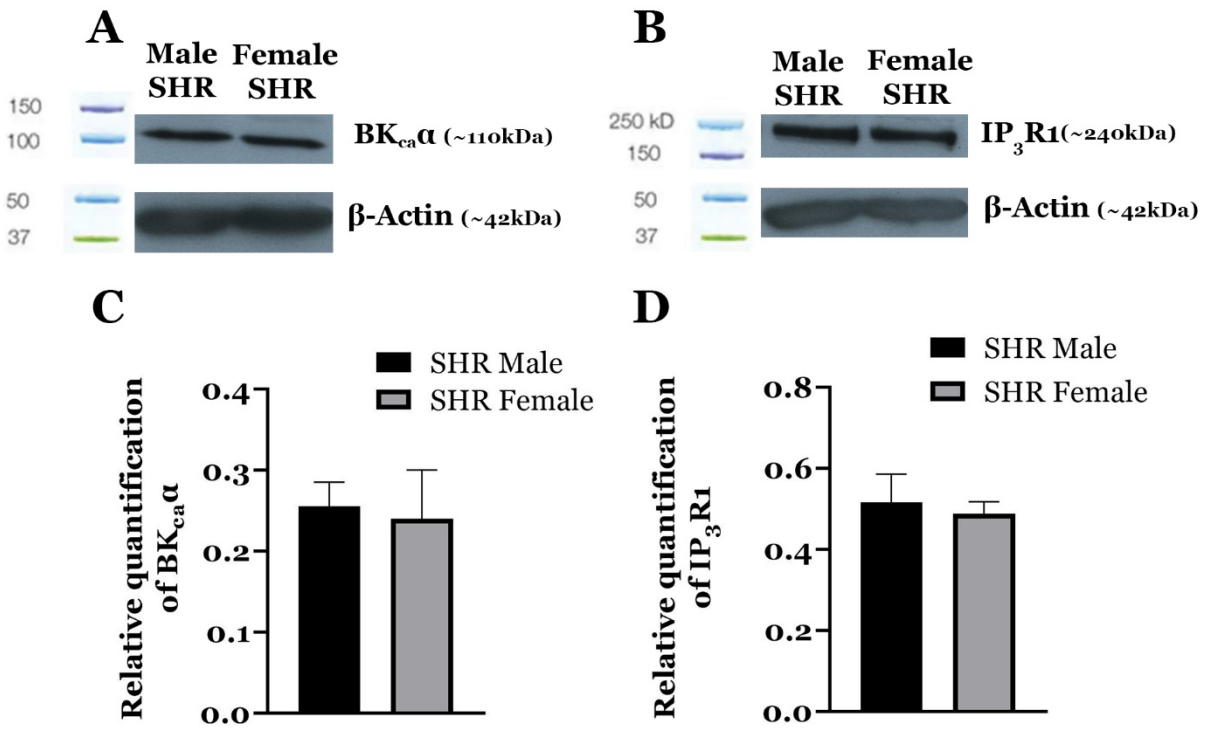

Figure 14. Comparison of $BK_{Ca}\alpha$ and IP_3R1 expression between male and female SHR mesenteric VSM cells. A-B: Representative blots showing expression of $BK_{Ca}\alpha$ (~110 kDa) and IP_3R1(~240 kDa) in male and female SHR mesenteric arteries. C-D: Bar graph summarizing the relative quantification of $BK_{Ca}\alpha$ and IP_3R1 (n= 3 rats). Values are mean±SEM.

BK_{Ca} channel inhibition failed to increase norepinephrine-induced vasoconstriction in SHR: Norepinephrine (NE) activates α1-adrenergic receptors in vascular smooth muscle cells and causes vasoconstriction by releasing Ca^{2+} from the SR through the PLC-IP_3 pathway (Exton, 1985). BK_{Ca} channel currents activated by Ca^{2+} released from the SR oppose the magnitude and duration of vasoconstriction (Wu & Marx, 2010). The hypothesis was that BK_{Ca} channel activation is significantly lower in response to IP_3-induced Ca^{2+} release in hypertension due to the loss of BK_{Ca}-IP_3R functional coupling. If BK_{Ca}-IP_3R functional coupling is missing in SHR mesenteric VSM cells, then the BK_{Ca} channel blockade will have minimal effect on NE-induced vasoconstriction in SHR. The possibility was investigated in an ex-vivo pressure myography experiment using endothelium-denuded mesenteric arteries.

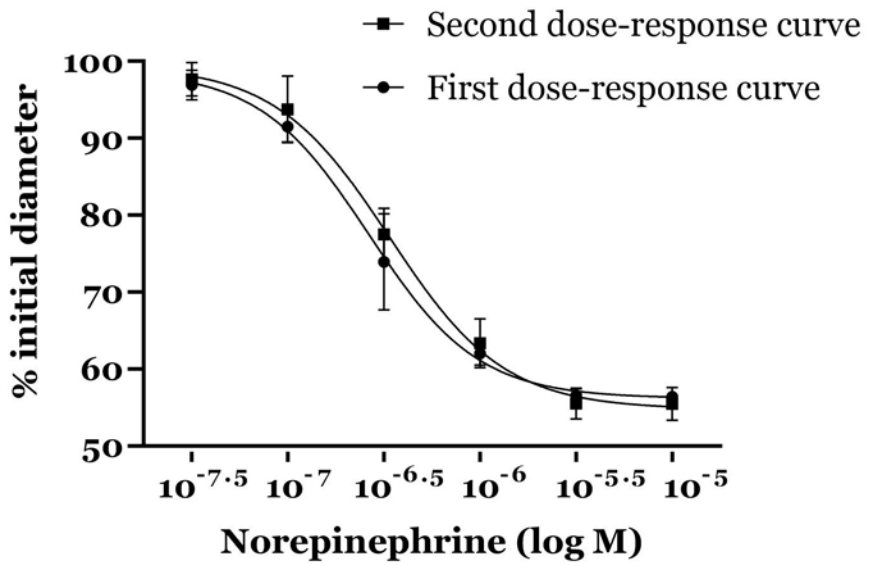

Figure 15. Evaluation of NE sensitization after repeated NE administration. Effect of NE ($10^{-7.5}$ – 10^{-5}M)-induced vasoconstriction compared between two dose-response relationships establish 30 minutes apart. N=3 arteries.

As part of the preliminary study, the possibility of mesenteric artery developing NE sensitization upon repeated NE administration was investigated. Single mesenteric artery isolated from 3 male SD rats each was mounted in myograph chamber and exposed to increasing concentrations of NE ($10^{-7.5}$ – 10^{-5}M). 2 dose-response curves were established 30 minutes apart. The arteries did not show any significant difference in NE-induced vasoconstriction between the 2 dose response curves. The result from this study is displayed in Figure 15.

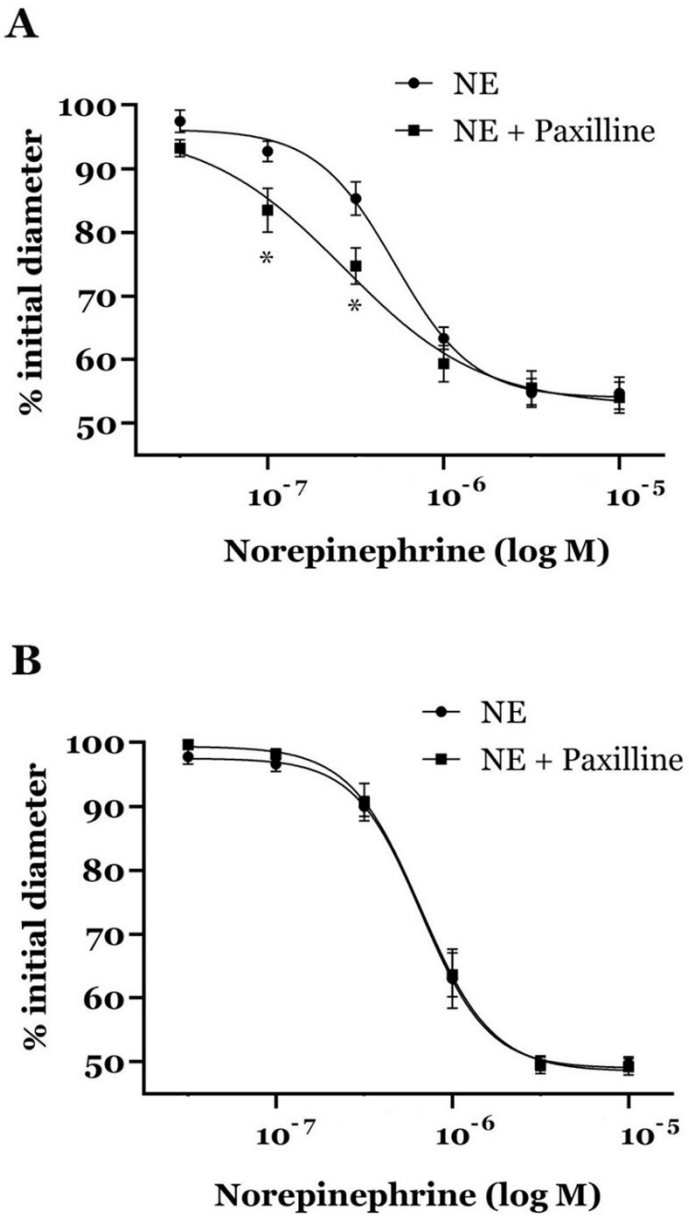

Figure 16. Effect of BK_{Ca} block on NE ($10^{-7.5}$ – 10^{-5}M)-induced vasoconstriction. A-B: NE concentration-%initial outer diameter relationship in SD (A) and SHR (B) arteries before and after incubation with paxilline (1μM). Values are mean±SEM (n=5 arteries). *P<0.05 indicates a significant difference from NE.

The outer diameter of the NE-treated arteries before and after the BK_{Ca} channel block with 1μM paxilline at intraluminal pressure of 60mmHg was measured (Figure 16A & 16B). Paxilline significantly increased norepinephrine-induced vasoconstriction in SD arteries (n=5) by ~10% (% initial diameter from 92.75±1.63 to 83.48±3.42) and ~12.5% (% initial diameter

from 85.31±2.62 to 74.71±2.85) at negative log molar concentrations, 10^{-7} and $10^{-6.5}$ respectively. Contrastingly, paxilline failed to significantly increase NE-induced vasoconstriction at any given NE concentration in SHR. From this result, it can be suggested that the loss of BK_{Ca}-IP_3 functional coupling reduced the contribution of K^+-efflux in opposing NE-induced vasoconstriction and, thus, reduced the effect of BK_{Ca} channel block in response to NE in SHR.

BK_{Ca} channel inhibition had no effect on ANG II-induced cellular hypertrophy and proliferation in SHR: Ang II-induced Gαq signaling increases $[Ca^{2+}]_i$ through stimulation of IP_3 production, which in turn activates calcineurin (CN)–NFAT and Ca^{2+}/Calmodulin–Dependent Protein Kinase II pathway to promote vascular hypertrophy and hyperplasia (Seo, Parikh & Ashley, 2020; Muthalif et al., 2002). BK_{Ca} channels can prevent excessive $[Ca^{2+}]_i$ through outward hyperpolarizing K^+ currents (Bentzen, Olesen, Rønn & Grunnet, 2014). To investigate the impact of BK_{Ca} channel block on ANG II-induced VSM cell hypertrophy and proliferation, cultured VSM cells were stimulated with Ang II (1μM) in the presence or absence of BK_{Ca} blocker, Paxilline (1μM). Both α-smooth muscle actin area and total cell area was measured to determine hypertrophic effects. ANG II significantly increased both α-smooth muscle actin area and VSM cell area in both SHR and SD rats compared to control (Figure 17G and 17H).

Paxilline treatment significantly augmented the hypertrophic effect of ANG II in SD, where α-smooth muscle actin area and total cell area of Paxilline treated ANG II group was ~15% (from 2493.31±106.85 to 2877.39±132.51μm^2, Figure 17G) and ~11% (from 3471.48±121.35 to 3854.86±129.99μm^2, Figure 17H) greater respectively, compared to the non-paxilline-treated ANG II group. The paxilline-induced increase in hypertrophic response was absent in SHR, pointing to a lack of BK_{Ca} activity after ANG II-induced increase in $[Ca^{2+}]_i$.

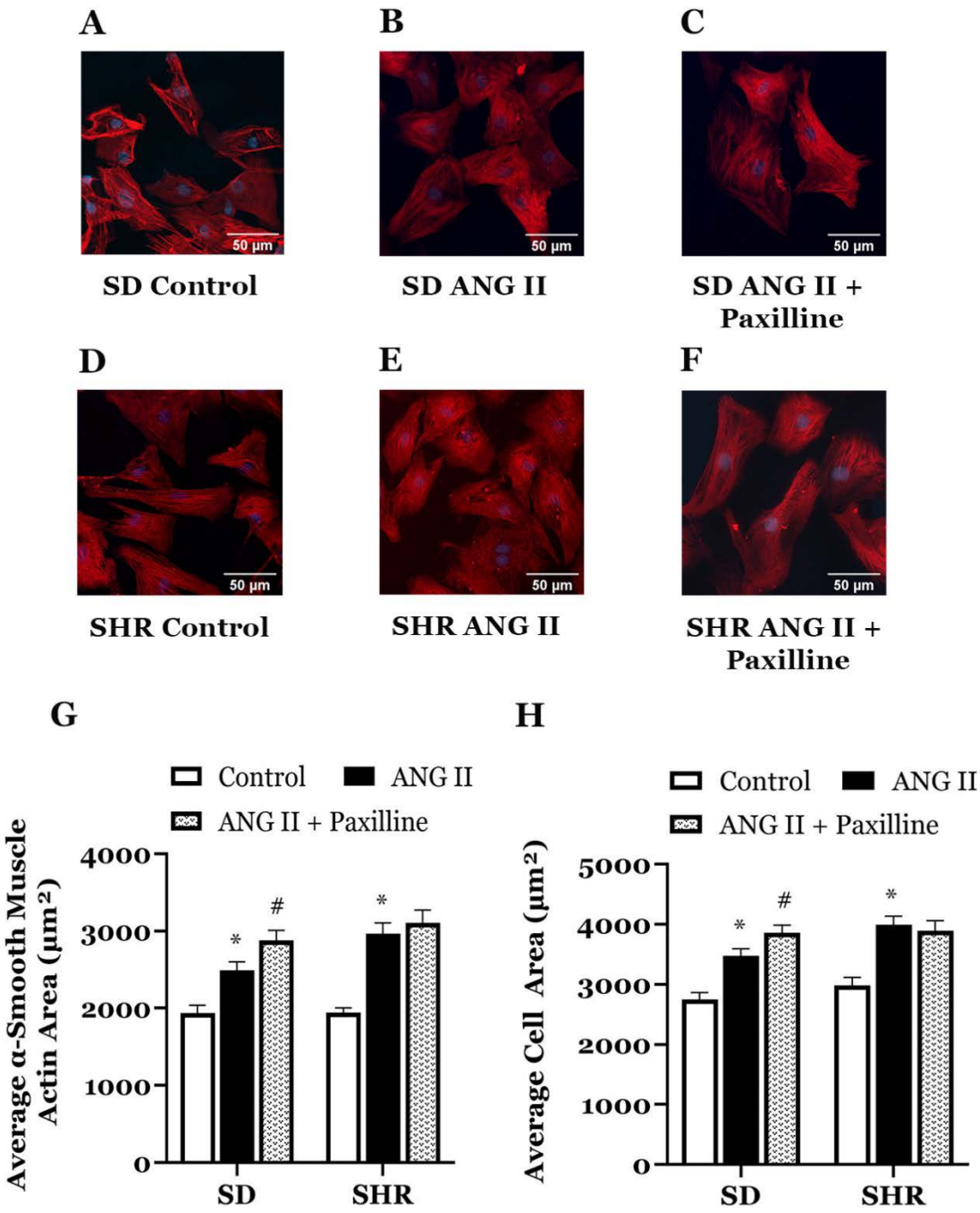

Figure 17. Effect of BK_{Ca} block on ANG II-induced hypertrophy in SHR and SD VSM cells. A-F: Immunofluorescence demonstration of the expression of smooth muscle-specific α-actin in the culture of VSM cells from SD (A-C) and SHR (D-F). Treatments include vehicle (A=SD, D=SHR, n= 87-94 cells), ANG II (1µM) (B=SD, E=SHR, n= 110-138 cells) or BK_{Ca} channel blocker (Paxilline, 1µM) + ANG II (C=SD, F=SHR, n = 85-137 cells). G: Bar graph summarizing the effect of paxilline (1µM) on ANG II-induced increase in average α-smooth muscle actin area. H: Bar graph summarizing the effect of paxilline (1µM) on ANG II-induced increase in average cell area measured from brightfield images (n= 88-122 cells). Values are mean±SEM. *$P<0.05$ indicates a significant difference from the control of the same strain. #$P<0.05$ indicates a significant difference from the ANG II group of the same strain.

Similarly, in WST-1 cell proliferation assay, ANG II significantly increased the proliferation of the cultured cells from SHR, and SD rats compared with the control (Figure 18). Paxilline treatment significantly increased ANG II-induced proliferation in SD by ~15% ($Absorbance_{(A440nm-A630nm)}$ from 0.15±0.01 to 0.17±0.01) while having no effect on cell proliferation in SHR (Figure 18).

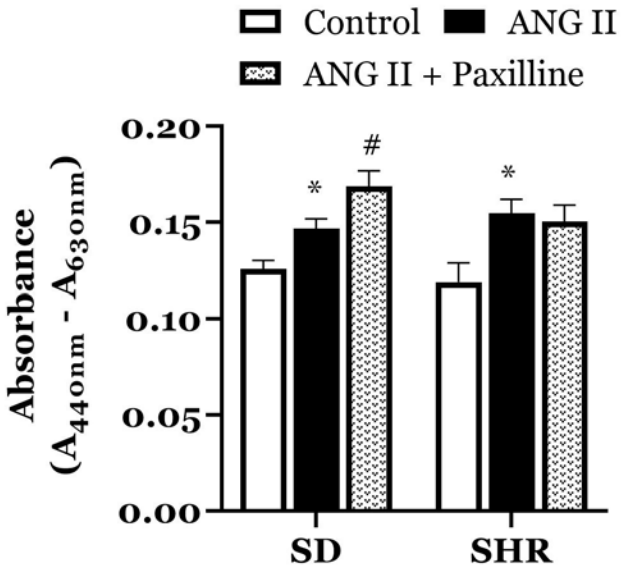

Figure 18. Effect of BK_{Ca} block on ANG II-induced proliferation in SHR and SD VSM cells. Bar graph summarizing the effect of paxilline (1μM) on ANG II-induced VSM cell proliferation in SHR and SD rats (n= 8 wells). Values are mean±SEM. *P<0.05 indicates a significant difference from the control of the same strain. #P<0.05 indicates a significant difference from the ANG II group of the same strain.

BK_{Ca} channel activation is significantly lower in SHR in response to SR Ca^{2+} release: The effect of SR Ca^{2+} released through IP_3Rs on BK_{Ca} channel activity was determined in VSM cells freshly isolated from rat mesenteric artery. Whole-cell BK_{Ca} currents were recorded in response to successive voltage pulses of 100ms duration, increasing in 20-mV increments from -40mV to +80mV in the absence or presence of 5-HT or a selective IP_3 receptor agonist, Adenophostin A. 5-HT binds to Gq/phospholipase C-coupled receptors and stimulate the production of IP_3 in VSM cells (Exton, 1985; Alexander, et al., 1985; Nagahama et al., 2000).

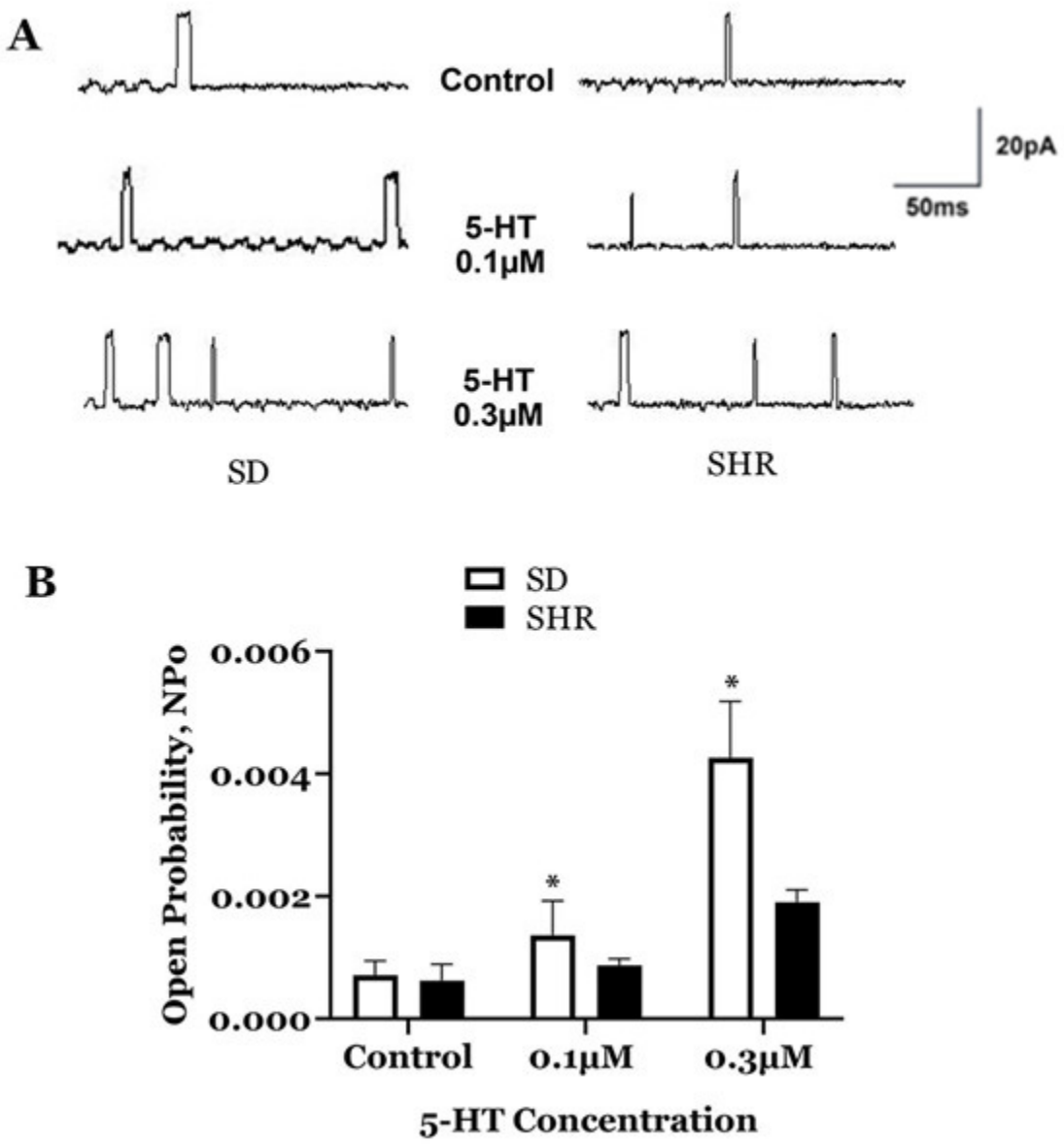

Figure 19. Effect of vasoconstrictor, 5-HT on the activity of BK_{Ca} channels recorded from cell-attached patches of rat mesenteric arterial VSM cells. Currents were recorded at room temperature with a pipette potential of +50 mV. A: Representative tracings showing the large-conductance K^+ channel currents recorded from cell-attached patches of VSM cells. B: Bar graph summarizing the open state probability (NPo) of BK_{Ca} channels during each treatment condition described above. *$P<0.05$ indicates a significant difference from the corresponding SHR value. Values presented are mean±SEM recorded from 4-5 cells.

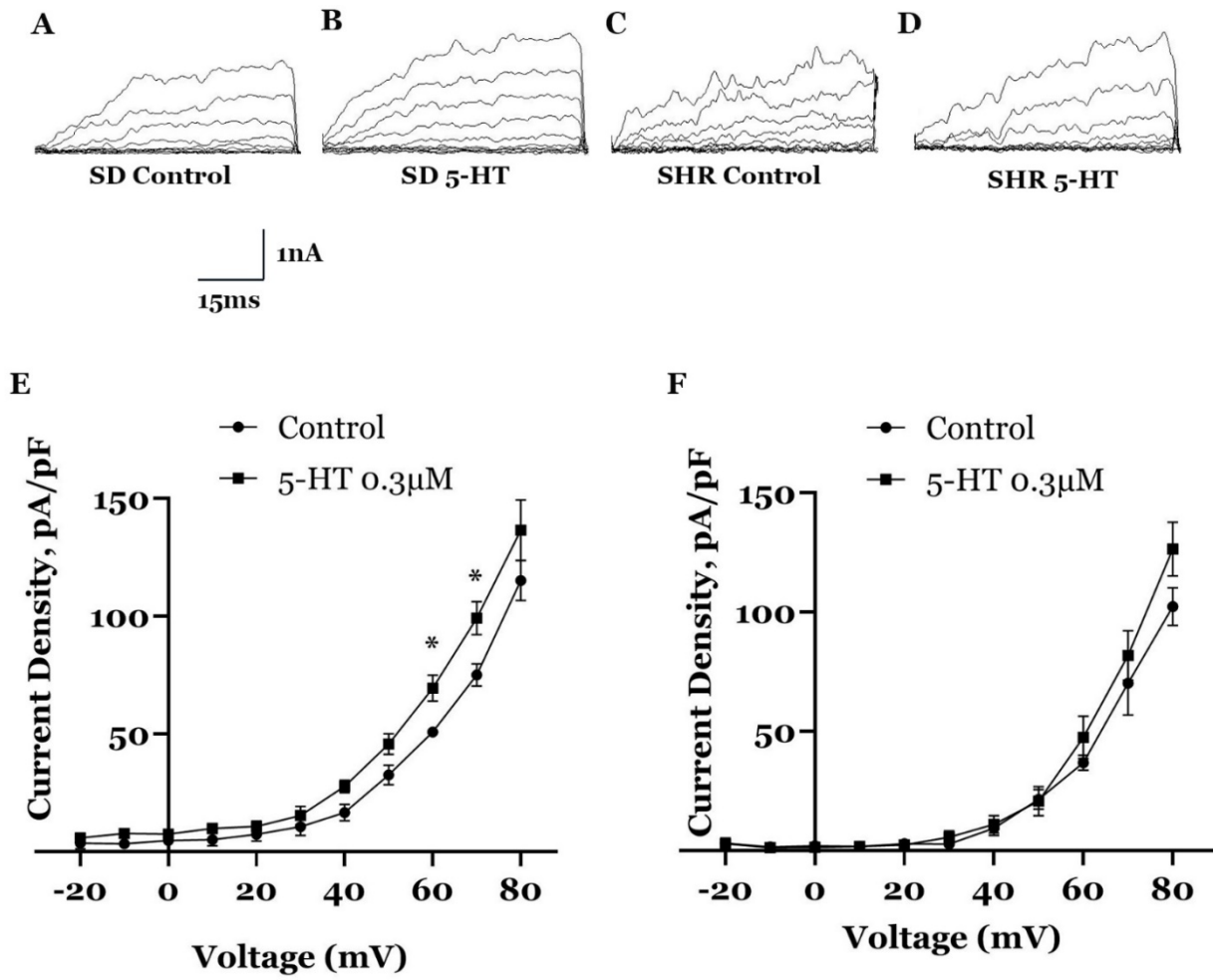

Figure 20. Effect of vasoconstrictor, 5-HT on the activity of large-conductance Ca^{2+}-activated K^+ (BK_{Ca}) channels of rat mesenteric arterial VSM cells. Whole-cell K^+ currents were recorded at room temperature in response to successive voltage pulses of 50ms duration, increasing in 10-mV increments from -20 mV to +80 mV before and after the treatment of 5-HT (0.3μM). A-D: representative tracings depicting the currents recorded from a single VSM cell before and after treatment with 5-HT (0.3μM, 5 min). E: I-V curve plots of BK_{Ca} currents in SD VSM cells at baseline and after application of 5-HT (0.3μM, 5 min). F: I-V curve plots of BK_{Ca} currents in SHR VSM cells at baseline and after application of 5-HT (0.3μM, 5 min). Values are mean±SEM (n=3 cells). *$P<0.05$ indicates a significant difference from the corresponding control value.

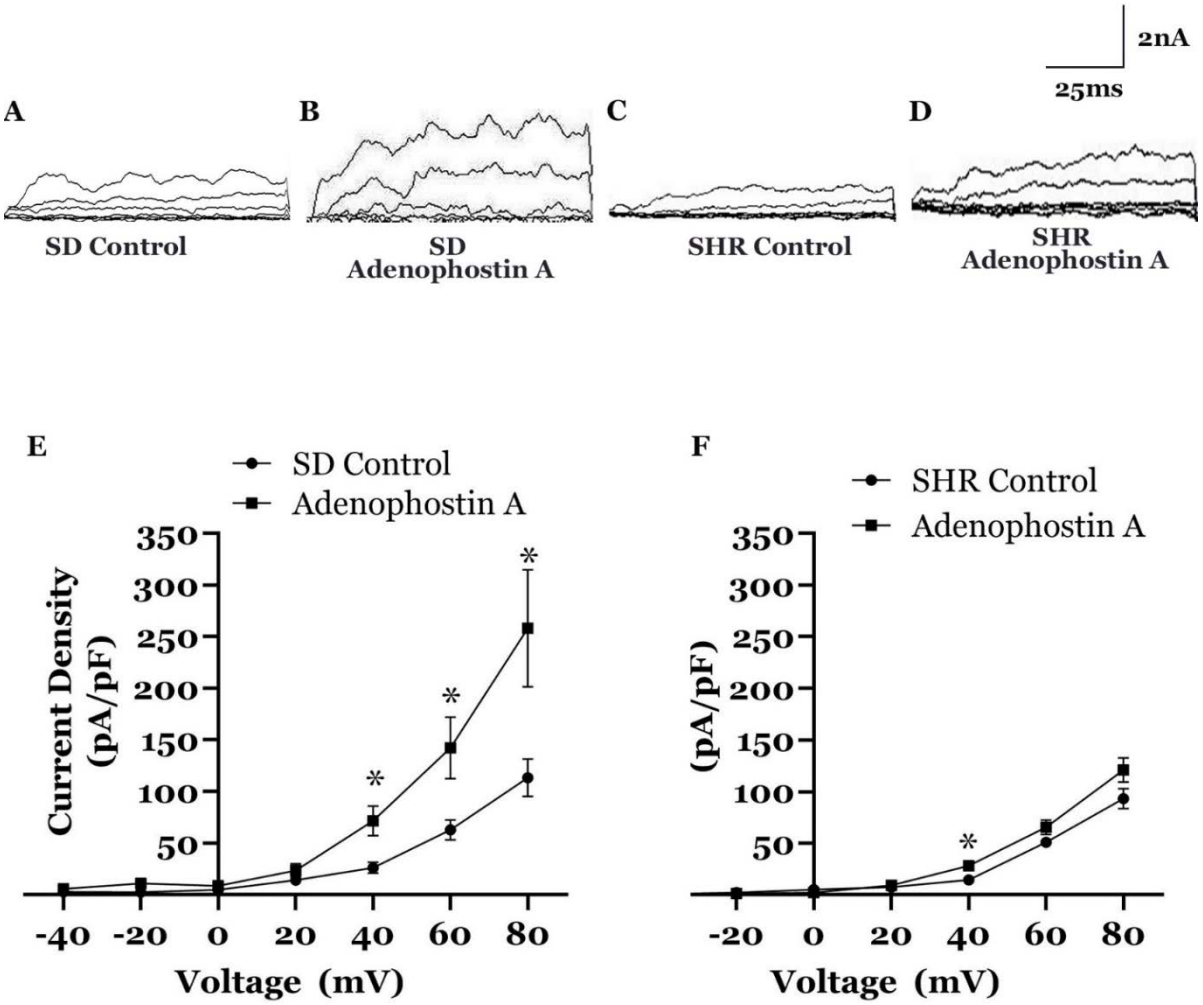

Figure 21. Effect of Adenophostin A on activity of large conductance Ca^{2+}-activated K^+ (BK_{Ca}) channels of rat mesenteric arterial VSM cells from SHR and SD rats. Whole-cell K^+ currents were recorded at room temperature in response to successive voltage pulses of 100ms duration, increasing in 20-mV increments from -40mV to +80mV before and after the treatment Adenophostin A (5μM). A-D: representative tracings depicting the currents recorded from a single VSM cell before and after treatment with Adenophostin A (5μM, 5 min). E-F: i-v curve plots of SD (E) and SHR (F) BK_{Ca} currents at baseline and after application of Adenophostin A (5μM, 5 min). Values are mean±SEM (n=5 -10 cells). *P<0.05 indicates a significant difference from the corresponding control value.

Data from the cell-attached patch-clamp experiment revealed that the open probability (NPo) of a single BK_{Ca} channel was significantly higher in VSM cells of SD rats than SHR in response to 0.1μM and 0.3μM 5-HT (Figure 19B). Similarly, in the whole-cell patch-clamp, the BK_{Ca} current density was significantly lower (by 18.62 pA/pF) in mesenteric VSM cells of SHR compared to SD at +60mV in response to bath application of 0.3μM 5-HT (Figure 20).

When the VSM cells were treated with Adenophostin A, BK_{Ca} current density at +60mV significantly increased in SD VSM cells from 62.84±9.60 pA/pF to 142.30±29.98 pA/pF (n=5 cells, $p<0.05$; Figure 21E), while in SHR VSM cells, the increase in BK_{Ca} current density was significantly lower (from 50.87±3.20 pA/pF to 65.62±7.14 pA/pF, n= 6 cells; Figure 21F) compared to SD. These results demonstrate that BK_{Ca} channel activation in hypertensive rats is lower than in normotensive rats in response to SR Ca^{2+} release through IP_3Rs.

No significant difference in BK_{Ca} channel activity between SD and WKY: Sprague-Dawley (SD) was chosen as the normotensive rat model. But WKY (Wister-Kyoto) rats are regarded as the most suitable control group for studying SHR rats (Huang, Wu & Peng, 2016). To justify the choice of picking SD as the normotensive control, whole-cell patch-clamp was performed in WKY mesenteric VSM cells to examine the increase in BK_{Ca} current density in response to the administration of selective IP_3R- agonist, Adenophostin A. If the result is comparable to SD, it can be assumed that the BK_{Ca}-IP_3R coupling integrity is comparable between SD and WKY.

The effect of selective IP_3R activation on BK_{Ca} channel activity was compared between freshly isolated SD and WKY rat VSM cells. Whole-cell BK_{Ca} currents were recorded in response to successive voltage pulses of 100ms duration, increasing in 20-mV increments from -40mV to +80mV in the absence or presence of Adenophostin A. BK_{Ca} current density increased significantly in both SD and WKY VSM cells when treated with Adenophostin A.

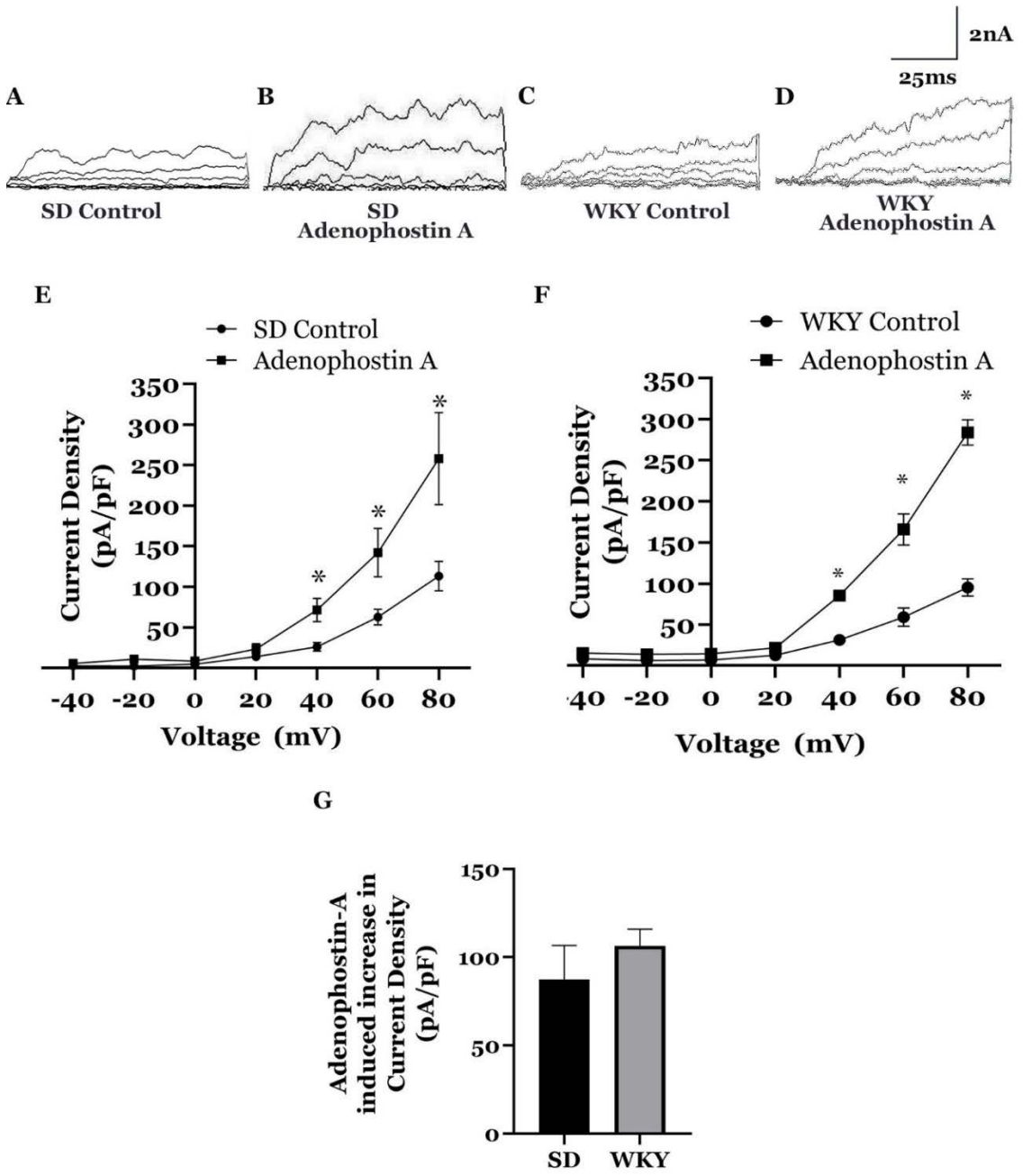

Figure 22. Comparison of BK_{Ca} channel current density between SD and WKY mesenteric arterial VSM cells in response to Adenophostin A. Whole-cell K^+ currents were recorded at room temperature in response to successive voltage pulses of 100ms duration, increasing in 20-mV increments from -40mV to +80mV before and after the treatment Adenophostin A (5μM). A-D: representative tracings depicting the currents recorded from a single VSM cell before and after treatment with Adenophostin A (5μM, 5 min). E-F: i-v curve plots of SD (E) and WKY (F) BK_{Ca} currents at baseline and after application of Adenophostin A (5μM, 5 min). G: Bar graph summarizing the Adenophostin A-induced increase in BK_{Ca} channel current density in SD and WKY VSM cells at +60mV. Values are mean±SEM (n=3 cells). *P<0.05 indicates a significant difference from the corresponding control value.

BK_{Ca} current density at +60mV significantly increased in SD VSM cells from 62.84±9.60 pA/pF to 142.30±29.98 pA/pF (n=5 cells, $p<0.05$; Figure 22E), while in WKY VSM cells, BK_{Ca} current density increased from 59.11±11.20 pA/pF to 165.70±19.18 pA/pF (n=7 cells; Figure 22F). The Adenophostin A-induced induced increase in average BK_{Ca} current density at +60mV between SD and WKY VSM cells was not significantly different (Figure 22G). These results demonstrate that BK_{Ca} channel activation in SD rats is similar to WKY in response to SR Ca^{2+} release through IP_3Rs.

Discussion

The present study was undertaken to evaluate the effect of the loss of functional coupling between IP_3 receptors on the SR and BK_{Ca} channels on the PM in mesenteric arterial smooth muscle cells in hypertension. The key findings are: 1) BK_{Ca} channel inhibition had no significant effect on vascular hypercontractility and hypertrophy in SHR, 2) BK_{Ca} activation is lower in SHR in response to IP_3R activation, despite having similar Ca^{2+}- and voltage-sensitivity to SD and 3) there is no significant difference in BK_{Ca} and IP_3R expression between SD and SHR VSM cells. These novel findings suggest that in SHR mesenteric VSM cells, the loss of IP_3R-BK_{Ca} functional coupling might be involved in vascular hypercontractility and hypertrophy.

In vascular smooth muscle cells, potassium channels are the main determinant of the resting membrane potential and regulate cell contraction and growth (Jackson, 2017; Brayden & Nelson, 1992). BK_{Ca} channels are large conductance potassium channels that regulate Ca^{2+} influx through voltage-activated Ca^{2+} channels (VGCC), $[Ca^{2+}]_{i,}$ and cellular contraction (Jackson, 2005). Vasoconstrictors, like ANG II, 5-HT, and NE that bind to Gq/phospholipase C-coupled receptors, stimulate the production of inositol 1,4,5-trisphosphate (IP_3) in VSM cells (Exton, 1985; Alexander, et al., 1985; Nagahama et al., 2000). IP_3 increases $[Ca^{2+}]_i$ and causes vasoconstriction by activating the SR membrane-localized IP_3 receptors (IP_3Rs). A large increase in $[Ca^{2+}]_i$ after the depletion of SR store through IP_3R channels activates BK_{Ca}-dependent

hyperpolarizing current and causes smooth muscle relaxation (Patterson, Henrie-Olson & Brenner, 2002).

The results of this present study demonstrate that when IP_3Rs are activated with specific IP_3R agonist in mesenteric VSM cells, the resulting BK_{Ca} channel activation from increased $[Ca^{2+}]_i$ is significantly lower in SHR compared to SD, despite no significant difference in Ca^{2+}- and voltage-sensitivity of BK_{Ca} channels between SHR and SD mesenteric VSM cells. Consistent with these electrophysiological findings, BK_{Ca} blocker, paxillin was without effect on NE-induced vasoconstriction in SHR mesenteric arteries while significantly increasing vasoconstriction in SD. Similarly, in cellular hypertrophy and proliferation assay, blocking BK_{Ca} channels had no effect on ANG II-induced hypertrophy or increased proliferation. The reduction in BK_{Ca} channel activation in SHR cannot be attributed to smaller Ca^{2+} transients as the live-cell Ca^{2+}-imaging experiment revealed that the Ca^{2+} transients generated by the application of NE or ANG II were significantly larger in SHR VSM cells compared to SD. The lack of BK_{Ca} activation in these experiments also cannot be explained by reduced $BK_{Ca}\alpha$ or IP_3R1 expression in SHR VSM cells as the western blot experiment revealed that expression of $BK_{Ca}\alpha$ or IP_3R1 is not significantly different between SHR and SD.

One possible explanation for the lack of BK_{Ca} activity indicated by the data could be related to the loss of functional coupling between the IP_3 receptors and the BK_{Ca} channels. Communication between discreet sites of Ca^{2+} release on the SR and BK_{Ca} channel on the plasma membrane is possible because of peripheral SR-PM coupling sites in native arterial myocytes. These coupling sites are found in specific subcellular regions, where the SR and the PM are kept in close appositions, providing a platform for BK_{Ca}-IP_3R functional and molecular connection (Chen, Quintanilla & Liou, 2019). BK_{Ca} channels require micromolar concentrations of intracellular Ca^{2+} to be activated at the normal resting membrane potential (Piskorowski & Aldrich, 2002). The basal concentration of Ca^{2+} in the cytoplasm of unstimulated VSM cells is 50-100 nM (Foskett, J. K., White, C., Cheung, K. H., & Mak, 2007), which is too low to activate

BK_{Ca} channels at normal resting membrane potential. IP_3Rs, upon activation, create Ca^{2+} microdomains with steep Ca^{2+} concentration gradients that rapidly form and dissipate near the opening of the IP_3R channel. While the Ca^{2+} concentration adjacent to the open channel may be ~100μM, the concentration may dip below 1μM as close as 1–2μm from the IP_3R opening (Naraghi, M., & Neher, 1997; Ríos, E., & Stern, 1997). SR-PM junctions or coupling sites bring IP_3Rs within 10-150 nm of BK_{Ca} channels (Poteser et al., 2016) and thus are vital for BK_{Ca} activation through IP_3R activation. This theory is substantiated by the findings reported by Pritchard et al. (2019), where the loss of SR-PM coupling sites caused near elimination of transient BK_{Ca} channel current activated by SR Ca^{2+} release events.

In conclusion, BK_{Ca} channel activation by IP_3-induced Ca^{2+} release provides an important negative feedback mechanism that opposes the vasoconstrictor responses (Yang et al., 2013). Loss of coupling between BK_{Ca} and Ca^{2+} release channels on the SR increases the sensitivity of the blood vessels to vasoconstrictor stimuli, increases total peripheral vascular resistance and systemic blood pressure, and causes hypertrophy and hyperplasia (Sausbier et al., 2005; Plüger et al., 2000; Brenner et al., 2000; Minamisawa et al., 2004; Wang et al., 2001). This study has demonstrated that BK_{Ca} activity in SHR is significantly lower in response to IP_3R activation compared to SD rats, despite having similar Ca^{2+}- and voltage sensitivity, similar channel expression and larger Ca^{2+} transients. This lack of activity could contribute to the development of vascular hypercontractility and hypertrophy in SHR.

CHAPTER 3: MOLECULAR MECHANISMS INVOLVED IN THE BK_{Ca}-IP_3R UNCOUPLING IN HYPERTENSION

Introduction

Vascular smooth muscle (VSM) cell contraction, relaxation, and growth is dependent on intracellular Ca^{2+}, a ubiquitous second messenger. These cells express multiple classes of K^+ channels, which regulate the $[Ca^{2+}]_i$ by controlling the cell membrane potential. Large conductance Ca^{2+}-activated K^+ (BK_{Ca}) channels are one of three calcium-sensitive potassium channels ubiquitously expressed in VSM cells. As BK_{Ca} channels have a relatively low affinity for Ca^{2+}, they require spatially and temporally localized large Ca^{2+} transients generated by Ca^{2+} release channels of sarcoplasmic reticulum and large depolarization to cause a substantial K^+ efflux. Since potassium ions are positive, a large efflux of K^+ significantly reduces membrane potential and provides vasorelaxation.

Unlike the ryanodine receptor (RyR) Ca^{2+} release channels, SR-localized Inositol 1,4,5-trisphosphate receptors (IP_3Rs) can be activated by vasoconstrictors without Ca^{2+} influx or depolarization (Fill & Copello, 2002). These agents stimulate the production of IP_3 in the cell, which activates IP_3Rs and elicits a highly localized Ca^{2+} transient known as Ca^{2+} puffs (Taylor & Tovey, 2010). Ca^{2+} concentration in these puffs may be as high as 100μM, enough to activate BK_{Ca} channels localized within 1μm of the opening of the IP_3Rs (Naraghi, M., & Neher, 1997; Ríos, E., & Stern, 1997).

While BK_{Ca} activation by IP_3R through the SR Ca^{2+} release pathway is well known, recent research by Zhao et al. (2010) has pointed to another mechanism through which IP_3Rs can influence the activity of BK_{Ca} channels independent of SR Ca^{2+} release. Zhao et al. (2010), through co-immunoprecipitation (coIP) experiment, have shown that IP_3Rs in VSM cells have a molecular connection with PM-localized BK_{Ca} channels, as IP_3Rs were able to pull down both alpha and beta subunits of BK_{Ca} channels. According to Zhao et al. (2010), IP_3Rs can increase

the BK_{Ca} Ca^{2+} sensitivity through IP_3 but only when there is a direct BK_{Ca}-IP_3R molecular connection (Zhao et al., 2010). This new finding is substantiated by previous research showing IP_3R coupling with cation channels on the plasma membrane and modulating their activity through IP_3 (Xi et al., 2008; Adebiyi et al., 2010).

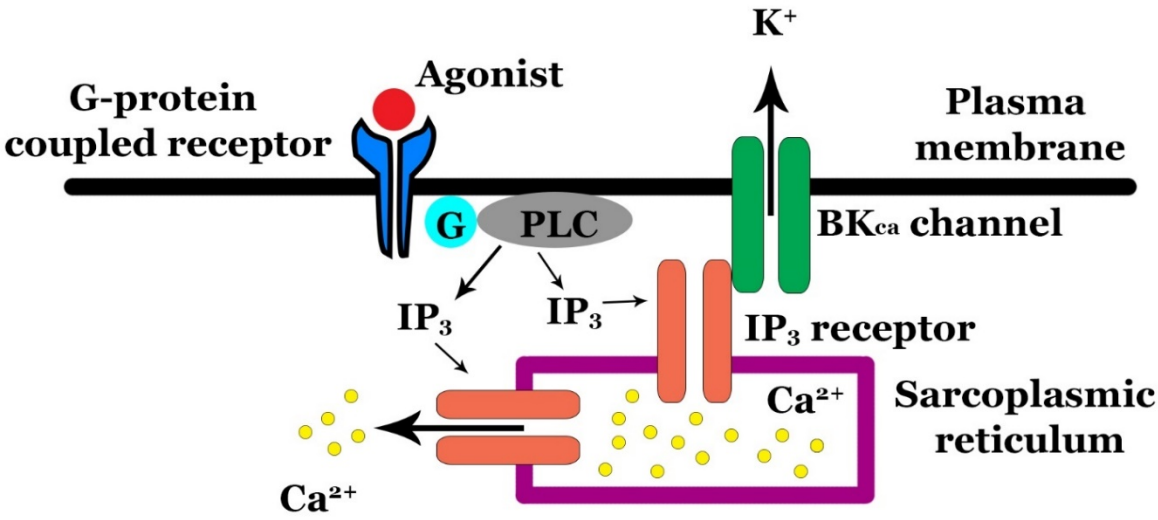

Figure 23. Model for BK_{Ca}-IP_3R molecular-coupling and regulation of BK_{Ca} channels by IP_3 receptors. Agonist activation of a G-protein coupled receptor activates phospholipase C (PLC), leading to the production of the calcium-mobilizing messenger, IP_3. IP_3 releases calcium from a critical sarcoplasmic reticulum store, which activates BK_{Ca} channels, causing vascular relaxation.

However, the research failed to provide conclusive evidence on whether the molecular connection between BK_{Ca} and IP_3R is a direct connection or a connection through an intermediate protein. A molecular connection between BK_{Ca} and IP_3R is possible because of the presence of SR-PM junctions. Different SR-PM tethering proteins bring the SR and PM close together and facilitate the formation of molecular coupling between ion channels. In VSM cells, Junctophilin 2 (JPH2) is the dominant SR-PM tethering protein, and the knockdown of this protein nearly abolishes BK_{Ca} activation through SR Ca^{2+} release and causes hypercontractility of arteries (Pritchard et al., 2019). JPH2 not only tethers SR and PM but also modulates the activity of SR-localized Ca^{2+} release channels and BK_{Ca} channels by coupling with them (Jayasinghe et al., 2012; Saeki et al., 2019). According to Jiang et al. (2019), the binding of JPH2

protein to the PM/SR membrane is possible through a reversible lipidation strategy called S-palmitoylation.

So far, no research has been conducted on the loss of BK_{Ca}-IP_3R molecular coupling in VSM cells in hypertension. The hypothesis is that the molecular connection between BK_{Ca} and IP_3R is missing in SHR VSM cells, preventing IP_3R from amplifying the Ca^{2+} sensitivity of co-localized BK_{Ca} channels. It can also be hypothesized that the loss of molecular connection is due to JPH2 dysregulation, either through reduced expression or loss of palmitoylation.

Thus, the present study was designed to evaluate BK_{Ca}-IP_3R molecular connection in SD and SHR mesenteric VSM cells. This study also compared the expression of JPH2 and examined the effect of JPH2 palmitoylation inhibition on BK_{Ca}-IP_3R coupling using a palmitoylation inhibitor called 2-Bromopalmitate (2-BP).

Materials and Methods

Chemicals: Crystallized papain, collagenase, and elastase were purchased from Worthington Biochemicals (Freehold, NJ). Rabbit anti-KCNMA1, anti-IP_3R1, anti-JPH2 primary antibodies and goat anti-rabbit secondary antibodies were purchased from Invitrogen (Waltham, MA). Soybean trypsin inhibitor, DTT, HEPES, 2-BP and other reagents were obtained from Sigma-Aldrich (St. Louis, MO). ANG II was purchased from Cayman Chemical (Ann Arbor, MI). WST-1 reagent was purchased from Abcam (Waltham, MA). Mouse anti-IP_3R1 primary antibody and Protein A/G PLUS-Agarose beads were purchased from Santa Cruz (California, USA),

Animals and tissue preparation: Third- and fourth-order mesenteric arteries were dissected from 4-6-month-old SHR and normotensive Sprague-Dawley (SD) rats of either sex purchased from Charles River Farms (Wilmington, MA). Mesenteric arteries of at least 3 rats of either sex were used per experiment. At least 3 mesenteric vascular beds were used per experiment for VSM cell isolation. Rats used for the experiments were housed at 22 ± 2°C on a 12 h-12 h light-dark cycle and provided with food and water ad libitum. Rats were euthanized for

experiments with a 150mg/kg intraperitoneal injection of sodium pentobarbital. All animal protocols were approved by the North Dakota State University Institutional Animal Care and Use Committee.

Mesenteric resistant arteries contribute greatly to the regulation of blood pressure by controlling peripheral vascular resistance (Christensen & Mulvany, 1993). These arteries experience both structural and functional alterations during the development of hypertension, which makes them an ideal candidate for cardiovascular research (Naito, Yoshida, Konishi & Ohara, 1998; Tatchum-Talom, Eyster & Martin, 2005; Schiffrin, 1992). Previous research has shown that mesenteric arteries of SHR not only display exaggerated constrictor responses to a variety of vasoconstrictors but also altered vasodilation (Pratt, Bonnet, Ludwig, Bonnet & Rusch, 2002; Chang, Lee, Wu & Chen, 2002).

Care was taken to prevent damage to the arteries during the isolation process. The mesentery was removed from each rat, third- and fourth-order mesenteric arteries were located and cleaned of fat and connective tissue, and placed in ice-cold low Ca^{2+} Tyrode's solution, containing in (mM): 145 NaCl, 4 KCl, 0.05 $CaCl_2$, 1 $MgCl_2$, 10 HEPES, and 10 dextrose.

Smooth muscle cell isolation: The collected arteries were subjected to enzymatic digestion for the isolation of single VSM cells as previously described by Sun et al. (1998). The arteries were incubated for 10 minutes in 2 ml of low Ca^{2+} Tyrode's solution containing 1 mg/ml albumin. Arteries were then incubated for 20 mins at 37°C in 2 ml of low Ca^{2+} Tyrode's solution in 1.5 mg/ml papain and 1 mg/mL DTT. Finally, the segments were incubated for 90 minutes at 37°C in 2 mg/mL collagenase, 0.5 mg/mL elastase, and 1 mg/ml soybean trypsin inhibitor. Tissues were then triturated gently using a Pasteur pipet to release single VSM cells. Isolated cells were then cultured in a 25cm^2 culture flask, which contained Dulbecco's modified Eagle medium (DMEM) supplemented with 10% fetal bovine serum, penicillin (100U/ml), and streptomycin (100µg/ml). Cells were passaged as they became confluent, and cells at 3^{rd}-5^{th} passages were used for experiments.

Co-immunoprecipitation (co-IP): For the comparison of BK_{Ca}-IP_3R1 molecular interaction between SD and SHR, mesenteric arteries were lysed in non-denaturating cell lysis buffer (Abcam, Cambridge, UK) with protease inhibitor mixture (ThermoFisher Scientific, Waltham, MA). For the analysis of BK_{Ca}-IP_3R1 molecular interaction in SD mesenteric VSM cells after palmitoylation inhibition, cultured mesenteric VSM cells were lysed. 1.5 mg cell lysate was incubated with 8μg rabbit polyclonal anti-KCNMA1 antibody for 2h followed by the addition of 20μl protein A/G PLUS–agarose beads (Santa Cruz Biotechnology, Dallas, TX) for 12h at 4 °C. After the incubation, samples were spun down and washed three times with PBS. Protein contents were then eluted with 2× SDS sample buffer, containing 65.8 mM Tris-HCl, pH: 6.8, 2.1% SDS, 26.3% (w/v) glycerol and 0.01% bromophenol blue. The total cell lysate was used as the positive control, while empty beads combined with cell lysate without anti-KCNMA1 antibody were used as the negative control. Samples were analyzed using Western Blot analysis with mouse monoclonal anti-IP_3R1 primary antibody (1:100) and horseradish peroxidase-conjugated anti-mouse secondary antibody (1:3000). Proteins were separated on 7.5% polyacrylamide gels by SDS-PAGE and electroblotted onto a nitrocellulose membrane. Membranes were blocked in TBS-T (0.08% Tween) containing 5% milk for 1h, followed by overnight incubation with mouse monoclonal anti-IP_3R1 primary antibody at 4°C. After washing with TBS-T, membranes were incubated for 1h with horseradish peroxidase-conjugated anti-mouse secondary antibody. Membranes were developed using enhanced chemiluminescence (ThermoFisher Scientific, Waltham, MA), and digital images were obtained using an AGFA CP1000 automatic film processor.

For the evaluation of the effect of loss of JPH2 palmitoylation on BK_{Ca}-IP_3R1 molecular interaction in SD VSM cells, cells were treated with 50μM 2-BP (JPH2 palmitoylation inhibitor) in serum-free media for 24 hours before the co-IP experiment. Cultured cells were then lysed and used for co-immunoprecipitation employing the same method described above.

Western blotting: JPH2 protein levels in rat mesenteric arteries were assessed by western blot analysis. Mesenteric arteries from 3 SHR and SD rats of either sex (2 male and 1 female rat of each strain) were isolated and homogenized by mechanical shearing with a Dounce homogenizer in ice-cold RIPA buffer. The Bradford method-based Bio-Rad protein assay kit (Bio-Rad, Hercules, California) was used for the quantification of solubilized protein. Bovine serum albumin (BSA) was used to establish the standard curve. Relative measurement of protein concentration was achieved through comparison with the standard curve. 35µg of protein was loaded in each well for the western blot analysis of JPH2 expression in SD and SHR mesenteric arteries. For the comparison of JPH2 expression between male and female SHR mesenteric arteries 25µg of protein was loaded in each well. Kaleidoscope (Bio-Rad, Hercules, California) was used for band referencing. Proteins were separated on 7.5% polyacrylamide gels by SDS-PAGE and electroblotted onto a nitrocellulose membrane. Membranes were blocked in TBS-T (0.08% Tween) containing 5% milk for 1h, followed by overnight incubation with rabbit polyclonal anti-JPH2 primary antibody (1:500) at 4°C. After washing with TBS-T, membranes were incubated for 1h with anti-rabbit horseradish peroxidase-conjugated secondary antibodies (1:3000). To ensure equal loading, the membranes were reprobed for β-actin after stripping using mouse monoclonal Anti-β-Actin antibody (1:1000). β-actin is a common housekeeping protein used in the western blot analysis of rodent mesenteric arteries (Stott et al., 2018; Silva et al., 2015; Troiano et al., 2021; Matsumoto et al., 2010). For stripping, a mild stripping buffer containing 199.8 mM glycine and 3.46 mM SDS was used (pH: 2.2). Briefly, the membrane was incubated twice with the stripping buffer for 8 minutes each. Afterwards the membrane was washed 3 times for 5 minutes each with TBST. After washing, the membrane was used again for β-actin staining. Membranes were developed using enhanced chemiluminescence (ThermoFisher Scientific, Waltham, MA), and digital images were obtained using an AGFA CP1000 automatic film processor. Relative protein expression values were obtained by dividing the raw values of JPH2 by the raw values of β-actin.

Cell proliferation assay: VSM cells were isolated from mesenteric arteries of 3 SD rats of either sex (2 male and 1 female rat of each strain) and cultured. VSM cells at 3rd passage were plated in a 96-well microplate and grown until 60% confluency. Fetal Bovine Serum (FBS)-supplemented DMEM media was then replaced with serum-free DMEM containing 50μM 2-bromopalmitic acid (2-BP) 24h before the experiment to serum starve the cells and inhibit JPH2 palmitoylation. Cellular proliferation of VSM cells was determined using the WST-1 (4-[3-(4-iodophenyl)-2-(4-nitrophenyl)-2H-5-tetrazolio]-1, 3-benzene disulfonate) reagent. The culture medium was replaced with 100 μl of the (1:10 dilution) WST-1 in a fresh medium in each well and incubated for 3h. Absorbance was measured using a multifunctional microplate reader (SpectraMax M5, Molecular Devices) at 440 nm, with a reference wavelength set at 630 nm.

Electrophysiological recordings: Patch-clamp recordings were used to measure BK_{Ca} channel activity in cultured mesenteric VSM cells at room temperature in the whole-cell voltage-clamp configuration as described previously (Modgil, Guo, O'Rourke & Sun, 2013; Sun et al., 1998). Axopatch 200B patch-clamp amplifier (Axon Instruments, Burlingame, CA) was used to control voltage-clamp and voltage-pulse generation, and pCLAMP 10.0 software (Molecular Devices, Sunnyvale, CA) was used to collect the current data. Voltage-activated currents were filtered at 1kHz and digitized at 5 kHz, and leakage current was subtracted digitally. Series resistance and total cell capacitance were obtained by adjusting series resistance and whole-cell capacitance using the Axopatch 200B amplifier control system.

Cultured cells were treated with 50μM 2-BP and serum-starved for 24 hours before the experiment. Afterward, the media was discarded from the culture dishes, and the cells were washed 3 times with a bath solution containing (in mM) 145 NaCl, 5.4 KCl, 1.8 $CaCl_2$, 1 $MgCl_2$, 5 HEPES, 10 dextrose; pH 7.4 (NaOH). Patch electrodes (resistance 3-4 MΩ) were fabricated from borosilicate glass pipettes and filled with pipette solution containing (in mM) 145 KCl, 5 NaCl, 0.37 $CaCl_2$, 2 $MgCl_2$, 10 HEPES, 1 EGTA, 7.5 dextrose; pH 7.2 (KOH). Cells were held at −60 mV, and 100-millisecond depolarizing step pulses of 20 mV increments from −40 to +80 mV

voltages were applied. BK_{Ca} current was divided by the capacitance and expressed as current density. Analysis was performed offline using Clampfit 10 software (Axon Instruments, Burlingame, CA).

Calculations and statistical analysis: Statistical analysis was performed using GraphPad Prism version 8.0.0 for Windows (San Diego, CA). Statistical differences between the experimental groups were analyzed using Student's t-test or one-way ANOVA followed by Dunnett's or Tukey's post hoc test for multiple comparisons, where appropriate. Statistical significance was established at a minimum of $P \leq 0.05$. All values were expressed as means ± SE. For whole-cell current amplitude at a given test potential, the peak current was measured using a peak detection routine in pClamp 10 software to generate the current-voltage relationship. Densitometric analysis of the western blot signals was performed using ImageJ software.

Results

IP_3R1 coimmunoprecipitates with BK_{Ca} channel α subunit in SD but not in SHR: Co-IP was performed to test the hypothesis that the molecular coupling between BK_{Ca} and IP_3R is lost in SHR VSM cells, disrupting the BK_{Ca}-IP_3R co-localization. BK_{Ca}-IP_3R co-localization is necessary for local molecular communication between these proteins and activation of BK_{Ca} channels by IP_3Rs via Ca^{2+} signaling (Zhao et al, 2010).

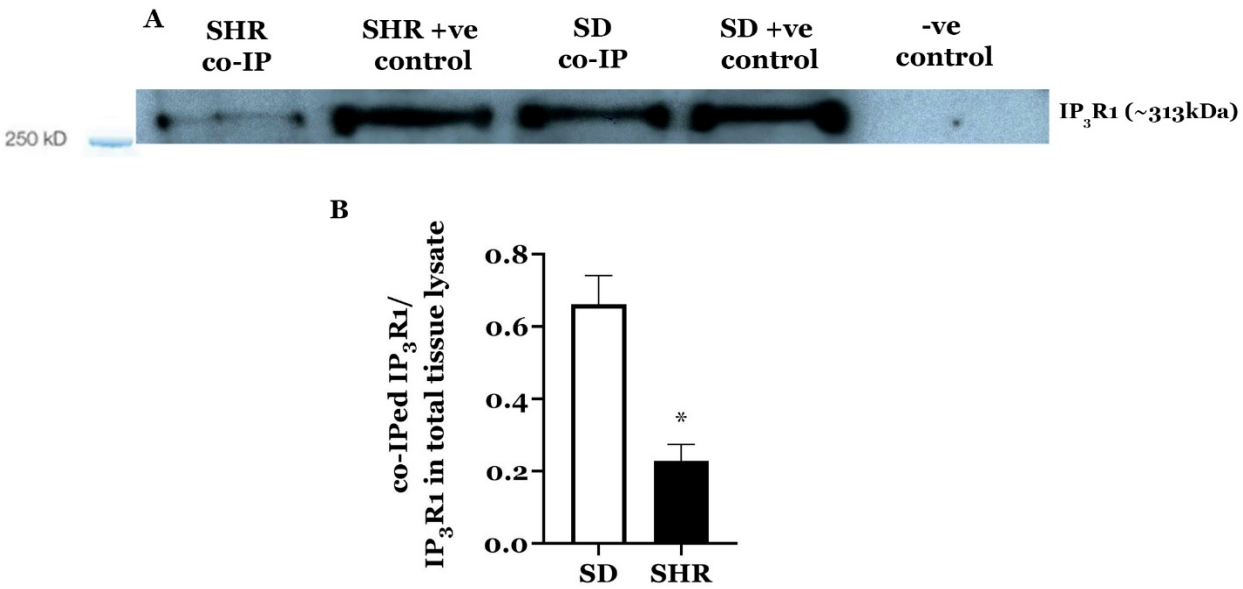

Figure 24. Molecular interaction between $BK_{Ca}\alpha$ and IP_3R1 in SD and SHR mesenteric VSM cells. A: IP_3R1 (`313 kDa) coimmunoprecipitation with BK_{Ca} channel α subunit from SD rat mesenteric arteries. Total cell lysate was used as positive control while empty beads incubated with cell lysate without anti-KCNMA1 antibody was used as negative control. B: Ratio of co-immunoprecipitated IP_3R1 vs IP_3R1 detected from total tissue lysate in (+) control lane (n= 3 rats). Values are mean±SEM. *$P<0.05$ indicates a significant difference from the corresponding SD value.

In the co-IP experiment, polyclonal $BK_{Ca}\alpha$ antibody co-immunoprecipitated IP_3R1 with $BK_{Ca}\alpha$ from SD rat mesenteric arterial lysate. The amount of IP_3R1 co-immunoprecipitated from SHR mesenteric arterial lysate was significantly lower than SD. Western blot analysis using monoclonal IP_3R1 antibody showed that the co-immunoprecipitated sample from SD rats generated a strong band, while in the case of SHR, the band was barely perceptible despite loading equal amount of protein (Figure 24A). (+ve) control samples of both SD and SHR, where total cell lysate was used, produced comparable bands showing that IP_3R1 expression is similar between them. (-ve) control lane did not generate any band as expected as (-ve) control sample contained empty beads. The ratio of co-IPed IP_3R1 to IP_3R1 in total tissue lysate is significantly lower in SHR compared to SD. Bar graph summarizing the ratio in SD and SHR VSM cells is shown in Figure 24B. These results strongly imply that interaction between BK_{Ca} and IP_3R is disrupted in SHR mesenteric VSM cells.

JPH2 expression in SHR VSM cells is not significantly different compared to SD: Western blot analysis was performed to examine the expression of JPH2 in SD and SHR mesenteric VSM cells. Relative protein expression values were obtained by dividing the raw values of JPH2 by the raw values of loading control, β-actin. In the western-blot experiment, the JPH2 expression level was not significantly different between SD and SHR mesenteric arteries. Representative blots showing the expression of JPH2 (~70 kDa) in SD and SHR VSM cells are shown in Figure 25A. Bar graph summarizing the relative quantification of JPH2 in SD and SHR VSM cells are shown in Figure 25B. Data from this experiment indicate that reduced JPH2 expression in SHR is not a factor behind disrupted BK_{Ca}-IP_3R molecular coupling.

The expression of JPH2 between male and female SHR mesenteric VSM cell was also compared. The results indicated that JPH2 expression level was not significantly different between male and female SHR mesenteric arteries. Representative blots showing expression of JPH2 (~70 kDa) in male and female SHR VSM cells are shown in Figure 25C. Bar graph summarizing the relative quantification of JPH2 is shown in Figure 25D.

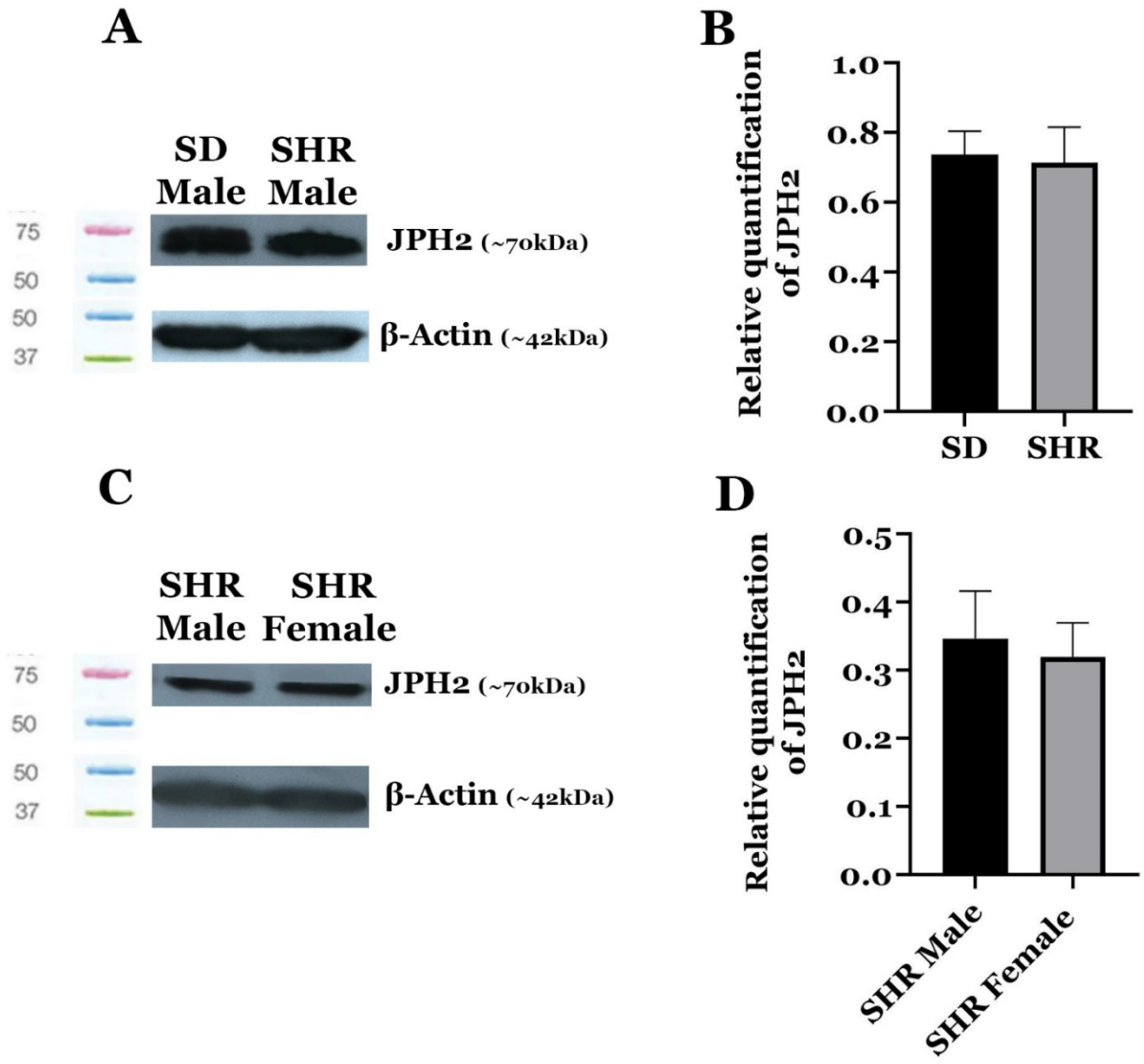

Figure 25. Expression of JPH2 in SD and SHR mesenteric VSM cells. A: Representative blots showing expression of JPH2 (~70 kDa) in small mesenteric arteries dissected from SHR and SD rats. B: Bar graph summarizing the relative quantification of JPH2 in SD and SHR VSM cells (n= 3 rats). C: Representative blots showing expression of JPH2 in male and female SHR mesenteric arteries. D: Bar graph summarizing the relative quantification of JPH2 (n= 3 rats). Values are mean±SEM.

$BK_{Ca}\alpha$ - IP_3R1 molecular connection is disrupted after inhibition of JPH2 palmitoylation: Co-IP was performed to test the effect of the loss of JPH2 palmitoylation on the molecular coupling between BK_{Ca} and IP_3R in cultured SD VSM cells. In this experiment, polyclonal $BK_{Ca}\alpha$ antibody co-immunoprecipitated IP_3R1 with $BK_{Ca}\alpha$ from untreated cell lysate but failed to co-immunoprecipitate in cells treated with 2-BP (50μM) for 24 hours. Western blot

analysis using monoclonal IP_3R1 antibody showed that the co-immunoprecipitated sample from untreated cells generated a strong band, while in the case of 2-BP treated cells, the band was barely perceptible despite loading an equal amount of protein (Figure 26A). The ratio of co-IPed IP_3R1 to IP_3R1 in total cell lysate is significantly lower in 2-BP treated SD VSM cells compared to untreated cells. Bar graph summarizing the ratio is shown in Figure 26B. These results strongly imply that JPH2 palmitoylation inhibition disrupts the BK_{Ca}-IP_3R co-localization.

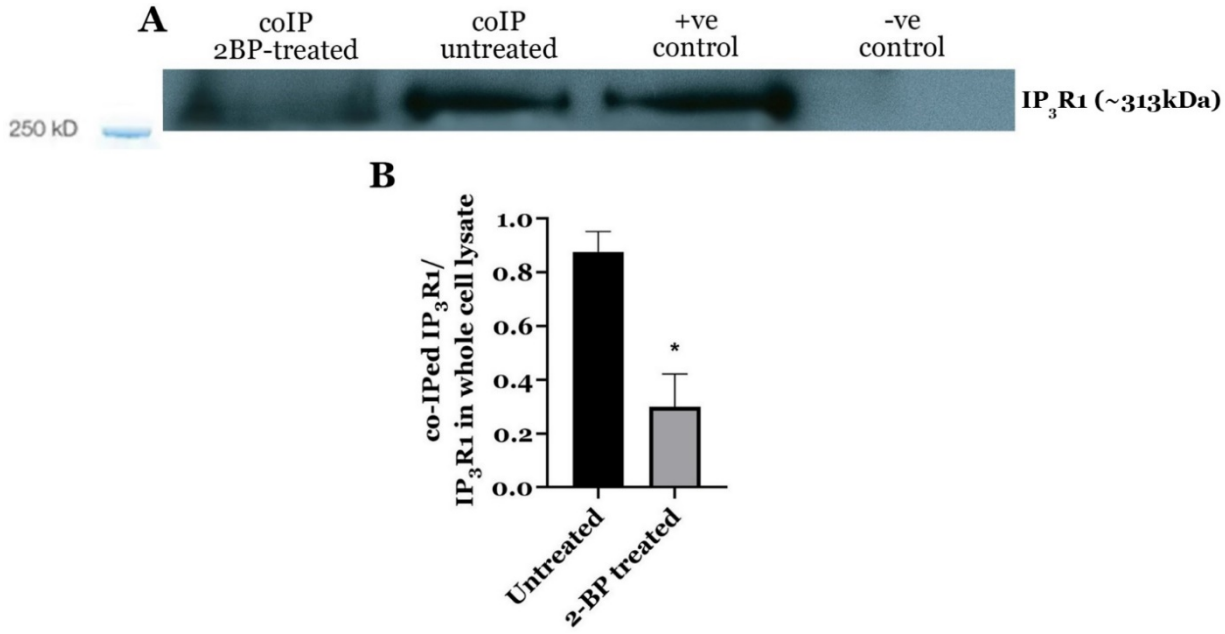

Figure 26. Effect of palmitoylation inhibition on molecular interaction between $BK_{Ca}\alpha$ and IP_3R1 in SD mesenteric VSM cells. A: IP_3R1 (`313 kDa) coimmunoprecipitation with BK_{Ca} channel α subunit is significantly reduced after 2-BP (50μM) treatment. Total cell lysate was used as positive control while empty beads incubated with cell lysate without anti-KCNMA1 antibody was used as negative control. B: Ratio of co-immunoprecipitated IP_3R1 vs IP_3R1 detected from total cell lysate in (+) control lane (n= 3 rats). Values are mean±SEM. *P<0.05 indicates a significant difference from the corresponding untreated control value.

JPH2 palmitoylation inhibition increased cellular proliferation in SD but not in SHR: WST-1 cell proliferation assay was performed to assess the effect of the loss of JPH2 palmitoylation on VSM cell proliferation. 2-BP (50μM) significantly increased the proliferation of the cultured cells from SD rats compared with control but was ineffective in SHR (Figure 27). 2BP treatment significantly increased cell proliferation in SD by ~24.84% while having no effect on cell proliferation in SHR.

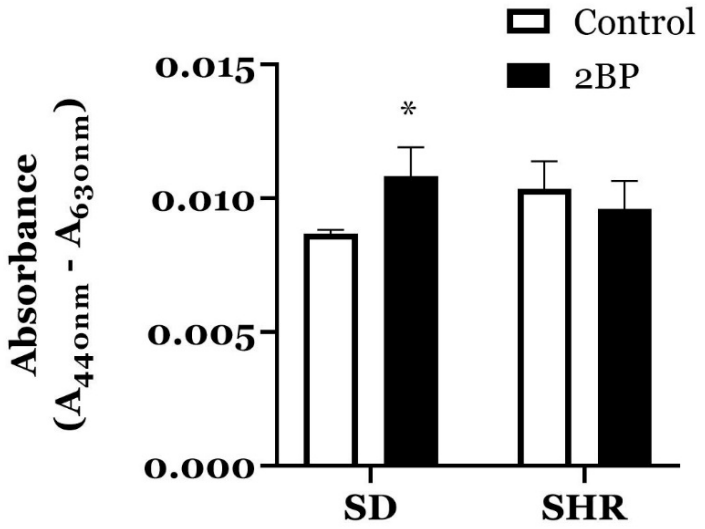

Figure 27. Effect of palmitoylation inhibition on SHR and SD VSM cell proliferation. Bar graph summarizing the effect of 2-BP (50μM) on VSM cell proliferation in SHR and SD rats (n= 4 wells with cells from 2 male rats). Values are mean±SEM. *P<0.05 indicates a significant difference from the control of the same strain.

Inhibition of JPH2 palmitoylation causes significant loss of BK_{Ca} current in response to SR Ca^{2+} release: The effect of the loss of JPH-2 palmitoylation on BK_{Ca} channel activity in response to SR Ca^{2+} released through IP_3Rs was determined in cultured SD VSM cells. Whole-cell BK_{Ca} currents were recorded in response to successive voltage pulses of 100ms duration, increasing in 20-mV increments from -40mV to +80mV in the absence or presence of a selective IP_3 receptor agonist, Adenophostin A.

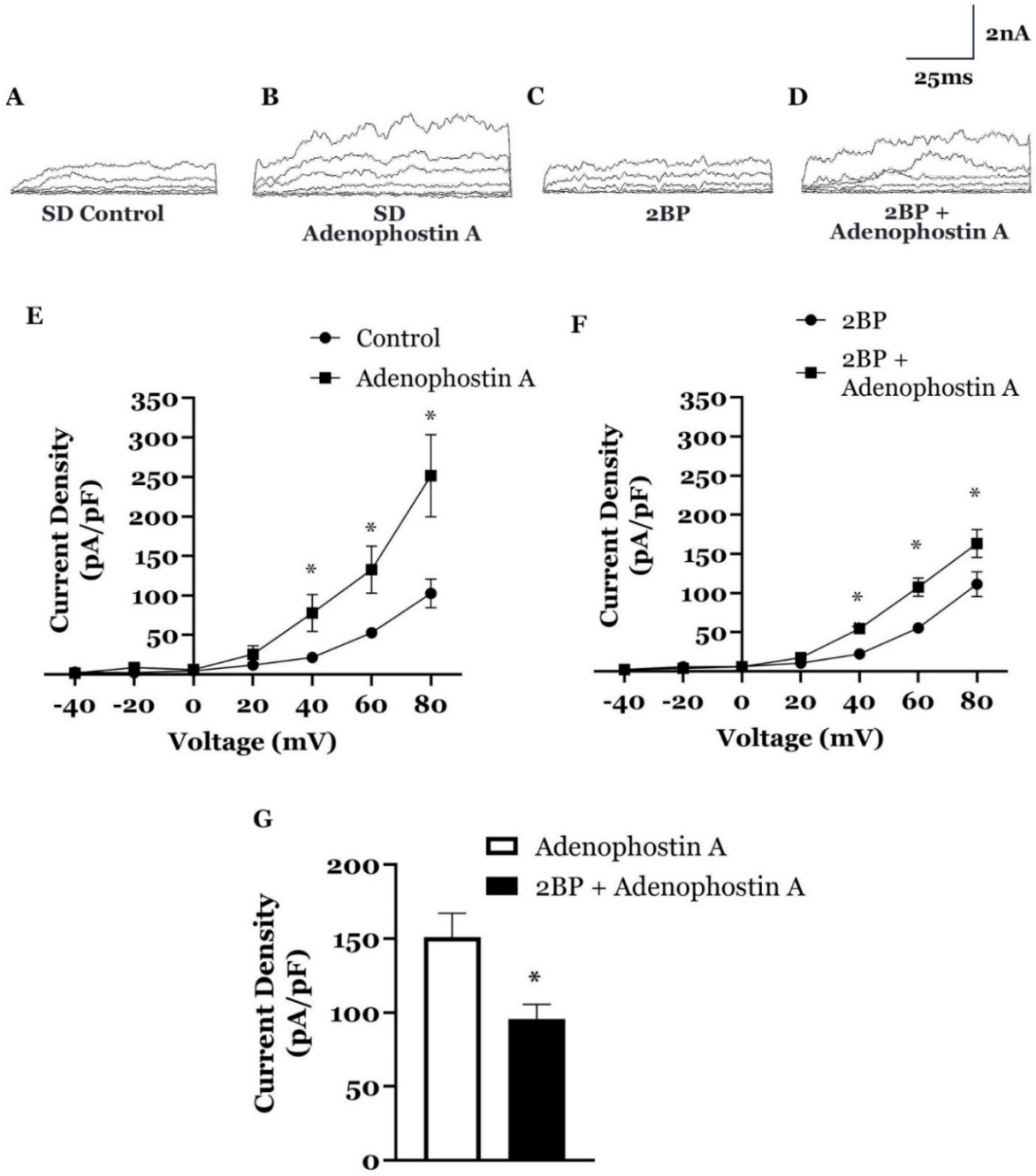

Figure 28. Effect of palmitoylation inhibition on Adenophostin A-induced BK_{Ca} current density in cultured SD VSM cells treated with 2-BP (50μM) for 24 hours. Whole-cell K^+ currents were recorded at room temperature in response to successive voltage pulses of 100ms duration, increasing in 20-mV increments from -40mV to +80mV before and after the treatment Adenophostin A (5μM). A-D: representative tracings depicting the currents recorded from a single VSM cell before and after treatment with Adenophostin A (5μM, 5 min). E-F: i-v curve plots of BK_{Ca} currents from untreated (E) and 2-BP treated (F) cells at baseline and after application of Adenophostin A (5μM, 5 min). G: Bar graph summarizing the effect of 2-BP (50μM) on Adenophostin A-induced BK_{Ca} current density at +60mV. Values are mean±SEM (n=5 -10 cells). *$P<0.05$ indicates a significant difference from the corresponding control value.

When the VSM cells were treated with Adenophostin A, BK_{Ca} current density at +60mV significantly increased in untreated control VSM cells from 52.77±5.10 pA/pF to 132.30±29.88 pA/pF (n=3 cells, $p<0.05$; Figure 28E), while in 2-BP treated VSM cells, the increase in BK_{Ca} current density was significantly lower (from 55.28±5.98 pA/pF to 114.08±17.75 pA/pF, n= 3 cells; Figure 28F) compared to untreated control. These results demonstrate the potential role played by JPH2 palmitoylation on BK_{Ca} channel activation in response to SR Ca^{2+} release through IP_3Rs.

Discussion

The present study was undertaken to examine the molecular coupling between IP_3 receptors on the SR and BK_{Ca} channels on the PM in mesenteric arterial smooth muscle cells. The key findings are: 1) BK_{Ca} channel α subunit coimmunoprecipitates with IP_3R1 in SD but the BK_{Ca}α -IP_3R1 co-immunoprecipitation is significantly reduced in SHR, 2) No difference in JPH2 expression despite reduced BK_{Ca}-IP_3R coupling, 3) Inhibition of JPH2 palmitoylation reduced BK_{Ca} activation and increased mesenteric VSM cell proliferation. These novel findings suggest that in SHR mesenteric VSM cells, the BK_{Ca}-IP_3R molecular connection is disrupted, and this disruption may be due to the loss of JPH2 palmitoylation rather than the loss of JPH2 itself.

While the mechanism of BK_{Ca} activation by Ca^{2+} released from the SR through the IP_3Rs is well known, the possibility of IP_3R activating BK_{Ca} channels without releasing Ca^{2+} from the SR has also been reported recently. According to Zhao et al. (2010), IP_3 increases BK_{Ca} Ca^{2+} sensitivity through molecular interaction between IP_3R and BK_{Ca}, independent of SR Ca^{2+} release. The ability of IP_3 to increase BK_{Ca} open probability (Po) is dependent on the localization of IP_3R in close proximity to BK_{Ca} and molecular interaction between these channels, as IP_3R blocker or IP_3R -ablation was able to prevent IP_3 from increasing BK_{Ca} Ca^{2+} sensitivity (Zhao et al. 2010). While Zhao et al. (2010) have shown that IP_3R1 is able to pull down BK_{Ca} channel in a co-immunoprecipitation experiment, it is not clear whether BK_{Ca} and IP_3R are directly connected or connected through an intermediate protein. Nonetheless, in the co-IP experiment,

the α subunit of the BK_{Ca} channel in SD VSM cell was able to pulldown significantly more IP_3R1 receptors with it compared to SHR. This result demonstrated that the molecular connection between IP_3R and BK_{Ca} might be reduced in SHR VSM cells, indicating the possibility of disrupted BK_{Ca}-IP_3R co-localization. This loss of molecular coupling may prevent IP_3R activation from amplifying the sensitivity of nearby BK_{Ca} channels (Zhao et al., 2008).

In excitable cells, there are multiple families of tethering proteins working in tandem to maintain the SR-PM junctions. However, in VSM cells, junctophilin-2 (JPH2), a member of the junctophilin family, is the predominant SR-Pm bridging protein. Originally thought to be just a structural protein, several studies have made it clear that JPH2 is also capable of regulating the functions of multiple Ca^{2+} handling proteins localized in the SR-PM junction. This observation has helped shed light on the critical role played by JPH2 in the formation of Ca^{2+} microdomains and proper Ca^{2+} signaling. JPH2 not only binds to the PM and SR but also to ion channels localized on both PM and SR. Co-immunoprecipitation and FRET (Förster resonance energy transfer) studies have shown that JPH2 is directly coupled to pore-forming subunits of L-type voltage-dependent calcium channels, BK_{Ca} channels, and ryanodine receptor (RyR) channels. Downregulation of JPH2 results in downregulation of other SR-PM tethering proteins, loss of SR-PM junctions, and perturbation of ion channels, leading to clinical diseases.

While JPH2 downregulation has been reported to cause VSM hypercontractility and hypertrophy, no significant difference in JPH2 expression between SD and SHR mesenteric VSM cells was observed. Although JPH2 expression is not downregulated in the VSM cells of 4–6-month-old SHR rats according to this study, it may be possible that the binding of JPH2 to the PM and SR is disrupted, preventing efficient functional and molecular coupling between BK_{Ca} and IP_3R. Jiang et al. (2019) reported that JPH2 binds to the PM and the SR through S-palmitoylation of its cysteine residues at the N- and C-terminal, respectively. S-palmitoylation is a common posttranslational modification employed by proteins to associate with membranes (Zaręba-Kozioł et al., 2018). In their study, Jiang et al. (2019) also demonstrated that inhibition

of JPH2 palmitoylation using 2-bromopalmitate (2-BP) can disrupt the SR-PM junctions without affecting the JPH2 expression level. While s-palmitoylation of JPH2 is necessary for its tethering ability, it is not known whether inhibition of JPH2 palmitoylation occurs in hypertension or not. It is also not known whether JPH2 palmitoylation has any effect on BK_{Ca}-IP_3R coupling.

In SHR VSM cells, the palmitoylation of JPH2 may be disrupted, leading to reduced BK_{Ca} channel activity after activation of IP_3R, which would explain the reduced BK_{Ca}-IP_3R molecular coupling despite having a normal level of JPH2 expression. To prove this hypothesis, a co-IP experiment on SD VSM cells after treating the cells with a palmitoylation inhibitor, 2BP was performed first. The result showed that inhibiting JPH2 palmitoylation disrupts BK_{Ca}-IP_3R molecular coupling, as IP_3R1 failed to co-immunoprecipitate with the BK_{Ca} channel α subunit in 2BP-treated SD VSM cells. Then the effect of the loss of JPH2 palmitoylation on BK_{Ca} channel activity in response to a specific IP_3R1 agonist, Adenophostin A using the whole-cell patch-clamp technique was examined. In this experiment, 2-BP (50 μM) treatment significantly reduced the BK_{Ca} current density in response to Adenophostin A. 2BP treatment of cultured SD VSM cells for 24 hours significantly reduced the BK_{Ca} current density in response to Adenophostin A**,** pointing to a potential loss of functional and molecular coupling between IP_3R and BK_{Ca}. Finally, a WST-1 cell proliferation assay to assess the effect of JPH2 palmitoylation inhibition on VSM cell proliferation was performed. In SD VSM cells, 2-BP treatment significantly increased cellular proliferation while having no effect in SHR. This result points to the potential loss of JPH2 palmitoylation in SHR VSM cells.

In conclusion, molecular coupling between IP_3R and BK_{Ca} channel provides an alternative pathway for IP_3R to influence the activity of BK_{Ca} without releasing Ca^{2+} from the SR. Defective molecular coupling may prevent IP_3R activation from amplifying the sensitivity of nearby BK_{Ca} channels (Zhao et al., 2008). Results from this study suggest that BK_{Ca}-IP_3R direct

coupling depends on not only their co-localization but also the proper tethering of JPH2 to the PM through palmitoylation.

CHAPTER 4: FUTURE DIRECTIONS

Further Investigation into The Role of JPH2 in Hypertension

Through the whole-cell patch-clamp experiment, this study showed that loss of palmitoylation negatively affects the BK_{Ca} channel current in response to IP_3R activation in SD VSM cells. It has also shown that loss of JPH2 palmitoylation disrupts BK_{Ca}-IP_3R coupling and increases cellular proliferation. However, it is no conclusive evidence of JPH2 palmitoylation playing a role in BK_{Ca} activity and hypertension. The lipid-based palmitoylation inhibiting compound (2-BP) used in this study is not specific to JPH2, as it may inhibit palmitoylation of other proteins (Draper & Smith, 2009). The mechanism through which it inhibits palmitoylation is also unknown.

There are several recently discovered non-lipid-based palmitoylation inhibitors that are significantly more selective in targeting the palmitoylation of a particular protein compared to 2-BP (Ducker et al., 2006; Draper & Smith, 2009). These are known as Compounds I-IV and are currently being evaluated as a potential therapeutic for treating cancer (Draper & Smith, 2009). It may be possible to use these compounds in the future to substantiate the findings from this study. It is also possible to detect palmitoylation of a specific protein in cells using immunoprecipitation and acyl-biotin exchange, as described by Brigidi & Bamji (2013). Using this technique, the palmitoylation level of JPH2 molecules can be compared between native SD and SHR VSM cells.

The possibility of JPH2 mutation should not be ruled out either, as mutation can hinder JPH2's ability to bind to the PM and SR without affecting the JPH2 expression level. It has been shown that mutation of the cysteine residues of JPH2 not only prevents JPH2 from biding to the lipid-raft domains of the PM through S-palmitoylation but also perturbs JPH2's ability to travel to the SR-PM junctions (Jiang et al., 2019). In patients with hypertrophic cardiomyopathy, S101R, Y141H, and S165F mutations of JPH2 have been reported (Landstrom et al., 2007). According to Landstrom et al. (2007), these mutations are localized to key locations of the

molecule and cause mislocalization of JPH2. JPH2 mutations has been shown to interfere with the cell's ability to effectively handle Ca^{2+} (Landstrom et al., 2007). As defects in Ca^{2+} signaling can lead to hypertrophy, loss of excitation-contraction coupling, and hypercontractility, it is possible that JPH2 in SHR VSM cells have mutations at different amino acids of the MORN motif.

Potential Role of Other Junctional Proteins in Hypertension

While the focus was on the predominantly expressed tethering protein JPH2 in this project, little is known about the expression and roles of other tethering proteins, such as E-syts, ORPs, $K_v2.1$, and $K_v2.2$, etc. in vascular smooth muscle cells.

According to Saheki et al. (2016), E-Syts may play a role in the transport of diacylglycerol (DAG) by forming a hydrophobic tunnel. E-Syts are also capable of binding to different lipids and transporting them between membranes (Schauder et al., 2014). DAG is produced alongside IP_3 when PIP_2 is hydrolyzed and acts as a second messenger (Kheifets, & Mochly-Rosen, 2007). DAG can influence the activity of different ion channels through the activation of protein kinase C (PKC). Ca^{2+} and K^+ channels have PKC phosphorylation sites, and the effect of PKC on these channels can be either stimulatory or inhibitory (Gada & Logothetis, 2022). SR-PM junctions can also recruit E-Syts when the Ca^{2+} levels rise, shortening the gap between SR and PM (Fernández-Busnadiego, Saheki & De Camilli, 2015). This shortening of the SR-PM gap brings the SR Ca^{2+} channels closer to the ion channels on the PM and facilitates ion channel coupling.

Another tethering protein, VAP, has also been implicated in maintaining Ca^{2+} homeostasis. According to De Vos et al. (2011), VAP tethers the membranes of mitochondria and SR and plays a role in Ca^{2+} exchange between them. Loss of VAP protein has been shown to interfere with the uptake of Ca^{2+} by these Ca^{2+} stores and causes a defect in Ca^{2+} signaling in the cell (De Vos et al., 2011).

TMEM proteins are essential for the activation of NFAT, a Ca^{2+}-sensitive transcription factor. NFAT interacts with an enzyme called calcineurin and regulates the hypertrophic growth

of blood vessels (Wilkins et al., 2004). TMEM proteins are also believed to be involved in the activation of STIM1 protein (Quintana et al., 2015). Activation of STM1 is required for STIM1-Orai1 coupling and efficient refilling of SR after SR emptying.

Further investigation into the role of the tethering proteins in the regulation of ion channel activity, lipid transport, and hypertrophic genes will help to get a better understanding of the importance of SR-PM junctions in blood pressure regulation.

IP_3R Binding to Other PM-Localized Ion Channels

In this project, only the coupling between BK_{Ca} channels and IP_3Rs was examined. However, IP_3Rs also couple with other PM-localized ion channels. Xi et al. (2008) reported that IP_3Rs are directly coupled to transient receptor potential canonical channels 3 (TRPC3) channel. Activation of this Ca^{2+}-permeable nonselective cation channel by IP_3 depends on its molecular coupling with IP_3R (Xi et al., 2008). Since the influx of Ca^{2+} through TRPC3 can activate nearby L-type Ca^{2+} channels and SR RyR channels, TRPC3-IP_3R coupling may play a role in the development of hypertension in SHR. Apart from BK_{Ca} and TRPC3, IP_3R's interactions with other Ca^{2+} and K^+ channels need to be investigated to get a complete picture of the role played by IP_3Rs in the control of blood pressure.

BK_{Ca}-IP3R Coupling in Pre-Hypertensive SHR

SHRs are known to remain pre-hypertensive for the first 6-8 weeks of their lives and then gradually develop hypertension over the next 12-14 weeks (Endemann et al., 1999). Vascular hypertrophy is believed to precede hypertension as pre-hypertensive rats have a significantly narrower arterial lumen and thicker arterial wall (Endemann et al., 1999). In this project, the focus was on 4-6 months old SHRs, at which point hypertension has fully developed. In the future, it will be necessary to investigate the state of BK_{Ca}-IP_3R coupling in newborn and juvenile SHRs to have a better understanding of its role in the development of vascular hypertrophy and hypertension.

CHAPTER 5: CONCLUSION

Hypertension is a significant risk factor for numerous cardiovascular diseases, including heart failure, vascular dementia, and stroke, and a leading cause of worldwide morbidity and mortality. Raised blood pressure causes 7.6 million premature deaths each year, about 13.5% of the global total (Lawes, Vander Hoorn & Rodgers, 2001). Much of the adverse effects of hypertension are mediated by changes in the structure and function of the vascular wall (Thom, 1997). Changes in vascular morphology and tone can increase vascular resistance and blood pressure (Touyz, 2012). The sympathetic nervous system, the renin-angiotensin-aldosterone system, and the immune system have all been implicated in the regulation of systemic vascular tone and resistance (Somlyo & Somlyo, 1994), making the process of understanding the precise mechanisms contributing to altered vascular reactivity particularly arduous.

Since the discovery of SR-PM junctions in 1957, it has been a hot topic of research in the scientific community. Numerous techniques have been developed to evaluate its role in Ca^{2+} signaling and vascular contraction. SR-PM junctions are the ideal membrane contact sites where PM and SR-localized ion channels can crosstalk. Given the crucial role played by ion channels in the regulation of blood pressure, ion channel coupling in SR-PM junctions demands a thorough understanding of their effects in the development of cardiovascular diseases. Current literature provides some vital information, but a lot of questions still remain unanswered.

My research aimed to identify the role of direct and indirect communication between the PM-localized BK_{Ca} channel and the SR-localized IP_3R channel in the development of hypercontractility and hypertrophy. A hypertensive animal model (spontaneously hypertensive rat) was used for this study. My hypothesis was that there is a loss of functional and molecular coupling between the IP_3 receptors and the BK_{Ca} channels in SHR VSM cells leading to reduced BK_{Ca} current after IP_3R activation.

The results of the present study, for the first time, demonstrate that BK_{Ca} channel activity is significantly lower in SHR VSM cells in response to IP_3-induced SR Ca^{2+} release. By using

patch-clamp, pressure myograph, and fluorescent microscopy, my studies have uncovered perturbation in the activity of ion channels, whose contribution to Ca^{2+} signaling is known to be significant. Many vasoconstrictors, like ANG II, 5-HT and NE stimulate the production of IP_3 in cells and cause vasoconstriction by activating the IP_3Rs (Exton, 1985; Alexander, et al., 1985; Nagahama et al., 2000). IP_3Rs create local Ca^{2+} transients having Ca^{2+} concentration of ~100μM and cause vasorelaxation by activating the BK_{Ca}-dependent hyperpolarizing (Patterson, Henrie-Olson & Brenner, 2002; Naraghi, M., & Neher, 1997; Ríos, E., & Stern, 1997). Considering BK_{Ca} channels are capable of reducing membrane voltage up to 20mV just from a single Ca^{2+} transient from the SR, loss of this communication between BK_{Ca} and IP_3R is significant regarding the development of hypercontractility and hypertrophy in SHR (Vetri et al., 2014).

My second novel finding was the loss of molecular coupling between BK_{Ca} and IP_3R in SHR VSM cells. My co-IP experiment revealed that the amount of IP_3R co-immunoprecipitating with BK_{Ca} channels in SHR was significantly lower compared to SD. This result indicates that BK_{Ca} and IP_3R are not as co-localized in SHR as in SD, which would significantly reduce BK_{Ca} activation in response to IP_3-induced SR Ca^{2+} release.

JPH2 is the predominantly expressed tethering protein in SR-PM junctions of VSM cells and has been proven to play a critical role in Ca^{2+} signaling and BK_{Ca} activity (Pritchard et al., 2019). However, there is no information regarding its expression in SHR VSM cells and its role in the development of hypertension in SHR. Using western blotting, my research has shown for the first time that JPH2 expression is not downregulated in SHR, despite the loss of BK_{Ca}-IP_3R molecular coupling. So, I explored the hypothesis that loss of palmitoylation may prevent JPH2 from binding to the PM and forming SR-PM coupling sites without affecting the expression of JPH2 protein. Through patch-clamp, western blot, and WST-1 proliferation assay, my studies have revealed that the loss of JPH2 palmitoylation significantly reduces BK_{Ca} activation in response to IP_3-induced SR Ca^{2+} release and increases VSM cell proliferation. Results from this

study will help understanding the role of protein palmitoylation in ion channel activity and raise questions regarding its role in hypertension.

An understanding of ion channel coupling under disease conditions may provide relevant caveats where BK_{Ca} channels are considered a therapeutic target in different cardiovascular disorders. I expect that the knowledge gained from my studies will fundamentally advance the field of ion channel-based therapeutics, especially in cardiovascular disorders.

REFERENCES

Abou-Saleh, H., Pathan, A. R., Daalis, A., Hubrack, S., Abou-Jassoum, H., Al-Naeimi, H., et al. (2013). Inositol 1,4,5-trisphosphate (IP3) receptor up-regulation in hypertension is associated with sensitization of Ca^{2+} release and vascular smooth muscle contractility. *J. Biol. Chem*. 288, 32941–32951. doi: 10.1074/jbc.M113.496802

Adebiyi, A., Zhao, G., Narayanan, D., Thomas-Gatewood, C. M., Bannister, J. P., & Jaggar, J. H. (2010). Isoform-selective physical coupling of TRPC3 channels to IP3 receptors in smooth muscle cells regulates arterial contractility. *Circulation research*, *106*(10), 1603–1612. https://doi.org/10.1161/CIRCRESAHA.110.216804

Adelman, J. P., Shen, K. Z., Kavanaugh, M. P., Warren, R. A., Wu, Y. N., Lagrutta, A., Bond, C. T., & North, R. A. (1992). Calcium-activated potassium channels expressed from cloned complementary DNAs. *Neuron*, *9*(2), 209–216. https://doi.org/10.1016/0896-6273(92)90160-f

Alexander, R. W., Brock, T. A., Gimbrone, M. A., Jr, & Rittenhouse, S. E. (1985). Angiotensin increases inositol trisphosphate and calcium in vascular smooth muscle. *Hypertension (Dallas, Tex.: 1979)*, *7*(3 Pt 1), 447–451.

Allen, B. G., & Walsh, M. P. (1994). The biochemical basis of the regulation of smooth-muscle contraction. *Trends in biochemical sciences*, *19*(9), 362–368. https://doi.org/10.1016/0968-0004(94)90112-0

Almassy, J., & Begenisich, T. (2012). The LRRC26 protein selectively alters the efficacy of BK channel activators. *Molecular pharmacology*, *81*(1), 21–30. https://doi.org/10.1124/mol.111.075234

Atkinson, N. S., Robertson, G. A., & Ganetzky, B. (1991). A component of calcium-activated potassium channels encoded by the Drosophila slo locus. *Science (New York, N.Y.)*, *253*(5019), 551–555. https://doi.org/10.1126/science.1857984

Bentzen, B. H., Olesen, S. P., Rønn, L. C., & Grunnet, M. (2014). BK channel activators and their therapeutic perspectives. *Frontiers in physiology*, *5*, 389. https://doi.org/10.3389/fphys.2014.00389

Berkefeld, H., Sailer, C. A., Bildl, W., Rohde, V., Thumfart, J. O., Eble, S., Klugbauer, N., Reisinger, E., Bischofberger, J., Oliver, D., Knaus, H. G., Schulte, U., & Fakler, B. (2006). BKCa-Cav channel complexes mediate rapid and localized Ca2+-activated K+ signaling. *Science (New York, N.Y.)*, *314*(5799), 615–620. https://doi.org/10.1126/science.1132915

Berridge M. J. (1993). Inositol trisphosphate and calcium signalling. *Nature*, *361*(6410), 315–325. https://doi.org/10.1038/361315a0

Berridge M. J. (2016). The Inositol Trisphosphate/Calcium Signaling Pathway in Health and Disease. *Physiological reviews*, *96*(4), 1261–1296. https://doi.org/10.1152/physrev.00006.2016

Berridge, M. J., Lipp, P., & Bootman, M. D. (2000). The versatility and universality of calcium signalling. *Nature reviews. Molecular cell biology*, *1*(1), 11–21. https://doi.org/10.1038/35036035

Boittin, F. X., Macrez, N., Halet, G., and Mironneau, J. (1999). Norepinephrine-induced Ca^{2+} waves depend on InsP(3) and ryanodine receptor activation in vascular myocytes. *Am. J. Physiol.* 277(1 Pt 1), C139–C151. doi: 10.1152/ajpcell.1999.277.1.C139

Bosanac, I., Michikawa, T., Mikoshiba, K., & Ikura, M. (2004). Structural insights into the regulatory mechanism of IP3 receptor. *Biochimica et biophysica acta*, *1742*(1-3), 89–102. https://doi.org/10.1016/j.bbamcr.2004.09.016

Brayden, J. E., & Nelson, M. T. (1992). Regulation of arterial tone by activation of calcium-dependent potassium channels. *Science (New York, N.Y.)*, *256*(5056), 532–535. https://doi.org/10.1126/science.1373909

Breckenridge, Ross. (2013). Animal Models of Myocardial Disease. Animal Models for the Study of Human Disease. 145-171. 10.1016/B978-0-12-415894-8.00007-5.

Brenner, R., Jegla, T. J., Wickenden, A., Liu, Y., & Aldrich, R. W. (2000). Cloning and functional characterization of novel large conductance calcium-activated potassium channel beta subunits, hKCNMB3 and hKCNMB4. *The Journal of biological chemistry*, *275*(9), 6453–6461. https://doi.org/10.1074/jbc.275.9.6453

Brenner, R., Peréz, G. J., Bonev, A. D., Eckman, D. M., Kosek, J. C., Wiler, S. W., Patterson, A. J., Nelson, M. T., & Aldrich, R. W. (2000). Vasoregulation by the beta1 subunit of the calcium-activated potassium channel. *Nature*, *407*(6806), 870–876. https://doi.org/10.1038/35038011

Brigidi, G. S., & Bamji, S. X. (2013). Detection of protein palmitoylation in cultured hippocampal neurons by immunoprecipitation and acyl-biotin exchange (ABE). *Journal of visualized experiments : JoVE*, (72), 50031. https://doi.org/10.3791/50031

Brisset, A. C., Hao, H., Camenzind, E., Bacchetta, M., Geinoz, A., Sanchez, J. C., Chaponnier, C., Gabbiani, G., & Bochaton-Piallat, M. L. (2007). Intimal smooth muscle cells of porcine and human coronary artery express S100A4, a marker of the rhomboid phenotype in vitro. *Circulation research*, *100*(7), 1055–1062. https://doi.org/10.1161/01.RES.0000262654.84810.6c

Brown, I., Diederich, L., Good, M. E., DeLalio, L. J., Murphy, S. A., Cortese-Krott, M. M., Hall, J. L., Le, T. H., & Isakson, B. E. (2018). Vascular Smooth Muscle Remodeling in Conductive and Resistance Arteries in Hypertension. *Arteriosclerosis, thrombosis, and vascular biology*, *38*(9), 1969–1985. https://doi.org/10.1161/ATVBAHA.118.311229

Brozovich, F. V., Nicholson, C. J., Degen, C. V., Gao, Y. Z., Aggarwal, M., & Morgan, K. G. (2016). Mechanisms of Vascular Smooth Muscle Contraction and the Basis for Pharmacologic Treatment of Smooth Muscle Disorders. *Pharmacological reviews*, *68*(2), 476–532. https://doi.org/10.1124/pr.115.010652

Butler, A., Tsunoda, S., McCobb, D. P., Wei, A., & Salkoff, L. (1993). mSlo, a complex mouse gene encoding "maxi" calcium-activated potassium channels. *Science (New York, N.Y.)*, *261*(5118), 221–224. https://doi.org/10.1126/science.7687074

Cárdenas, C., Müller, M., McNeal, A., Lovy, A., Jaňa, F., Bustos, G., Urra, F., Smith, N., Molgó, J., Diehl, J. A., Ridky, T. W., & Foskett, J. K. (2016). Selective Vulnerability of Cancer Cells by Inhibition of Ca(2+) Transfer from Endoplasmic Reticulum to Mitochondria. *Cell reports*, *14*(10), 2313–2324. https://doi.org/10.1016/j.celrep.2016.02.030

Catterall W. A., Swanson T. M. (2015). Structural basis for pharmacology of voltage-gated sodium and calcium channels. *Mol. Pharmacol.* 88 141–150. 10.1124/mol.114.097659

Chai, Q., Wang, X. L., Zeldin, D. C., & Lee, H. C. (2013). Role of caveolae in shear stress-mediated endothelium-dependent dilation in coronary arteries. *Cardiovascular research*, *100*(1), 151–159. https://doi.org/10.1093/cvr/cvt157

Chang, C. L., Chen, Y. J., & Liou, J. (2017). ER-plasma membrane junctions: Why and how do we study them?. Biochimica et biophysica acta. Molecular cell research, 1864(9), 1494–1506. https://doi.org/10.1016/j.bbamcr.2017.05.018

Chang, C. L., Hsieh, T. S., Yang, T. T., Rothberg, K. G., Azizoglu, D. B., Volk, E., Liao, J. C., & Liou, J. (2013). Feedback regulation of receptor-induced Ca2+ signaling mediated by E-Syt1 and Nir2 at endoplasmic reticulum-plasma membrane junctions. *Cell reports*, *5*(3), 813–825. https://doi.org/10.1016/j.celrep.2013.09.038

Chang, H. R., Lee, R. P., Wu, C. Y., & Chen, H. I. (2002). Nitric oxide in mesenteric vascular reactivity: a comparison between rats with normotension and hypertension. *Clinical and experimental pharmacology & physiology*, *29*(4), 275–280. https://doi.org/10.1046/j.1440-1681.2002.03643.x

Chen, Y. W., Chen, Y. F., Chen, Y. T., Chiu, W. T., & Shen, M. R. (2016). The STIM1-Orai1 pathway of store-operated Ca2+ entry controls the checkpoint in cell cycle G1/S transition. *Scientific reports*, *6*, 22142. https://doi.org/10.1038/srep22142

Chen M., Petkov G. V. (2009). Identification of large conductance calcium activated potassium channel accessory beta4 subunit in rat and mouse bladder smooth muscle. J. Urol. 182, 374–381 10.1016/j.juro.2009.02.109

Chen, Y. J., Quintanilla, C. G., & Liou, J. (2019). Recent insights into mammalian ER-PM junctions. *Current opinion in cell biology*, *57*, 99–105. https://doi.org/10.1016/j.ceb.2018.12.011

Christensen KL, Mulvany MJ. Mesenteric arcade arteries contribute substantially to vascular resistance in conscious rats. *J Vasc Res*. 1993;30:73–9.

Chung, J., Torta, F., Masai, K., Lucast, L., Czapla, H., Tanner, L. B., Narayanaswamy, P., Wenk, M. R., Nakatsu, F., & De Camilli, P. (2015). INTRACELLULAR TRANSPORT. PI4P/phosphatidylserine countertransport at ORP5- and ORP8-mediated ER-plasma membrane contacts. *Science (New York, N.Y.)*, *349*(6246), 428–432. https://doi.org/10.1126/science.aab1370

Collier, M. L., Ji, G., Wang, Y., & Kotlikoff, M. I. (2000). Calcium-induced calcium release in smooth muscle: loose coupling between the action potential and calcium release. *The Journal of general physiology*, *115*(5), 653–662. https://doi.org/10.1085/jgp.115.5.653

Contreras, G. F., Castillo, K., Enrique, N., Carrasquel-Ursulaez, W., Castillo, J. P., Milesi, V., Neely, A., Alvarez, O., Ferreira, G., González, C., & Latorre, R. (2013). A BK (Slo1) channel journey from molecule to physiology. *Channels (Austin, Tex.)*, *7*(6), 442–458. https://doi.org/10.4161/chan.26242

Cox, D. H., & Aldrich, R. W. (2000). Role of the beta1 subunit in large-conductance Ca(2+)-activated K(+) channel gating energetics. Mechanisms of enhanced Ca(2+) sensitivity. *The Journal of general physiology*, *116*(3), 411–432. https://doi.org/10.1085/jgp.116.3.411

De Vos, K. J., Mórotz, G. M., Stoica, R., Tudor, E. L., Lau, K. F., Ackerley, S., Warley, A., Shaw, C. E., & Miller, C. C. (2012). VAPB interacts with the mitochondrial protein PTPIP51 to regulate calcium homeostasis. *Human molecular genetics*, *21*(6), 1299–1311. https://doi.org/10.1093/hmg/ddr559

Ducker, C. E., Griffel, L. K., Smith, R. A., Keller, S. N., Zhuang, Y., Xia, Z., Diller, J. D., & Smith, C. D. (2006). Discovery and characterization of inhibitors of human palmitoyl acyltransferases. *Molecular cancer therapeutics*, *5*(7), 1647–1659. https://doi.org/10.1158/1535-7163.MCT-06-0114

Dupont, G., Combettes, L., Bird, G. S., & Putney, J. W. (2011). Calcium oscillations. *Cold Spring Harbor perspectives in biology*, *3*(3), a004226. https://doi.org/10.1101/cshperspect.a004226

Draper, J. M., & Smith, C. D. (2009). Palmitoyl acyltransferase assays and inhibitors (Review). *Molecular membrane biology*, *26*(1), 5–13. https://doi.org/10.1080/09687680802683839

Echevarría, W., Leite, M. F., Guerra, M. T., Zipfel, W. R., & Nathanson, M. H. (2003). Regulation of calcium signals in the nucleus by a nucleoplasmic reticulum. *Nature cell biology*, *5*(5), 440–446. https://doi.org/10.1038/ncb980

Elmarakby, A. A., & Sullivan, J. C. (2021). Sex differences in hypertension: lessons from spontaneously hypertensive rats (SHR). *Clinical science (London, England : 1979)*, *135*(15), 1791–1804. https://doi.org/10.1042/CS20201017

Endemann, D., Touyz, R. M., Li, J. S., Deng, L. Y., & Schiffrin, E. L. (1999). Altered angiotensin II-induced small artery contraction during the development of hypertension in spontaneously hypertensive rats. *American journal of hypertension*, *12*(7), 716–723. https://doi.org/10.1016/s0895-7061(99)00036-9

Endo M. (2009). Calcium-induced calcium release in skeletal muscle. *Physiological reviews*, *89*(4), 1153–1176. https://doi.org/10.1152/physrev.00040.2008

Exton J. H. (1985). Mechanisms involved in alpha-adrenergic phenomena. *The American journal of physiology*, *248*(6 Pt 1), E633–E647. https://doi.org/10.1152/ajpendo.1985.248.6.E633

Fan, G., Baker, M. R., Wang, Z., Seryshev, A. B., Ludtke, S. J., Baker, M. L., & Serysheva, I. I. (2018). Cryo-EM reveals ligand induced allostery underlying $InsP_3R$ channel gating. *Cell research*, *28*(12), 1158–1170. https://doi.org/10.1038/s41422-018-0108-5

Fan, G., Baker, M. L., Wang, Z., Baker, M. R., Sinyagovskiy, P. A., Chiu, W., Ludtke, S. J., & Serysheva, I. I. (2015). Gating machinery of InsP3R channels revealed by electron cryomicroscopy. *Nature*, *527*(7578), 336–341. https://doi.org/10.1038/nature15249

Fernández-Busnadiego, R., Saheki, Y., & De Camilli, P. (2015). Three-dimensional architecture of extended synaptotagmin-mediated endoplasmic reticulum-plasma membrane contact sites. *Proceedings of the National Academy of Sciences of the United States of America*, *112*(16), E2004–E2013. https://doi.org/10.1073/pnas.1503191112

Ferris, C. D., Cameron, A. M., Bredt, D. S., Huganir, R. L., & Snyder, S. H. (1991). Inositol 1,4,5-trisphosphate receptor is phosphorylated by cyclic AMP-dependent protein kinase at serines 1755 and 1589. *Biochemical and biophysical research communications*, *175*(1), 192–198. https://doi.org/10.1016/s0006-291x(05)81219-7

Ferris, C. D., Huganir, R. L., & Snyder, S. H. (1990). Calcium flux mediated by purified inositol 1,4,5-trisphosphate receptor in reconstituted lipid vesicles is allosterically regulated by adenine nucleotides. *Proceedings of the National Academy of Sciences of the United States of America*, *87*(6), 2147–2151. https://doi.org/10.1073/pnas.87.6.2147

Fill, M., & Copello, J. A. (2002). Ryanodine receptor calcium release channels. *Physiological reviews*, *82*(4), 893–922. https://doi.org/10.1152/physrev.00013.2002

Finkel T. (1999). Myocyte hypertrophy: the long and winding RhoA'd. The Journal of clinical investigation, 103(12), 1619–1620. https://doi.org/10.1172/JCI7459

Flynn, G. E., & Zagotta, W. N. (2001). Conformational changes in S6 coupled to the opening of cyclic nucleotide-gated channels. *Neuron*, *30*(3), 689–698. https://doi.org/10.1016/s0896-6273(01)00324-5

Foskett, J. K., White, C., Cheung, K. H., & Mak, D. O. (2007). Inositol trisphosphate receptor Ca^{2+} release channels. *Physiological reviews*, *87*(2), 593–658. https://doi.org/10.1152/physrev.00035.2006

Fox, P. D., Haberkorn, C. J., Akin, E. J., Seel, P. J., Krapf, D., & Tamkun, M. M. (2015). Induction of stable ER-plasma-membrane junctions by Kv2.1 potassium channels. *Journal of cell science*, *128*(11), 2096–2105. https://doi.org/10.1242/jcs.166009

Futatsugi, A., Nakamura, T., Yamada, M. K., Ebisui, E., Nakamura, K., Uchida, K., Kitaguchi, T., Takahashi-Iwanaga, H., Noda, T., Aruga, J., & Mikoshiba, K. (2005). IP3 receptor types 2 and 3 mediate exocrine secretion underlying energy metabolism. *Science (New York, N.Y.)*, *309*(5744), 2232–2234. https://doi.org/10.1126/science.1114110

Gada, K. D., & Logothetis, D. E. (2022). Protein Kinase C regulation of ion channels: the involvement of PIP_2. *The Journal of biological chemistry*, 102035. Advance online publication. https://doi.org/10.1016/j.jbc.2022.102035

Garbino, A., van Oort, R. J., Dixit, S. S., Landstrom, A. P., Ackerman, M. J., & Wehrens, X. H. (2009). Molecular evolution of the junctophilin gene family. *Physiological genomics*, *37*(3), 175–186. https://doi.org/10.1152/physiolgenomics.00017.2009

Garbino, A., & Wehrens, X. H. (2010). Emerging role of junctophilin-2 as a regulator of calcium handling in the heart. *Acta pharmacologica Sinica*, *31*(9), 1019–1021. https://doi.org/10.1038/aps.2010.116

Giordano, F., Saheki, Y., Idevall-Hagren, O., Colombo, S. F., Pirruccello, M., Milosevic, I., Gracheva, E. O., Bagriantsev, S. N., Borgese, N., & De Camilli, P. (2013). PI(4,5)P(2)-dependent and Ca(2+)-regulated ER-PM interactions mediated by the extended synaptotagmins. *Cell*, *153*(7), 1494–1509. https://doi.org/10.1016/j.cell.2013.05.026

Grayson, T. H., Haddock, R. E., Murray, T. P., Wojcikiewicz, R. J., & Hill, C. E. (2004). Inositol 1,4,5-trisphosphate receptor subtypes are differentially distributed between smooth muscle and endothelial layers of rat arteries. *Cell calcium*, *36*(6), 447–458. https://doi.org/10.1016/j.ceca.2004.04.005

Henkart, M., Landis, D. M., & Reese, T. S. (1976). Similarity of junctions between plasma membranes and endoplasmic reticulum in muscle and neurons. *The Journal of cell biology*, *70*(2 pt 1), 338–347. https://doi.org/10.1083/jcb.70.2.338

Henning, R. J., Bourgeois, M., & Harbison, R. D. (2018). Poly(ADP-ribose) Polymerase (PARP) and PARP Inhibitors: Mechanisms of Action and Role in Cardiovascular Disorders. *Cardiovascular toxicology*, *18*(6), 493–506. https://doi.org/10.1007/s12012-018-9462-2

Hermann, A., Sitdikova, G. F., & Weiger, T. M. (2015). Oxidative Stress and Maxi Calcium-Activated Potassium (BK) Channels. *Biomolecules*, *5*(3), 1870–1911. https://doi.org/10.3390/biom5031870

Hibino H., Inanobe A., Furutani K., Murakami S., Findlay I., Kurachi Y. (2010). Inwardly rectifying potassium channels: their structure, function, and physiological roles. *Physiol. Rev*. 90 291–366. 10.1152/physrev.00021.2009

Hill, M. A., & Meininger, G. A. (2016). Small artery mechanobiology: Roles of cellular and non-cellular elements. *Microcirculation (New York, N.Y. : 1994)*, *23*(8), 611–613. https://doi.org/10.1111/micc.12323

Hill, M. A., Zou, H., Potocnik, S. J., Meininger, G. A., and Davis, M. J. (2001). Arteriolar smooth muscle mechanotransduction: Ca^{2+} signaling pathways underlying myogenic reactivity. *J. Appl. Physiol.* 91, 973–983. doi: 10.1152/jappl.2001.91.2.973

Hirota, J., Furuichi, T., & Mikoshiba, K. (1999). Inositol 1,4,5-trisphosphate receptor type 1 is a substrate for caspase-3 and is cleaved during apoptosis in a caspase-3-dependent manner. *The Journal of biological chemistry*, *274*(48), 34433–34437. https://doi.org/10.1074/jbc.274.48.34433

Hristov K. L., Afeli S. A. Y., Parajuli S. P., Cheng Q., Rovner E. S., Petkov G. V. (2013). Neurogenic detrusor overactivity is associated with decreased expression and function of the large conductance voltage- and Ca(2+)-activated K(+) channels. PLoS ONE 8:e68052 10.1371/journal.pone.0068052

Huang, S. M., Wu, Y. L., Peng, S. L., Peng, H. H., Huang, T. Y., Ho, K. C., & Wang, F. N. (2016). Inter-Strain Differences in Default Mode Network: A Resting State fMRI Study on Spontaneously Hypertensive Rat and Wistar Kyoto Rat. *Scientific reports*, *6*, 21697. https://doi.org/10.1038/srep21697

Hutchings, C. J., Colussi, P., & Clark, T. G. (2019). Ion channels as therapeutic antibody targets. *mAbs*, *11*(2), 265–296. https://doi.org/10.1080/19420862.2018.1548232

Intengan, H. D., & Schiffrin, E. L. (2000). Structure and mechanical properties of resistance arteries in hypertension: role of adhesion molecules and extracellular matrix determinants. *Hypertension (Dallas, Tex. : 1979)*, *36*(3), 312–318. https://doi.org/10.1161/01.hyp.36.3.312

Iwai, M., Tateishi, Y., Hattori, M., Mizutani, A., Nakamura, T., Futatsugi, A., Inoue, T., Furuichi, T., Michikawa, T., & Mikoshiba, K. (2005). Molecular cloning of mouse type 2 and type 3 inositol 1,4,5-trisphosphate receptors and identification of a novel type 2 receptor splice variant. *The Journal of biological chemistry*, *280*(11), 10305–10317. https://doi.org/10.1074/jbc.M413824200

Jackson W. F. (2005). Potassium channels in the peripheral microcirculation. *Microcirculation (New York, N.Y. : 1994)*, *12*(1), 113–127. https://doi.org/10.1080/10739680590896072

Jackson W. F. (2017). Potassium Channels in Regulation of Vascular Smooth Muscle Contraction and Growth. *Advances in pharmacology (San Diego, Calif.)*, *78*, 89–144. https://doi.org/10.1016/bs.apha.2016.07.001

Jadeja, R. N., Rachakonda, V., Bagi, Z., & Khurana, S. (2015). Assessing Myogenic Response and Vasoactivity In Resistance Mesenteric Arteries Using Pressure Myography. *Journal of visualized experiments: JoVE*, (101), e50997. https://doi.org/10.3791/50997

Jaggar, J. H., and Nelson, M. T. (2000). Differential regulation of Ca^{2+} sparks and Ca^{2+} waves by UTP in rat cerebral artery smooth muscle cells. *Am. J. Physiol. Cell Physiol.* 279, C1528–C1539. doi: 10.1152/ajpcell.2000.279.5.C1528

Jaggar, J. H., Porter, V. A., Lederer, W. J., & Nelson, M. T. (2000). Calcium sparks in smooth muscle. *American journal of physiology. Cell physiology*, *278*(2), C235–C256. https://doi.org/10.1152/ajpcell.2000.278.2.C235

Jayasinghe, I. D., Baddeley, D., Kong, C. H., Wehrens, X. H., Cannell, M. B., & Soeller, C. (2012). Nanoscale organization of junctophilin-2 and ryanodine receptors within peripheral couplings of rat ventricular cardiomyocytes. *Biophysical journal*, *102*(5), L19–L21. https://doi.org/10.1016/j.bpj.2012.01.034

Jiang, M., Hu, J., White, F., Williamson, J., Klymchenko, A. S., Murthy, A., Workman, S. W., & Tseng, G. N. (2019). *S*-Palmitoylation of junctophilin-2 is critical for its role in tethering the sarcoplasmic reticulum to the plasma membrane. *The Journal of biological chemistry*, *294*(36), 13487–13501. https://doi.org/10.1074/jbc.RA118.006772

Johnson, B., Leek, A. N., Solé, L., Maverick, E. E., Levine, T. P., & Tamkun, M. M. (2018). Kv2 potassium channels form endoplasmic reticulum/plasma membrane junctions via interaction with VAPA and VAPB. *Proceedings of the National Academy of Sciences of the United States of America*, *115*(31), E7331–E7340. https://doi.org/10.1073/pnas.1805757115

Kasri, N. N., Bultynck, G., Smyth, J., Szlufcik, K., Parys, J. B., Callewaert, G., Missiaen, L., Fissore, R. A., Mikoshiba, K., & de Smedt, H. (2004). The N-terminal Ca2+-independent calmodulin-binding site on the inositol 1,4,5-trisphosphate receptor is responsible for calmodulin inhibition, even though this inhibition requires Ca2+. *Molecular pharmacology*, *66*(2), 276–284. https://doi.org/10.1124/mol.66.2.276

Kheifets, V., & Mochly-Rosen, D. (2007). Insight into intra- and inter-molecular interactions of PKC: design of specific modulators of kinase function. *Pharmacological research*, *55*(6), 467–476. https://doi.org/10.1016/j.phrs.2007.04.014

Koga, T., Yoshida, Y., Cai, J. Q., Islam, M. O., & Imai, S. (1994). Purification and characterization of 240-kDa cGMP-dependent protein kinase substrate of vascular smooth muscle. Close resemblance to inositol 1,4,5-trisphosphate receptor. *The Journal of biological chemistry*, *269*(15), 11640–11647.

Koval, O. M., Fan, Y., & Rothberg, B. S. (2007). A role for the S0 transmembrane segment in voltage-dependent gating of BK channels. *The Journal of general physiology*, *129*(3), 209–220. https://doi.org/10.1085/jgp.200609662

Kume, S., Muto, A., Inoue, T., Suga, K., Okano, H., & Mikoshiba, K. (1997). Role of inositol 1,4,5-trisphosphate receptor in ventral signaling in Xenopus embryos. *Science (New York, N.Y.)*, *278*(5345), 1940–1943. https://doi.org/10.1126/science.278.5345.1940

Landstrom, A. P., Beavers, D. L., & Wehrens, X. H. (2014). The junctophilin family of proteins: from bench to bedside. *Trends in molecular medicine*, *20*(6), 353–362. https://doi.org/10.1016/j.molmed.2014.02.004

Landstrom, A. P., Weisleder, N., Batalden, K. B., Bos, J. M., Tester, D. J., Ommen, S. R., Wehrens, X. H., Claycomb, W. C., Ko, J. K., Hwang, M., Pan, Z., Ma, J., & Ackerman, M. J. (2007). Mutations in JPH2-encoded junctophilin-2 associated with hypertrophic cardiomyopathy in humans. *Journal of molecular and cellular cardiology*, *42*(6), 1026–1035. https://doi.org/10.1016/j.yjmcc.2007.04.006

Lawes, C. M., Vander Hoorn, S., Rodgers, A., & International Society of Hypertension (2008). Global burden of blood-pressure-related disease, 2001. *Lancet (London, England)*, *371*(9623), 1513–1518. https://doi.org/10.1016/S0140-6736(08)60655-8

Lee, U. S., & Cui, J. (2010). BK channel activation: structural and functional insights. *Trends in neurosciences*, *33*(9), 415–423. https://doi.org/10.1016/j.tins.2010.06.004

Lewis R. S. (2011). Store-operated calcium channels: new perspectives on mechanism and function. *Cold Spring Harbor perspectives in biology*, *3*(12), a003970. https://doi.org/10.1101/cshperspect.a003970

Li, Q., & Yan, J. (2016). Modulation of BK Channel Function by Auxiliary Beta and Gamma Subunits. *International review of neurobiology*, *128*, 51–90. https://doi.org/10.1016/bs.irn.2016.03.015

Libby P. (2002). Inflammation in atherosclerosis. *Nature*, *420*(6917), 868–874. https://doi.org/10.1038/nature01323

Lim, S. T., Antonucci, D. E., Scannevin, R. H., & Trimmer, J. S. (2000). A novel targeting signal for proximal clustering of the Kv2.1 K+ channel in hippocampal neurons. *Neuron*, *25*(2), 385–397. https://doi.org/10.1016/s0896-6273(00)80902-2

Lin, Q., Zhao, G., Fang, X., Peng, X., Tang, H., Wang, H., Jing, R., Liu, J., Lederer, W. J., Chen, J., & Ouyang, K. (2016). IP_3 receptors regulate vascular smooth muscle contractility and hypertension. *JCI insight*, *1*(17), e89402. https://doi.org/10.1172/jci.insight.89402

Linde, C. I., Karashima, E., Raina, H., Zulian, A., Wier, W. G., Hamlyn, J. M., et al. (2012). Increased arterial smooth muscle Ca^{2+} signaling, vasoconstriction, and myogenic reactivity in Milan hypertensive rats. *Am. J. Physiol. Heart Circ. Physiol.* 302, H611–H620. doi: 10.1152/ajpheart.00950.2011

Lino Cardenas, C. L., Kessinger, C. W., Cheng, Y., MacDonald, C., MacGillivray, T., Ghoshhajra, B., Huleihel, L., Nuri, S., Yeri, A. S., Jaffer, F. A., Kaminski, N., Ellinor, P., Weintraub, N. L., Malhotra, R., Isselbacher, E. M., & Lindsay, M. E. (2018). An HDAC9-MALAT1-BRG1 complex mediates smooth muscle dysfunction in thoracic aortic aneurysm. *Nature communications*, *9*(1), 1009. https://doi.org/10.1038/s41467-018-03394-7

Lovell, P. V., & McCobb, D. P. (2001). Pituitary control of BK potassium channel function and intrinsic firing properties of adrenal chromaffin cells. The Journal of neuroscience : the official journal of the Society for Neuroscience, 21(10), 3429–3442. https://doi.org/10.1523/JNEUROSCI.21-10-03429.2001

Manford A. G., Stefan C. J., Yuan H. L., Macgurn J. A., and Emr S. D. (2012) ER-to-plasma membrane tethering proteins regulate cell signaling and ER morphology. *Dev. Cell* 23, 1129–1140 10.1016/j.devcel.2012.11.004

Marban, E., & Koretsune, Y. (1990). Cell calcium, oncogenes, and hypertrophy. *Hypertension (Dallas, Tex. : 1979)*, *15*(6 Pt 1), 652–658. https://doi.org/10.1161/01.hyp.15.6.652

Marche, P., Herembert, T., & Zhu, D. L. (1995). Molecular mechanisms of vascular hypertrophy in the spontaneously hypertensive rat. *Clinical and experimental pharmacology & physiology. Supplement*, *22*(1), S114–S116. https://doi.org/10.1111/j.1440-1681.1995.tb02844.x

Marty A. (1981). Ca-dependent K channels with large unitary conductance in chromaffin cell membranes. *Nature*, *291*(5815), 497–500. https://doi.org/10.1038/291497a0

Matsumoto, T., Kobayashi, T., Ishida, K., Taguchi, K., & Kamata, K. (2010). Enhancement of mesenteric artery contraction to 5-HT depends on Rho kinase and Src kinase pathways in the ob/ob mouse model of type 2 diabetes. British journal of pharmacology, 160(5), 1092–1104. https://doi.org/10.1111/j.1476-5381.2010.00753.x

Mayet, J., & Hughes, A. (2003). Cardiac and vascular pathophysiology in hypertension. *Heart (British Cardiac Society)*, *89*(9), 1104–1109. https://doi.org/10.1136/heart.89.9.1104

McManus, O. B., Helms, L. M., Pallanck, L., Ganetzky, B., Swanson, R., & Leonard, R. J. (1995). Functional role of the beta subunit of high conductance calcium-activated potassium channels. *Neuron*, *14*(3), 645–650. https://doi.org/10.1016/0896-6273(95)90321-6

Minamisawa, S., Oshikawa, J., Takeshima, H., Hoshijima, M., Wang, Y., Chien, K. R., Ishikawa, Y., & Matsuoka, R. (2004). Junctophilin type 2 is associated with caveolin-3 and is down-regulated in the hypertrophic and dilated cardiomyopathies. *Biochemical and biophysical research communications*, *325*(3), 852–856. https://doi.org/10.1016/j.bbrc.2004.10.107

Moczydlowski E. G. (2004). BK channel news: full coverage on the calcium bowl. *The Journal of general physiology*, *123*(5), 471–473. https://doi.org/10.1085/jgp.200409069

Modgil, A., Guo, L., O'Rourke, S. T., & Sun, C. (2013). Apelin-13 inhibits large-conductance Ca^{2+}-activated K+ channels in cerebral artery smooth muscle cells via a PI3-kinase dependent mechanism. *PloS one*, *8*(12), e83051. https://doi.org/10.1371/journal.pone.0083051

Morrow, J. P., Zakharov, S. I., Liu, G., Yang, L., Sok, A. J., & Marx, S. O. (2006). Defining the BK channel domains required for beta1-subunit modulation. *Proceedings of the National Academy of Sciences of the United States of America*, *103*(13), 5096–5101. https://doi.org/10.1073/pnas.0600907103

Mound, A., Rodat-Despoix, L., Bougarn, S., Ouadid-Ahidouch, H., & Matifat, F. (2013). Molecular interaction and functional coupling between type 3 inositol 1,4,5-trisphosphate receptor and BK_{ca} channel stimulate breast cancer cell proliferation. *European journal of cancer (Oxford, England : 1990)*, *49*(17), 3738–3751. https://doi.org/10.1016/j.ejca.2013.07.013

Muthalif, M. M., Karzoun, N. A., Benter, I. F., Gaber, L., Ljuca, F., Uddin, M. R., Khandekar, Z., Estes, A., & Malik, K. U. (2002). Functional significance of activation of calcium/calmodulin-dependent protein kinase II in angiotensin II--induced vascular hyperplasia and hypertension. *Hypertension (Dallas, Tex.: 1979)*, *39*(2 Pt 2), 704–709. https://doi.org/10.1161/hy0202.103823

Naito Y, Yoshida H, Konishi C, Ohara N. Differences in responses to norepinephrine and adenosine triphosphate in isolated perfused mesenteric vascular beds between normotensive and spontaneously hypertensive rats. *J. Cardiovasc. Pharmacol.* 1998;32:807–818.

Nagahama, T., Hayashi, K., Ozawa, Y., Takenaka, T., & Saruta, T. (2000). Role of protein kinase C in angiotensin II-induced constriction of renal microvessels. *Kidney international*, *57*(1), 215–223. https://doi.org/10.1046/j.1523-1755.2000.00822.x

Naraghi, M., & Neher, E. (1997). Linearized buffered Ca^{2+} diffusion in microdomains and its implications for calculation of [Ca^{2+}] at the mouth of a calcium channel. *The Journal of neuroscience : the official journal of the Society for Neuroscience*, *17*(18), 6961–6973. https://doi.org/10.1523/JNEUROSCI.17-18-06961.1997

Nimigean, C. M., & Magleby, K. L. (1999). The beta subunit increases the Ca2+ sensitivity of large conductance Ca2+-activated potassium channels by retaining the gating in the bursting states. *The Journal of general physiology*, *113*(3), 425–440. https://doi.org/10.1085/jgp.113.3.425

Nishi, M., Sakagami, H., Komazaki, S., Kondo, H., & Takeshima, H. (2003). Coexpression of junctophilin type 3 and type 4 in brain. *Brain research. Molecular brain research*, *118*(1-2), 102–110. https://doi.org/10.1016/s0169-328x(03)00341-3

Orci, L., Ravazzola, M., Le Coadic, M., Shen, W. W., Demaurex, N., & Cosson, P. (2009). From the Cover: STIM1-induced precortical and cortical subdomains of the endoplasmic reticulum. *Proceedings of the National Academy of Sciences of the United States of America*, *106*(46), 19358–19362. https://doi.org/10.1073/pnas.0911280106

Paknejad, N., & Hite, R. K. (2018). Structural basis for the regulation of inositol trisphosphate receptors by Ca^{2+} and IP_3. *Nature structural & molecular biology*, *25*(8), 660–668. https://doi.org/10.1038/s41594-018-0089-6

Patterson, A. J., Henrie-Olson, J., & Brenner, R. (2002). Vasoregulation at the molecular level: a role for the beta1 subunit of the calcium-activated potassium (BK) channel. *Trends in cardiovascular medicine*, *12*(2), 78–82. https://doi.org/10.1016/s1050-1738(01)00146-3

Petersen, O. H., Courjaret, R., & Machaca, K. (2017). Ca2+ tunnelling through the ER lumen as a mechanism for delivering Ca2+ entering via store-operated Ca2+ channels to specific target sites. The Journal of physiology, 595(10), 2999–3014. https://doi.org/10.1113/JP272772

Petkov G. V. (2014). Central role of the BK channel in urinary bladder smooth muscle physiology and pathophysiology. *American journal of physiology. Regulatory, integrative and comparative physiology*, *307*(6), R571–R584. https://doi.org/10.1152/ajpregu.00142.2014

Piskorowski, R., & Aldrich, R. W. (2002). Calcium activation of BK_{ca} potassium channels lacking the calcium bowl and RCK domains. *Nature*, *420*(6915), 499–502. https://doi.org/10.1038/nature01199

Piskorowski, R. A., & Aldrich, R. W. (2006). Relationship between pore occupancy and gating in BK potassium channels. *The Journal of general physiology*, *127*(5), 557–576. https://doi.org/10.1085/jgp.200509482

Plüger, S., Faulhaber, J., Fürstenau, M., Löhn, M., Waldschütz, R., Gollasch, M., Haller, H., Luft, F. C., Ehmke, H., & Pongs, O. (2000). Mice with disrupted BK channel beta1 subunit gene feature abnormal Ca(2+) spark/STOC coupling and elevated blood pressure. *Circulation research*, *87*(11), E53–E60. https://doi.org/10.1161/01.res.87.11.e53

Popescu, L. M., Gherghiceanu, M., Mandache, E., & Cretoiu, D. (2006). Caveolae in smooth muscles: nanocontacts. *Journal of cellular and molecular medicine*, *10*(4), 960–990. https://doi.org/10.1111/j.1582-4934.2006.tb00539.x

Poteser, M., Leitinger, G., Pritz, E., Platzer, D., Frischauf, I., Romanin, C., & Groschner, K. (2016). Live-cell imaging of ER-PM contact architecture by a novel TIRFM approach reveals extension of junctions in response to store-operated Ca^{2+}-entry. *Scientific reports*, *6*, 35656. https://doi.org/10.1038/srep35656

Pratt PF, Bonnet S, Ludwig LM, Bonnet P, Rusch NJ. Upregulation of L-type Ca2+ channels in mesenteric and skeletal arteries of SHR. *Hypertension*. 2002;40:214–9.

Pritchard, H., Griffin, C. S., Yamasaki, E., Thakore, P., Lane, C., Greenstein, A. S., & Earley, S. (2019). Nanoscale coupling of junctophilin-2 and ryanodine receptors regulates vascular smooth muscle cell contractility. *Proceedings of the National Academy of Sciences of the United States of America*, *116*(43), 21874–21881. https://doi.org/10.1073/pnas.1911304116

Prakriya, M., & Lewis, R. S. (2015). Store-Operated Calcium Channels. *Physiological reviews*, *95*(4), 1383–1436. https://doi.org/10.1152/physrev.00020.2014

Prole, D. L., & Taylor, C. W. (2019). Structure and Function of IP_3 Receptors. *Cold Spring Harbor perspectives in biology*, *11*(4), a035063. https://doi.org/10.1101/cshperspect.a035063

Quintana, A., Rajanikanth, V., Farber-Katz, S., Gudlur, A., Zhang, C., Jing, J., Zhou, Y., Rao, A., & Hogan, P. G. (2015). TMEM110 regulates the maintenance and remodeling of mammalian ER-plasma membrane junctions competent for STIM-ORAI signaling. *Proceedings of the National Academy of Sciences of the United States of America*, *112*(51), E7083–E7092. https://doi.org/10.1073/pnas.1521924112

Ríos, E., & Stern, M. D. (1997). Calcium in close quarters: microdomain feedback in excitation-contraction coupling and other cell biological phenomena. *Annual review of biophysics and biomolecular structure*, *26*, 47–82. https://doi.org/10.1146/annurev.biophys.26.1.47

Rodríguez-Prados, M., Rojo-Ruiz, J., Aulestia, F. J., García-Sancho, J., & Alonso, M. T. (2015). A new low-Ca^{2+} affinity GAP indicator to monitor high Ca^{2+} in organelles by luminescence. *Cell calcium*, *58*(6), 558–564. https://doi.org/10.1016/j.ceca.2015.09.002

Saeki, T., Suzuki, Y., Yamamura, H., Takeshima, H., & Imaizumi, Y. (2019). A junctophilin-caveolin interaction enables efficient coupling between ryanodine receptors and BK_{ca} channels in the Ca^{2+} microdomain of vascular smooth muscle. *The Journal of biological chemistry*, *294*(35), 13093–13105. https://doi.org/10.1074/jbc.RA119.008342

Saheki, Y., Bian, X., Schauder, C. M., Sawaki, Y., Surma, M. A., Klose, C., Pincet, F., Reinisch, K. M., & De Camilli, P. (2016). Control of plasma membrane lipid homeostasis by the extended synaptotagmins. *Nature cell biology*, *18*(5), 504–515. https://doi.org/10.1038/ncb3339

Saleem, H., Tovey, S. C., Molinski, T. F., & Taylor, C. W. (2014). Interactions of antagonists with subtypes of inositol 1,4,5-trisphosphate (IP_3) receptor. *British journal of pharmacology*, *171*(13), 3298–3312. https://doi.org/10.1111/bph.12685

Salkoff L., Butler A., Ferreira G., Santi C., Wei A. (2006). High-conductance potassium channels of the SLO family. Nat. Rev. Neurosci. 7, 921–931 10.1038/nrn1992

Sartore, S., Chiavegato, A., Faggin, E., Franch, R., Puato, M., Ausoni, S., & Pauletto, P. (2001). Contribution of adventitial fibroblasts to neointima formation and vascular remodeling: from innocent bystander to active participant. *Circulation research*, *89*(12), 1111–1121. https://doi.org/10.1161/hh2401.100844

Sausbier, M., Arntz, C., Bucurenciu, I., Zhao, H., Zhou, X. B., Sausbier, U., Feil, S., Kamm, S., Essin, K., Sailer, C. A., Abdullah, U., Krippeit-Drews, P., Feil, R., Hofmann, F., Knaus, H. G., Kenyon, C., Shipston, M. J., Storm, J. F., Neuhuber, W., Korth, M., ... Ruth, P. (2005). Elevated blood pressure linked to primary hyperaldosteronism and impaired vasodilation in BK channel-deficient mice. *Circulation*, *112*(1), 60–68. https://doi.org/10.1161/01.CIR.0000156448.74296.FE

Schauder, C. M., Wu, X., Saheki, Y., Narayanaswamy, P., Torta, F., Wenk, M. R., De Camilli, P., & Reinisch, K. M. (2014). Structure of a lipid-bound extended synaptotagmin indicates a role in lipid transfer. *Nature*, *510*(7506), 552–555. https://doi.org/10.1038/nature13269

Schiffrin EL. Reactivity of small blood vessels in hypertension: relation with structural changes. *State of the art lecture Hypertension*. 1992;19:II1–9.

Schreiber, M., & Salkoff, L. (1997). A novel calcium-sensing domain in the BK channel. *Biophysical journal*, *73*(3), 1355–1363. https://doi.org/10.1016/S0006-3495(97)78168-2

Scruggs, A. M., Grabauskas, G., & Huang, S. K. (2020). The Role of KCNMB1 and BK Channels in Myofibroblast Differentiation and Pulmonary Fibrosis. American journal of respiratory cell and molecular biology, 62(2), 191–203. https://doi.org/10.1165/rcmb.2019-0163OC

Seo, K., Parikh, V. N., & Ashley, E. A. (2020). Stretch-Induced Biased Signaling in Angiotensin II Type 1 and Apelin Receptors for the Mediation of Cardiac Contractility and Hypertrophy. *Frontiers in physiology*, *11*, 181. https://doi.org/10.3389/fphys.2020.00181

Shruti S., Clem R. L., Barth A. L. (2008). A seizure-induced gain-of-function in BK channels is associated with elevated firing activity in neocortical pyramidal neurons. Neurobiol. Dis. 30, 323–330 10.1016/j.nbd.2008.02.002

Sienaert, I., De Smedt, H., Parys, J. B., Missiaen, L., Vanlingen, S., Sipma, H., & Casteels, R. (1996). Characterization of a cytosolic and a luminal Ca2+ binding site in the type I inositol 1,4,5-trisphosphate receptor. *The Journal of biological chemistry*, *271*(43), 27005–27012. https://doi.org/10.1074/jbc.271.43.27005

Silva, D. F., de Almeida, M. M., Chaves, C. G., Braz, A. L., Gomes, M. A., Pinho-da-Silva, L., Pesquero, J. L., Andrade, V. A., Leite, M., de Albuquerque, J. G., Araujo, I. G., Nunes, X. P., Barbosa-Filho, J. M., Cruz, J., Correia, N., & de Medeiros, I. A. (2015). TRPM8 Channel Activation Induced by Monoterpenoid Rotundifolone Underlies Mesenteric Artery Relaxation. PloS one, 10(11), e0143171. https://doi.org/10.1371/journal.pone.0143171

Simonetti, G., & Mohaupt, M. (2007). Kalzium und Blutdruck [Calcium and blood pressure]. *Therapeutische Umschau. Revue therapeutique*, *64*(5), 249–252. https://doi.org/10.1024/0040-5930.64.5.249

Simpson P. C. (1988). Role of proto-oncogenes in myocardial hypertrophy. The American journal of cardiology, 62(11), 13G–19G. https://doi.org/10.1016/0002-9149(88)90026-4

Soltysinska, E., Bentzen, B. H., Barthmes, M., Hattel, H., Thrush, A. B., Harper, M. E., Qvortrup, K., Larsen, F. J., Schiffer, T. A., Losa-Reyna, J., Straubinger, J., Kniess, A., Thomsen, M. B., Brüggemann, A., Fenske, S., Biel, M., Ruth, P., Wahl-Schott, C., Boushel, R. C., Olesen, S. P., ... Lukowski, R. (2014). KCNMA1 encoded cardiac BK channels afford protection against ischemia-reperfusion injury. *PloS one*, *9*(7), e103402. https://doi.org/10.1371/journal.pone.0103402

Somlyo, A. P., & Somlyo, A. V. (1994). Signal transduction and regulation in smooth muscle. *Nature*, *372*(6503), 231–236. https://doi.org/10.1038/372231a0

Stott, J. B., Barrese, V., Suresh, M., Masoodi, S., & Greenwood, I. A. (2018). Investigating the Role of G Protein βγ in Kv7-Dependent Relaxations of the Rat Vasculature. Arteriosclerosis, thrombosis, and vascular biology, 38(9), 2091–2102. https://doi.org/10.1161/ATVBAHA.118.311360

Sun, C. W., Alonso-Galicia, M., Taheri, M. R., Falck, J. R., Harder, D. R., & Roman, R. J. (1998). Nitric oxide-20-hydroxyeicosatetraenoic acid interaction in the regulation of K+ channel activity and vascular tone in renal arterioles. *Circulation research*, *83*(11), 1069–1079. https://doi.org/10.1161/01.res.83.11.1069

Supattapone, S., Danoff, S. K., Theibert, A., Joseph, S. K., Steiner, J., & Snyder, S. H. (1988). Cyclic AMP-dependent phosphorylation of a brain inositol trisphosphate receptor decreases its release of calcium. *Proceedings of the National Academy of Sciences of the United States of America*, *85*(22), 8747–8750. https://doi.org/10.1073/pnas.85.22.8747

Szteyn, K., & Singh, H. (2020). BK_{ca} Channels as Targets for Cardioprotection. *Antioxidants (Basel, Switzerland)*, *9*(8), 760. https://doi.org/10.3390/antiox9080760

Takei, K., Shin, R. M., Inoue, T., Kato, K., & Mikoshiba, K. (1998). Regulation of nerve growth mediated by inositol 1,4,5-trisphosphate receptors in growth cones. *Science (New York, N.Y.)*, *282*(5394), 1705–1708. https://doi.org/10.1126/science.282.5394.1705

Takeshima, H., Komazaki, S., Nishi, M., Iino, M., & Kangawa, K. (2000). Junctophilins: a novel family of junctional membrane complex proteins. *Molecular cell*, *6*(1), 11–22. https://doi.org/10.1016/s1097-2765(00)00003-4

Tao-Cheng J. H. (2018). Activity-dependent decrease in contact areas between subsurface cisterns and plasma membrane of hippocampal neurons. Molecular brain, 11(1), 23. https://doi.org/10.1186/s13041-018-0366-7

Taylor, C. W., Genazzani, A. A., & Morris, S. A. (1999). Expression of inositol trisphosphate receptors. *Cell calcium*, *26*(6), 237–251. https://doi.org/10.1054/ceca.1999.0090

Taylor, C. W., & Tovey, S. C. (2010). IP(3) receptors: toward understanding their activation. *Cold Spring Harbor perspectives in biology*, *2*(12), a004010. https://doi.org/10.1101/cshperspect.a004010

Tatchum-Talom R, Eyster KM, Martin DS. Sexual dimorphism in angiotensin II-induced hypertension and vascular alterations. *Can J Physiol Pharmacol.* 2005;83:413–22.

Thom, S. (1997). Arterial structural modifications in hypertension. Effects of treatment. *European heart journal*, *18 Suppl E*, E2–E4. https://doi.org/10.1016/s0195-668x(97)90001-4

Thillaiappan, N. B., Chavda, A. P., Tovey, S. C., Prole, D. L., & Taylor, C. W. (2017). Ca^{2+} signals initiate at immobile IP_3 receptors adjacent to ER-plasma membrane junctions. *Nature communications*, *8*(1), 1505. https://doi.org/10.1038/s41467-017-01644-8

Touyz, R. M. (2012). New insights into mechanisms of hypertension. *Current opinion in nephrology and hypertension*, *21*(2), 119–121. https://doi.org/10.1097/MNH.0b013e328350a50f

Touyz, R. M., Alves-Lopes, R., Rios, F. J., Camargo, L. L., Anagnostopoulou, A., Arner, A., & Montezano, A. C. (2018). Vascular smooth muscle contraction in hypertension. *Cardiovascular research*, *114*(4), 529–539. https://doi.org/10.1093/cvr/cvy023

Touyz, R. M., Tolloczko, B., & Schiffrin, E. L. (1994). Mesenteric vascular smooth muscle cells from spontaneously hypertensive rats display increased calcium responses to angiotensin II but not to endothelin-1. *Journal of hypertension*, *12*(6), 663–673.

Troiano, J. A., Potje, S. R., Graton, M. E., Gonçalves, E. T., Tostes, R. C., & Antoniali, C. (2021). Caveolin-1/Endothelial Nitric Oxide Synthase Interaction Is Reduced in Arteries From Pregnant Spontaneously Hypertensive Rats. Frontiers in physiology, 12, 760237. https://doi.org/10.3389/fphys.2021.760237

Tseng-Crank, J., Godinot, N., Johansen, T. E., Ahring, P. K., Strøbaek, D., Mertz, R., Foster, C. D., Olesen, S. P., & Reinhart, P. H. (1996). Cloning, expression, and distribution of a Ca(2+)-activated K+ channel beta-subunit from human brain. *Proceedings of the National Academy of Sciences of the United States of America*, *93*(17), 9200–9205. https://doi.org/10.1073/pnas.93.17.9200

Uchida, K., Aramaki, M., Nakazawa, M., Yamagishi, C., Makino, S., Fukuda, K., Nakamura, T., Takahashi, T., Mikoshiba, K., & Yamagishi, H. (2010). Gene knock-outs of inositol 1,4,5-trisphosphate receptors types 1 and 2 result in perturbation of cardiogenesis. *PloS one*, *5*(9), e12500. https://doi.org/10.1371/journal.pone.0012500

Vetri, F., Saha Roy Choudhury, M., Sundivakkam, P., & Pelligrino, D. A. (2014). BK_{ca} channels as physiological regulators: A focused review. *Journal of Receptor, Ligand and Channel Research*, 3. https://doi.org/10.2147/jrlcr.s36065

Wallner, M., Meera, P., & Toro, L. (1996). Determinant for beta-subunit regulation in high-conductance voltage-activated and Ca(2+)-sensitive K+ channels: an additional transmembrane region at the N terminus. *Proceedings of the National Academy of Sciences of the United States of America*, *93*(25), 14922–14927. https://doi.org/10.1073/pnas.93.25.14922

Wallner, M., Meera, P., & Toro, L. (1999). Molecular basis of fast inactivation in voltage and Ca2+-activated K+ channels: a transmembrane beta-subunit homolog. *Proceedings of the National Academy of Sciences of the United States of America*, *96*(7), 4137–4142. https://doi.org/10.1073/pnas.96.7.4137

Wang, B., & Brenner, R. (2006). An S6 mutation in BK channels reveals beta1 subunit effects on intrinsic and voltage-dependent gating. *The Journal of general physiology*, *128*(6), 731–744. https://doi.org/10.1085/jgp.200609596

Wang, Y., Chen, J., Wang, Y., Taylor, C. W., Hirata, Y., Hagiwara, H., Mikoshiba, K., Toyo-oka, T., Omata, M., & Sakaki, Y. (2001). Crucial role of type 1, but not type 3, inositol 1,4,5-trisphosphate (IP(3)) receptors in IP(3)-induced Ca(2+) release, capacitative Ca(2+) entry, and proliferation of A7r5 vascular smooth muscle cells. *Circulation research*, *88*(2), 202–209. https://doi.org/10.1161/01.res.88.2.202

Wang, Y., Li, G., Goode, J., Paz, J. C., Ouyang, K., Screaton, R., Fischer, W. H., Chen, J., Tabas, I., & Montminy, M. (2012). Inositol-1,4,5-trisphosphate receptor regulates hepatic gluconeogenesis in fasting and diabetes. *Nature*, *485*(7396), 128–132. https://doi.org/10.1038/nature10988

Weaver, A. K., Olsen, M. L., McFerrin, M. B., & Sontheimer, H. (2007). BK channels are linked to inositol 1,4,5-triphosphate receptors via lipid rafts: a novel mechanism for coupling [Ca(2+)](i) to ion channel activation. *The Journal of biological chemistry*, *282*(43), 31558–31568. https://doi.org/10.1074/jbc.M702866200

Wehbe, N., Nasser, S. A., Pintus, G., Badran, A., Eid, A. H., & Baydoun, E. (2019). MicroRNAs in Cardiac Hypertrophy. International journal of molecular sciences, 20(19), 4714. https://doi.org/10.3390/ijms20194714

Weiger, T. M., Holmqvist, M. H., Levitan, I. B., Clark, F. T., Sprague, S., Huang, W. J., Ge, P., Wang, C., Lawson, D., Jurman, M. E., Glucksmann, M. A., Silos-Santiago, I., DiStefano, P. S., & Curtis, R. (2000). A novel nervous system beta subunit that downregulates human large conductance calcium-dependent potassium channels. *The Journal of neuroscience : the official journal of the Society for Neuroscience*, *20*(10), 3563–3570. https://doi.org/10.1523/JNEUROSCI.20-10-03563.2000

Wilkins, B. J., Dai, Y. S., Bueno, O. F., Parsons, S. A., Xu, J., Plank, D. M., Jones, F., Kimball, T. R., & Molkentin, J. D. (2004). Calcineurin/NFAT coupling participates in pathological, but not physiological, cardiac hypertrophy. *Circulation research*, *94*(1), 110–118. https://doi.org/10.1161/01.RES.0000109415.17511.18

Wilkins, B. J., & Molkentin, J. D. (2004). Calcium-calcineurin signaling in the regulation of cardiac hypertrophy. *Biochemical and biophysical research communications*, *322*(4), 1178–1191. https://doi.org/10.1016/j.bbrc.2004.07.121

Womack M. D., Khodakhah K. (2004). Dendritic control of spontaneous bursting in cerebellar Purkinje cells. J. Neurosci. 24, 3511–3521 10.1523/JNEUROSCI.0290-04.2004

Wu, M. M., Buchanan, J., Luik, R. M., & Lewis, R. S. (2006). Ca2+ store depletion causes STIM1 to accumulate in ER regions closely associated with the plasma membrane. *The Journal of cell biology*, *174*(6), 803–813. https://doi.org/10.1083/jcb.200604014

Wu, R. S., & Marx, S. O. (2010). The BK potassium channel in the vascular smooth muscle and kidney: α- and β-subunits. *Kidney international*, *78*(10), 963–974. https://doi.org/10.1038/ki.2010.325

Xi, Q., Adebiyi, A., Zhao, G., Chapman, K. E., Waters, C. M., Hassid, A., & Jaggar, J. H. (2008). IP3 constricts cerebral arteries via IP3 receptor-mediated TRPC3 channel activation and independently of sarcoplasmic reticulum Ca2+ release. *Circulation research*, *102*(9), 1118–1126. https://doi.org/10.1161/CIRCRESAHA.108.173948

Xia, X. M., Ding, J. P., Zeng, X. H., Duan, K. L., & Lingle, C. J. (2000). Rectification and rapid activation at low Ca2+ of Ca2+-activated, voltage-dependent BK currents: consequences of rapid inactivation by a novel beta subunit. *The Journal of neuroscience : the official journal of the Society for Neuroscience*, *20*(13), 4890–4903. https://doi.org/10.1523/JNEUROSCI.20-13-04890.2000

Xu, W., & Lipscombe, D. (2001). Neuronal Ca(V)1.3alpha(1) L-type channels activate at relatively hyperpolarized membrane potentials and are incompletely inhibited by dihydropyridines. *The Journal of neuroscience : the official journal of the Society for Neuroscience*, *21*(16), 5944–5951. https://doi.org/10.1523/JNEUROSCI.21-16-05944.2001

Xu, H., & Ren, D. (2015). Lysosomal physiology. *Annual review of physiology*, *77*, 57–80. https://doi.org/10.1146/annurev-physiol-021014-071649

Yahagi, K., Kolodgie, F. D., Lutter, C., Mori, H., Romero, M. E., Finn, A. V., & Virmani, R. (2017). Pathology of Human Coronary and Carotid Artery Atherosclerosis and Vascular Calcification in Diabetes Mellitus. *Arteriosclerosis, thrombosis, and vascular biology*, *37*(2), 191–204. https://doi.org/10.1161/ATVBAHA.116.306256

Yamada, M., Miyawaki, A., Saito, K., Nakajima, T., Yamamoto-Hino, M., Ryo, Y., Furuichi, T., & Mikoshiba, K. (1995). The calmodulin-binding domain in the mouse type 1 inositol 1,4,5-trisphosphate receptor. *The Biochemical journal*, *308 (Pt 1)*(Pt 1), 83–88. https://doi.org/10.1042/bj3080083

Yan, J., & Aldrich, R. W. (2012). BK potassium channel modulation by leucine-rich repeat-containing proteins. *Proceedings of the National Academy of Sciences of the United States of America*, *109*(20), 7917–7922. https://doi.org/10.1073/pnas.1205435109

Yang, Y., Li, P. Y., Cheng, J., Cai, F., Lei, M., Tan, X. Q., Li, M. L., Liu, Z. F., & Zeng, X. R. (2013). IP_3 decreases coronary artery tone via activating the BK_{ca} channel of coronary artery smooth muscle cells in pigs. *Biochemical and biophysical research communications*, *439*(3), 363–368. https://doi.org/10.1016/j.bbrc.2013.08.079

Yang, J., McBride, S., Mak, D. O., Vardi, N., Palczewski, K., Haeseleer, F., & Foskett, J. K. (2002). Identification of a family of calcium sensors as protein ligands of inositol trisphosphate receptor Ca(2+) release channels. *Proceedings of the National Academy of Sciences of the United States of America*, *99*(11), 7711–7716. https://doi.org/10.1073/pnas.102006299

Yellen G. (2002). The voltage-gated potassium channels and their relatives. *Nature*, *419*(6902), 35–42. https://doi.org/10.1038/nature00978

Yoshikawa, F., Morita, M., Monkawa, T., Michikawa, T., Furuichi, T., & Mikoshiba, K. (1996). Mutational analysis of the ligand binding site of the inositol 1,4,5-trisphosphate receptor. *The Journal of biological chemistry*, *271*(30), 18277–18284. https://doi.org/10.1074/jbc.271.30.18277

Yuan, P., Leonetti, M. D., Pico, A. R., Hsiung, Y., & MacKinnon, R. (2010). Structure of the human BK channel Ca2+-activation apparatus at 3.0 A resolution. *Science (New York, N.Y.)*, *329*(5988), 182–186. https://doi.org/10.1126/science.1190414

Zamponi G. W., Striessnig J., Koschak A., Dolphin A. C. (2015). The physiology, pathology, and pharmacology of voltage-gated calcium channels and their future therapeutic potential. *Pharmacol. Rev.* 67 821–870. 10.1124/pr.114.009654

Zaręba-Kozioł, M., Figiel, I., Bartkowiak-Kaczmarek, A., & Włodarczyk, J. (2018). Insights Into Protein *S*-Palmitoylation in Synaptic Plasticity and Neurological Disorders: Potential and

Limitations of Methods for Detection and Analysis. *Frontiers in molecular neuroscience*, *11*, 175. https://doi.org/10.3389/fnmol.2018.00175

Zhao, G., Adebiyi, A., Blaskova, E., Xi, Q., & Jaggar, J. H. (2008). Type 1 inositol 1,4,5-trisphosphate receptors mediate UTP-induced cation currents, Ca^{2+} signals, and vasoconstriction in cerebral arteries. *American journal of physiology. Cell physiology*, *295*(5), C1376–C1384. https://doi.org/10.1152/ajpcell.00362.2008

Zhao, G., Neeb, Z. P., Leo, M. D., Pachuau, J., Adebiyi, A., Ouyang, K., Chen, J., & Jaggar, J. H. (2010). Type 1 IP_3 receptors activate BK_{ca} channels via local molecular coupling in arterial smooth muscle cells. *The Journal of general physiology*, *136*(3), 283–291. https://doi.org/10.1085/jgp.201010453